

DOE/BC/15102-3
(OSTI ID: 783119)

THE INFLUENCE OF FOLD AND FRACTURE DEVELOPMENT ON
RESERVOIR BEHAVIOR OF THE LISBURNE GROUP OF NORTHERN
ALASKA

Semi-Annual Report
May 2000-January 2001

By:
Wesley K. Wallace
Catherine L. Hanks
Michael T. Whalen
Jerry Jensen
J. Ryan Shackleton
Margarete A. Jadamec
Michelle M. McGee
Alexandre V. Karpov

Date Published: July 2001

Work Performed Under Contract No. DE-AC26-98BC15102

University of Alaska
Fairbanks, Alaska



**National Energy Technology Laboratory
National Petroleum Technology Office
U.S. DEPARTMENT OF ENERGY
Tulsa, Oklahoma**

DISCLAIMER

This report was prepared as an account of work sponsored by an agency of the United States Government. Neither the United States Government nor any agency thereof, nor any of their employees, makes any warranty, expressed or implied, or assumes any legal liability or responsibility for the accuracy, completeness, or usefulness of any information, apparatus, product, or process disclosed, or represents that its use would not infringe privately owned rights. Reference herein to any specific commercial product, process, or service by trade name, trademark, manufacturer, or otherwise does not necessarily constitute or imply its endorsement, recommendation, or favoring by the United States Government or any agency thereof. The views and opinions of authors expressed herein do not necessarily state or reflect those of the United States Government.

This report has been reproduced directly from the best available copy.

The Influence of Fold and Fracture Development on Reservoir Behavior of the
Lisburne Group of Northern Alaska

By
Wesley K. Wallace
Catherine L. Hanks
Michael T. Whalen
Jerry Jensen
J. Ryan Shackleton
Margarete A. Jadamec
Michelle M. McGee
Alexandre V. Karpov

July 2001

Work Performed Under Contract DE-AC26-98BC15102

Prepared for
U.S. Department of Energy
Assistant Secretary for Fossil Energy

Robert E. Lemmon, Technology Manager
National Petroleum Technology Office
P.O. Box 3628
Tulsa, OK 74101

Prepared by
Geophysical Institute
University of Alaska
P.O. Box 757320
Fairbanks, AK 99775-5780

Table of contents

Part A: Introduction and project summary

Definition of problem and objectives	A-1
Scope of this report	A-2
Geologic setting	A-3
References	A-6

Part B: Baseline stratigraphy of the Lisburne Group, by Michelle M. McGee and Michael T. Whalen

Abstract	B-1
Objective	B-1
Methods	B-1
Observations and interpretations	B-2
Stratigraphic sections	
Section FC	B-3
Section FW	B-3
Section EF	B-4
Section EF2	B-4
Section MF and MF2	B-5
Discussion/Conclusions	B-5
Research plan for project completion	B-6
Recommended approach for future similar research	B-7
References	B-7
Table	B-8
Figures	B-9

Part C: Kinematic evolution of thrust-truncated folds by M. A. Jadamec

Abstract	C-1
Introduction	C-2
Methods	C-2
Preliminary Results	C-3
Field Mapping	C-3
Surveying	C-3
Discussion	C-4
Future work	C-5
References	C-5

Figures	C-7
Tables	C-16

Part D: The relationship between fracturing, asymmetric folding, and normal faulting in Lisburne Group carbonates: West Porcupine Lake Valley, northeastern Brooks Range, Alaska

by **J.R. Shackleton, C.L. Hanks, and W.K. Wallace**

Abstract	D-1
Introduction	D-2
Fractures and folds	D-3
Mechanical stratigraphy and fracture development	D-3
Geologic setting	D-4
Lisburne Group stratigraphy	D-5
Methodology	D-5
Preliminary Observations	D-7
Mechanical stratigraphy of the Lisburne Group	D-7
Map scale and mesoscopic scale structures	D-8
Fracturing	D-9
Preliminary interpretations	D-10
Mechanism of folding	D-10
Influence of mechanical stratigraphy on folds in the area	D-10
Normal faulting	D-11
Fracturing	D-11
Future research	D-12
References	D-13

Part E: Flow modeling

by **A.V. Karpov, J. L. Jensen and C. L. Hanks**

Introduction	E-1
Literature overview	E-1
Fracture Statistical Properties	E-1
Fracture Property Assessment	E-2
Lisburne Formation Fracture Analysis	E-2
Data Description	E-2
Analysis Results	E-2
NNW fractures	E-3
ENE fracture set	E-3
Fracture Modeling	E-4

Future work	E-5
Acknowledgements	E-5
References	E-5
Appendix A. Sample L-moment calculations	E-6
Appendix B. Jack-knifing Analysis	E-7

List of figures

Part A: Introduction and project summary

- Figure 1. Map of western part of northeastern Brooks Range A-8
- Figure 2. Generalized geologic map of the Porcupine Lake structural low A-9
- Figure 3. Schematic cross section showing the major structural domains and features in western Porcupine Lake valley. A-10

Part B: Baseline stratigraphy of the Lisburne Group

- Figure 1. Map illustrating locations of stratigraphic sections. B-9
- Figure 2. Generalized section through the Wachsmuth (?) and Alapah Limestone. B-10
- Figure 3. Illustrates the locations of sections FC and FW. B-10
- Figure 4. Key to symbols used in stratigraphic sections. B-11
- Figure 5. Measured stratigraphic section FC. B-12
- Figure 6. Measured stratigraphic section FW. B-13
- Figure 7. Measured stratigraphic section EF. B-14
- Figure 8. Photo showing location of EF section. B-15
- Figure 9. Measured stratigraphic section from EF2. B-16
- Figure 10. Photo illustrating Middle Alapah-Upper Alapah contact in EF2 section B-17
- Figure 11. Photo illustrates the dark and light banding in the Lower Alapah. B-17
- Figure 12. Measured stratigraphic section from MF2. B-18
- Figure 13. Silicified burrows on a large block of talus between sections MF and MF2. B-19
- Figure 14. Measured stratigraphic section from MF2. B-20
- Figure 15. Measured stratigraphic section from MF. B-21

Part C: Kinematic evolution of thrust-truncated folds

- Figure 1. Map of the northeastern Brooks Range C-7
- Figure 2. Scaled cross section across the continental divide thrust-front C-8
- Figure 3. Preliminary map of field area south of Porcupine Lake Valley C-9
- Figure 4. (A) Structural character of frontal anticline in SPLV.
(B) Fold with interpretations. C-10

Figure 5. (A) Structural style of hangingwall anticline south of the frontal anticline in SPLV.	
(B) Fold with interpretations.	C-11
Figure 6. (A) West fold in MFS.	
(B) Fold with interpretations.	C-12
Figure 7. (A) East fold in MFS.	
(B) Fold with interpretations.	C-13
Figure 8. (A) Structures in UMF.	
(B) UMF anticline with interpretations.	C-14
Figure 8. (C) UMF syncline.	
(D) UMF fault.	C-15

Part D: The relationship between fracturing, asymmetric folding, and normal faulting in Lisburne Group carbonates: West Porcupine Lake Valley, northeastern Brooks Range, Alaska

Figure 1: Regional Structure and tectonic map of the Brooks Range and North Slope of Alaska.	D-16
Figure 2. A: Diagram showing fracture orientation with increasing strain	D-17
B: Stearns and Friedman's (1969) model for fractures related to folds.	D-17
Figure 3: Simplified models for detachment folds.	D-18
Figure 4: Suppe and Medwedeff's (1990) model for fault propagation folding.	D-19
Figure 5: Model for fault bend folding (from Suppe, 1983).	D-20
Figure 6: Lithostratigraphy and mechanical stratigraphy of the NE Brooks Range.	D-21
Figure 7: The geologic map of the western portion of the northeastern Brooks Range.	D-22
Figure 8: Cross section through the northeastern Brooks Range.	D-23
Figure 9: Generalized lithostratigraphy of the Endicott, Lisburne, and Sadlerochit groups in the northeastern Brooks Range.	D-24
Figure 10: Photograph of the stratigraphy in West Porcupine Lake Valley.	D-25
Figure 11: Generalized Mechanical Stratigraphy of the Kayak Shale, Lisburne Group, and Sadlerochit Group in West Porcupine Lake Valley.	D-26
Figure 12: Geologic map of West Porcupine Lake Valley.	D-27
Figure 13: Unbalanced cross section through West Porcupine Lake Valley.	D-28
Figure 14: West view of Camp Syncline with sample locations.	D-29

Figure 15: Northeast view (strike sub- perpendicular) of open anticline and syncline with sample locations. D-30

Figure 16: Preliminary interpretive sketch of selected fracture sets recorded in the lower portion of Camp Syncline. D-31

Part E: Flow modeling

Figure 1. Results of Monte Carlo simulations on probability plots for NS fracture height. E-8

Figure 2. L-moment plot with fracture height and spacing sample points. E-9

Figure 3. “Jack-knifing” simulation results shown on L-moment plot. E-9

Figure 4. Probability plots for NS fracture spacing. E-10

Figure 5. Probability plots for EW fracture height. E-10

Figure 6. Probability plots for EW fracture spacing. E-11

Figure 7. Fracman model of megafractures E-11

Figure 8. Fracman model showing only fracture traces E-12

List of tables

Part B: Baseline stratigraphy of the Lisburne Group

Table 1. Summary of outcrop data collected in the northeastern Brooks Range during summer 1999	B-8
--	-----

Part C: Kinematic evolution of thrust-truncated folds

Table 1. Preliminary summary of MFS, UMF, and SPLV fold properties.	C-16
---	------

Part E: Flow modeling

Table 1. Model distribution types and parameters for fracture properties	E-4
--	-----

Table 2. Input parameters for fracture generation in Fracman.	E-5
---	-----

Abstract

The Carboniferous Lisburne Group is a major carbonate reservoir unit in northern Alaska. The Lisburne is detachment folded where it is exposed throughout the northeastern Brooks Range, but is relatively undeformed in areas of current production in the subsurface of the North Slope. The objectives of this study are to develop a better understanding of four major aspects of the Lisburne:

1. The geometry and kinematics of detachment folds and their truncation by thrust faults.
2. The influence of folding on fracture patterns.
3. The influence of deformation on fluid flow.
4. Lithostratigraphy and its influence on folding, faulting, fracturing, and reservoir characteristics.

The Lisburne in the main axis of the Brooks Range is characteristically deformed into imbricate thrust sheets with asymmetrical hangingwall anticlines and footwall synclines. In contrast, the Lisburne in the northeastern Brooks Range is characterized by symmetrical detachment folds. The focus of our 2000 field studies was at the boundary between these structural styles in the vicinity of Porcupine Lake, in the Arctic National Wildlife Refuge. The northern edge of thrust-truncated folds in Lisburne is marked by a local range front that likely represents an eastward continuation of the central Brooks Range front. This is bounded to the north by a gently dipping panel of Lisburne with local asymmetrical folds. The leading edge of the flat panel is thrust over Permian to Cretaceous rocks in a synclinal depression. These younger rocks overlie symmetrically detachment-folded Lisburne, as is extensively exposed to the north.

Six partial sections were measured in the Lisburne of the flat panel and local range front. The Lisburne here is about 700 m thick and is interpreted to consist primarily of the Wachsmuth and Alapah Limestones, with only a thin veneer of Wahoo Limestone. The Wachsmuth is gradational between the underlying Mississippian Kayak Shale and the overlying Mississippian Alapah. The Alapah consists of a lower resistant member of alternating limestone and chert, a middle recessive member, and an upper resistant member that is similar to Wahoo in the northeastern Brooks Range. Two major episodes of transgression and shallowing-upward are represented by the Lisburne of the area.

Asymmetrical folds, mostly truncated by thrust faults, were studied in and south of the local range front. These probably originated as detachment folds based on their mechanical stratigraphy and the transition to detachment folds to the north. Several thrust-truncated folds and one unbroken fold were surveyed to document their geometry. A portion of the local range front was mapped to document changes in fold geometry along strike in three dimensions. The thrust-truncated folds typically are north-vergent hangingwall anticlines with a hangingwall flat in the backlimb and an overturned hangingwall ramp in the forelimb.

Fracture patterns were documented in the gently dipping panel of Lisburne with asymmetrical folds. Four sets of steeply dipping extension fractures were identified, with strikes to the 1) N, 2) E, 3) N to NW, and 4) NE. The relative timing of these fracture sets is complex and unclear. En echelon sets of fractures are common, and display normal or strike-slip sense. Penetrative structures are locally well developed, especially in association with folds. Two sets of normal faults are well developed in the area, and are unusual for the Brooks Range. One set is parallel to and another is transverse to the strike of the folds. The normal faults cut across folds, but may have been active late during folding because fold geometry differs across faults and some folding apparently continued after normal faulting.

In addition to field studies, models were developed for fracture distribution and fluid flow in Lisburne that has been relatively little deformed. Outcrop data from the eastern Sadlerochit Mountains documented NNW- and ENE-striking fracture sets. For both sets of fractures, a better fit to the data is obtained with a lognormal rather than an exponential distribution model for fracture height and spacing. Results of the statistical analyses were used as input to generate models of fracture sets using FracMan software. Such models will form the basis for later models to assess fluid flow and optimum borehole trajectory in fractured Lisburne.

Introduction and geologic setting

Definition of problem and objectives

Carbonate rocks of the Carboniferous Lisburne Group are found throughout a vast region of northern Alaska, including the subsurface of the North Slope and the northern Brooks Range. The Lisburne is a major hydrocarbon reservoir in the North Slope: It was the original target at Prudhoe Bay and is the currently producing reservoir in the Lisburne oil field. Folded and thrust-faulted Lisburne has been a past exploration target in the foothills of the Brooks Range, and will become increasingly more important with growing interest in exploration for gas. It also is an important potential future target for oil and gas exploration in the coastal plain of the Arctic National Wildlife Refuge (1002 area). However, relatively little is known about the reservoir characteristics and behavior of the Lisburne and how they change as a result of deformation.

As in many carbonate reservoirs, most of the hydrocarbon production from the Lisburne Group in the subsurface is from naturally occurring fractures. Natural fractures play an essential role in production from the reservoir, but the geologic factors that control the origin, distribution, and character of these fractures are poorly understood. In the Lisburne oil field, less than 10% of the 2 billion barrels in place is recoverable at the present time. A clearer understanding of the nature and origin of these fractures has the potential to aid in the development of secondary and tertiary recovery programs for a reservoir that is large but difficult to produce.

Future targets for exploration in the Lisburne likely will be along the northern edge of the Brooks Range orogen, where the Lisburne has been modified by fold-and-thrust deformation. Such deformation has long been recognized both to enhance porosity and permeability, largely through the formation of fractures, and to reduce them by compression, as reflected by the formation of cleavage and stylolites. However, the ability to predict patterns of porosity/permeability enhancement or reduction and how they vary within a particular fold trap remain quite limited. Recent rapid advances in the understanding of the geometry and kinematics of different types of folds that form in fold-and-thrust settings offer great potential to improve the systematic understanding of porosity/permeability enhancement or reduction in fold traps, but these advances have only begun to be applied.

The Lisburne Group is a structurally competent unit that overlies an incompetent unit. Hence, the Lisburne undergoes a progressive evolution as shortening increases, from its undeformed state, to tightening detachment folds, to detachment folds that either continue to tighten or are truncated by thrust faults, depending on whether they are symmetrical or asymmetrical. How trap geometry and reservoir characteristics vary as this evolution progresses is not systematically understood, particularly with respect to differences in lithology and position within a fold. The basic objective of this study is to document and develop predictive models for structurally induced changes in reservoir geometry and characteristics at different stages in the evolution of detachment folds in the Lisburne Group.

Extensive exposures of the Lisburne Group in the northeastern Brooks Range fold-and-thrust belt offer the opportunity to develop a clearer understanding of the origin, distribution, and character of structurally induced enhancement and reduction of porosity and permeability in the Lisburne Group. The Lisburne Group has deformed into detachment folds evolved to different degrees, and thus provides a series of natural experiments in which to observe those structures and to develop models both for their formation and for the resulting patterns of enhancement and reduction of porosity and permeability. The results of these field-based observations and models

can then be used to develop quantitative models for characterization of Lisburne reservoirs and the fluid flow within them. Such models can be applied to a spectrum of traps from relatively undeformed to highly folded and thrust faulted.

This study of the Lisburne Group has the following major objectives:

- Establish 'baseline' reservoir characteristics in a relatively undeformed section and develop fracture and fluid flow models and a wellbore placement strategy in such reservoir.
- Document the evolution of trap-scale fold geometry with increasing shortening, with emphasis on changes in thickness across the fold and with respect to mechanical stratigraphy.
- Characterize the differences between folds that continue to shorten by tightening vs. those that are cut by thrust faults as shortening increases.
- Determine patterns in reservoir enhancement and destruction within a fold trap as a function of mechanical stratigraphy and of position within folds at different stages of evolution.
- Use observations of natural folds to constrain predictive models for the evolution of trap-scale fold geometry with increasing shortening and for the resulting modifications of reservoir characteristics.
- Use observations of natural folds and predictive fold models as a basis for fracture models for fluid flow and wellbore placement strategies in fold traps.

The results of this study will apply to current production in relatively undeformed Lisburne and to future exploration in deformed Lisburne. At least as important is the fact that the results will apply generally to carbonate reservoirs and to folded reservoirs, both of which are major producers and exploration targets worldwide.

Scope of this report

This report summarizes the results of this project's second season of field work, which was conducted during the summer of 2000. The report presents initial examples of compiled data and preliminary interpretations and analysis of field observations, and reflects progress to January 2001. Results of further data compilation, analysis, and interpretation will be presented in future reports. Except for an update on fracture and flow modeling, the report does not address studies begun during the first (1999) season of field work for the project. Progress on these studies will be presented in the second annual report.

Participants in this report include three Master's students (M.A. Jadamec, J.R. Shackleton, and A.V. Karpov), a Ph.D. student (M.M. McGee), a micropaleontological analyst (A.P. Krumhardt), three University of Alaska faculty (W.K. Wallace, C.L. Hanks, and M.T. Whalen), and one Texas A & M faculty (J.L. Jensen).

The report consists of five parts that each summarize a different aspect of the study and are written by different authors. These include:

- Introduction and geologic setting, by W.K. Wallace
- Stratigraphy of the Lisburne Group in the Porcupine Lake area, by M.M. McGee, M.T. Whalen, and A.P. Krumhardt
- Kinematic evolution of thrust-truncated folds, by M.A. Jadamec
- The relationship between fracturing, asymmetric folding, and normal faulting in Lisburne Group carbonates: West Porcupine Lake valley, by J.R. Shackleton, C.L. Hanks, and W.K. Wallace
- Lisburne Group fracture distribution and flow modeling, by A.V. Karpov, J.L. Jensen, and C.L. Hanks

Geologic Setting

The Lisburne Group is the most abundant and widely distributed rock unit in the northern Brooks Range, where it forms the range front in most places and extends a significant distance southward into the range. This unit displays two distinct structural styles in different parts of the northern Brooks Range. Imbricately stacked thrust sheets characterize the Lisburne south of the range front in the western and central Brooks Range and south of the projection of the range front into the eastern Brooks Range. These thrust sheets commonly display asymmetrical hangingwall anticlines and footwall synclines, but only rare asymmetrical folds that have not been cut by thrust faults. In contrast, the northeastern Brooks Range is characterized by symmetrical detachment folds only rarely cut by thrust faults. The "Continental Divide thrust front" marks the boundary between these two structural styles (Figure A-1).

The focus of the first summer of field work for this study was on the Lisburne and its structures north of the Continental Divide thrust front, in the detachment-folded Lisburne of the northeastern Brooks Range. The second summer of field work addressed the asymmetrically folded and imbricated Lisburne south of the thrust front. This report presents preliminary results from that second field season. The structural style south of the Continental Divide thrust front is exceptionally well exposed along the southern margin of an important structural low near Porcupine Lake (Figure A-1). This area was the geographic focus of the studies presented in this report.

Regional stratigraphy and its structural implications

Little published information is available on the stratigraphy in the Porcupine Lake area. Major differences in stratigraphy exist across the Continental Divide thrust front beneath the Mississippian Kayak Shale, but the differences are much less clear higher in the section. North of the thrust front, a complex of penetratively deformed and slightly metamorphosed pre-Middle Devonian sedimentary and subordinate volcanic rocks forms depositional basement and is unconformably overlain by a thin veneer of Mississippian Kekiktuk Conglomerate. To the south, a much expanded clastic succession exists downward from the stratigraphic position of the Kekiktuk Conglomerate and the underlying basement rocks are not exposed (e.g., Imm et al., 1993). This clastic succession probably is equivalent to the succession documented to the east-northeast by Anderson et al. (1994), where the Middle Devonian (and younger?) Ulungarat formation unconformably overlies basement and is in turn unconformably overlain by Mississippian Kekiktuk Conglomerate with a small angular discordance.

The Kekiktuk Conglomerate is conformably overlain by a succession that consists of the Mississippian Kayak Shale, carbonate rocks of the Mississippian and Pennsylvanian Lisburne Group, and shale and subordinate sandstone of the Permian and Lower Triassic Sadlerochit Group (or its equivalents) is present on both sides of the Continental Divide thrust front. Preliminary work (detailed in chapter B of this report) indicates that the Lisburne south of the thrust front is thicker and that intervals of thick-bedded and coarse-grained limestone make up a greater part of the succession than to the north.

The stratigraphic succession has a profound influence on the character of structures on both sides of the Continental Divide thrust front. Basement to the north forms thick fault-bend folded thrust sheets, whereas the clastic succession to the south is detached from basement and forms thinner imbricate thrust sheets (Wallace, 1993). The Lisburne serves as a competent structural member

bounded by structural detachments in the underlying and overlying incompetent shales on both sides of the boundary, but forms thrust-truncated folds to the south and detachment folds to the north.

These are the stratigraphic units most relevant to this report. Other units that are locally preserved within the Porcupine Lake structural low are mentioned below.

Structural domains of the Porcupine Lake structural low

The Porcupine Lake structural low and a similar low at Bathtub Ridge to the east-northeast lie along structural strike with the range front of the central Brooks Range. They display similar structural characteristics to that range front and probably represent remnants of its eastern continuation. This range front originated as the leading edge of far-displaced allochthons in Late Jurassic to Early Cretaceous time (Moore et al., 1994a), but was structurally modified and attained the structural relief responsible for its present topographic expression in Paleocene time (O'Sullivan et al., 1997). In the eastern Brooks Range, the older range front became isolated within the range as the deformation front migrated forward to form the northeastern Brooks Range in Eocene and later time (Wallace and Hanks, 1990; Hanks et al., 1994; O'Sullivan, 1994). The Porcupine Lake and Bathtub Ridge structural lows locally preserve rocks and structures that have been uplifted and eroded elsewhere along the former range front.

A zone that consists of four distinct structural domains defines the boundary in structural styles between the central and northeastern Brooks Range across the Porcupine Lake structural low (Figures A-2 & A-3). The southernmost domain is a local range front that forms the southern edge of the lower topography of the structural low to the north. This range front is typical of the range front of the central Brooks Range, which lies along strike. It is marked by a distinct topographic front defined by folds at the leading edges of overlapping thrust sheets. This range front marks the northern edge of the structural style characteristic of the northern part of the main axis of the Brooks Range (Moore et al., 1994a; Wallace et al., 1997). South-dipping Lisburne thrust sheets are bounded by décollements in the underlying Kayak Shale and overlying Sadlerochit Group. Asymmetrical hangingwall anticlines and footwall synclines commonly mark the leading and trailing edges of these thrust sheets. Local unbroken asymmetrical folds suggest that the hangingwall anticlines and footwall synclines formed by thrust-breakthrough of the steep limbs of asymmetrical folds.

The domain north of the local range front consists of an extensive, nearly flat-lying panel of Lisburne and Sadlerochit (Figures A-2 & A-3) that locally displays unbroken asymmetrical folds and is cut by two sets of normal faults, one parallel to and another transverse to regional structure. In the lowest part of the regional structural low, this panel is overlain by a klippe of Carboniferous to Cretaceous rocks that are probably equivalent to remnants of south-derived allochthons preserved along the central Brooks Range front and in the western Brooks Range. The leading edge of the flat-lying panel is locally exposed as a hangingwall anticline in Lisburne thrust over rocks of the Sadlerochit Group.

To the north of the flat panel, a synclinal depression centered near Porcupine Lake (Figures A-2 & A-3) preserves strata that have been eroded throughout most of the northeastern Brooks Range except near its northern range front. In addition to the Permian and Triassic Sadlerochit Group, these rocks include the Triassic Shublik Formation, the Jurassic and Lower Cretaceous Kingak Shale, the Lower Cretaceous Kongakut Formation, and the Lower Cretaceous Bathtub Graywacke. The youngest part of this succession includes probable equivalents of foreland basin

deposits found in similar synclinal lows along strike to the west along the central Brooks Range front and to the east in Bathtub syncline. Local exposures of folded Lisburne within this synclinal depression suggest that it marks the southern extent of the symmetrical detachment folds characteristic of the northeastern Brooks Range.

A fourth domain is exposed only to the east (Figure A-2), where imbricated Lisburne and older rocks form a structural high that plunges westward beneath the Permian and younger rocks preserved in the synclinal depression. This structural high is bounded to the south by a thrust fault along the leading edge of the flat panel and to the north by a thrust fault that was itself folded when symmetrical detachment folds formed in the underlying Lisburne and Sadlerochit. The core of the structural high consists of imbricated coarse-grained siliciclastic rocks that are structurally bounded above and below by folded and imbricated Lisburne. The siliciclastic rocks lie beneath the sub-Lisburne décollement (in Kayak) and are probably equivalent to a parautochthonous Middle Devonian to Mississippian clastic wedge (Ulungarat and Kekiktuk Formations) that is exposed to the east.

Questions about the Porcupine Lake structural low

The structural characteristics of the Porcupine Lake structural low raise a number of unresolved questions that are relevant to this project. These questions are only briefly introduced here, but will be addressed in more detail in other parts of this report and in future research.

The most central of these questions is why structural style changes across the low from thrust-truncated asymmetrical folds to symmetrical detachment folds. Wallace (1993) suggested several possible controlling factors, including changes across the boundary in mechanical stratigraphy, dip of the basal detachment, amount of depositional and structural overburden, and/or amount of shortening. The role of each of these factors will be explored in future work, but field observations have already confirmed that differences in mechanical stratigraphy exist across the boundary. Specifically, the Lisburne south of the boundary is thicker and more competent than to the north, and the stratigraphic character and structural behavior of the underlying rocks changes across the boundary. Additional questions related to these stratigraphic differences may have bearing on interpretation of the factors controlling structural style.

The Endicott Mountains allochthon is interpreted to have been displaced a large distance northward over parautochthonous rocks of the North Slope and northeastern Brooks Range (Mull et al., 1987, 1989; Moore et al., 1994a & b). The Upper Devonian Hunt Fork Shale, Noatak Sandstone, and Kanayut Conglomerate are stratigraphic units found only in the allochthon. However, direct equivalents of the parautochthonous section are found in the overlying rocks of the allochthon, including the Kayak Shale, Lisburne Limestone, and Siksikpuk Formation, and distinction between the allochthon and parautochthon is difficult in this part of the section. The northern edge of the Endicott Mountains allochthon has generally been interpreted to lie a significant distance to the south of the Porcupine Lake structural low (e.g., Mull et al., 1989; Imm et al., 1993; Moore et al., 1994b). However, two observations suggest the possibility that the leading edge of the Endicott Mountains allochthon might extend northward to the northern edge of the flat panel. First, the northern edge of the flat panel is locally seen to be a thrust fault whose displacement is indeterminate. Second, the stratigraphy of the Lisburne and Sadlerochit-equivalent rocks of the flat panel and local range front differ somewhat from those of the known parautochthon to the north. Detailed stratigraphic study is required to determine whether or not these rocks belong to the allochthon. The location of the northern edge of the Endicott Mountains allochthon could have a bearing on the change from thrust-truncated to untruncated folds in the

Lisburne, although this change in structural style does not coincide with the allochthon boundary farther west (Wallace et al., 1997).

A similar question involves the stratigraphic affinity of the sub-Kayak clastic rocks in the structural high east of the Porcupine Lake structural low. Based on their location and character, these rocks most likely are equivalent to the parautochthonous Middle Devonian to Mississippian Ulungarat and Kekiktuk Formations. However, the possibility must also be considered that they are equivalents of the Kanayut Conglomerate of the Endicott Mountains allochthon. The identity of these rocks has major implications for structural interpretation, but requires detailed stratigraphic study to resolve.

Two other questions involve structural characteristics of the Porcupine Lake structural low that are apparently absent from the central Brooks Range front. First, why does the flat panel exist, and why are the folds within it not generally truncated by thrust faults? Second, why are two different sets of normal faults so prominently developed within the flat panel? The answers to these questions are obviously relevant to our studies of fold and fracture evolution within the flat panel.

Location of the field studies included in this report

The focus of the 2000 field season was on the stratigraphy, folding, thrust truncation, and fracturing of Lisburne that has been asymmetrically folded. Consequently, the field observations summarized in this report are from the local range front and flat panel domains of the Porcupine Lake area (Figures A-2 & A-3). Lisburne stratigraphy appears to be the same in the two domains and is described in Chapter B. Chapter C describes the structure of the western part of the flat panel, including asymmetrical folds, normal faults, and associated fractures. Chapter D describes thrust-truncated asymmetrical folds along the local range front south of the central part of the Porcupine Lake structural low.

References

- Anderson, A.V., Wallace, W.K., and Mull, C.G., 1994, Depositional record of a major tectonic transition in northern Alaska: Middle Devonian to Mississippian rift-basin margin deposits, upper Kongakut River region, eastern Brooks Range, Alaska, *in* Thurston, D., and Fujita, K., eds., 1992 Proceedings International Conference on Arctic Margins, U.S. Minerals Management Service Outer Continental Shelf Study 94-0040, p. 71-76.
- Hanks, C.L., Wallace, W.K., and O'Sullivan, P., 1994, The Cenozoic structural evolution of the northeastern Brooks Range, Alaska, *in* Thurston, D., and Fujita, K., eds., 1992 Proceedings International Conference on Arctic Margins, U.S. Minerals Management Service Outer Continental Shelf Study 94-0040, p. 263-268.
- Imm, T.A., Dillon, J.T., and Bakke, A.A., 1993, Generalized geologic map of the Arctic National Wildlife Refuge, northeastern Brooks Range, Alaska: Alaska Division of Geological and Geophysical Surveys Special Report 42, scale 1:500,000, 1 sheet.
- Moore, T.E., Wallace, W.K., Bird, K.J., Karl, S.M., Mull, C.G., and Dillon, J.T., 1994a, Chapter 3: Geology of northern Alaska, *in* Plafker, G., and Berg, H.C., eds., The geology of Alaska: The Geology of North America, Geological Society of America, Boulder, Colorado, v. G1, p. 49-140.
- Moore, T.E., Wallace, W.K., Mull, C.G., Karl, S.M., and Bird, K.J., 1994b, Generalized geologic map and sections for northern Alaska, *in* Plafker, G., and Berg, H.C., eds., The geology of Alaska: The Geology of North America, Geological Society of America, Boulder, Colorado, v. G1, p. Plate 6.

- Mull, C.G., Roeder, D.H., Tailleur, I.L., Pessel, G.H., Grantz, A., and May, S.D., 1987, Geologic sections and maps across Brooks Range and Arctic Slope to Beaufort Sea: Geological Society of America Map and Chart Series MC-28S, scale 1:500,000, 1 sheet.
- Mull, C.G., Adams, K.E., and J.T. Dillon, J.T., 1989, Stratigraphy and structure of the Doonerak Fenster and Endicott Mountains allochthon, central Brooks Range, *in* Mull, C.G., and Adams, K.E., eds., Dalton Highway, Yukon River to Prudhoe Bay, Alaska, Bedrock geology of the eastern Koyukuk basin, central Brooks Range, and east central Arctic Slope: Alaska Division of Geological and Geophysical Surveys Guidebook 7, v. 2, p. 203-217.
- O'Sullivan, P.B., 1994, Timing of Tertiary episodes of cooling in response to uplift and erosion, northeastern Brooks Range, Alaska, *in* Thurston, D., and Fujita, K., eds., 1992 Proceedings International Conference on Arctic Margins, U.S. Minerals Management Service Outer Continental Shelf Study 94-0040, p. 269-274.
- O'Sullivan, P.B., Murphy, J.M., and Blythe, A.E., 1997, Late Mesozoic and Cenozoic thermotectonic evolution of the central Brooks Range and adjacent North Slope foreland basin, Alaska: Including fission track results from the Trans-Alaska Crustal Transect (TACT): *Journal of Geophysical Research*, v. 102, no. B9, p. 20,821-20,845.
- Wallace, W.K., 1993, Detachment folds and a passive-roof duplex: Examples from the northeastern Brooks Range, Alaska, *in* Solie, D.N., and Tannian, F., eds., Short Notes on Alaskan Geology 1993: Alaska Division of Geological and Geophysical Surveys Geologic Report 113, p. 81-99.
- Wallace, W.K., and Hanks, C.L., 1990, Structural provinces of the northeastern Brooks Range, Arctic National Wildlife Refuge, Alaska: *American Association of Petroleum Geologists Bulletin*, v. 74, no. 7, p. 1100-1118.
- Wallace, W.K., Moore, T.E., and Plafker, G., 1997, Multistory duplexes with forward dipping roofs, north central Brooks Range, Alaska: *Journal of Geophysical Research*, v. 102, no. B9, p. 20,773-20,796.

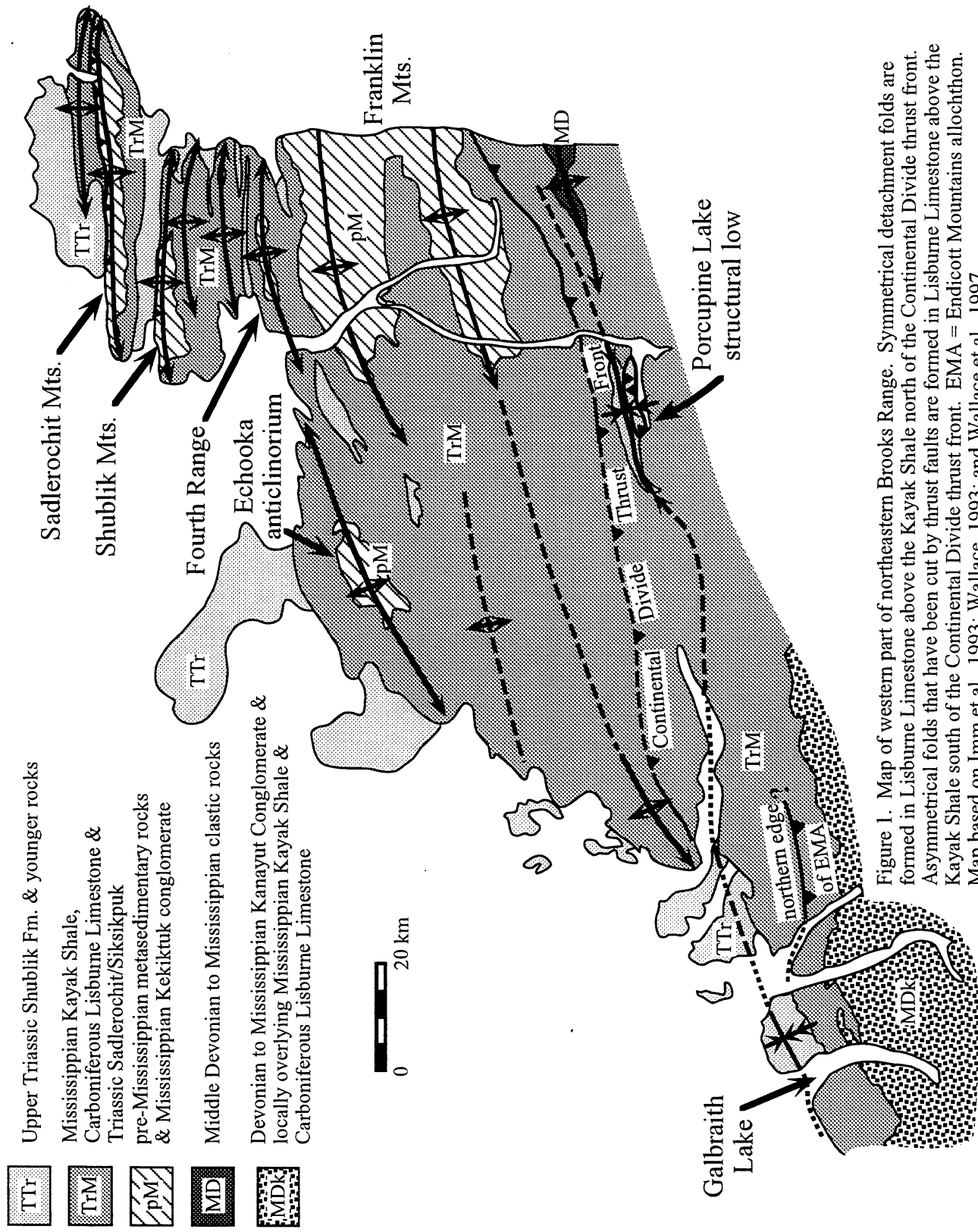


Figure 1. Map of western part of northeastern Brooks Range. Symmetrical detachment folds are formed in Lisburne Limestone above the Kayak Shale north of the Continental Divide thrust front. Asymmetrical folds that have been cut by thrust faults are formed in Lisburne Limestone above the Kayak Shale south of the Continental Divide thrust front. EMA = Endicott Mountains allochthon. Map based on Imm et al., 1993; Wallace, 1993; and Wallace et al., 1997.

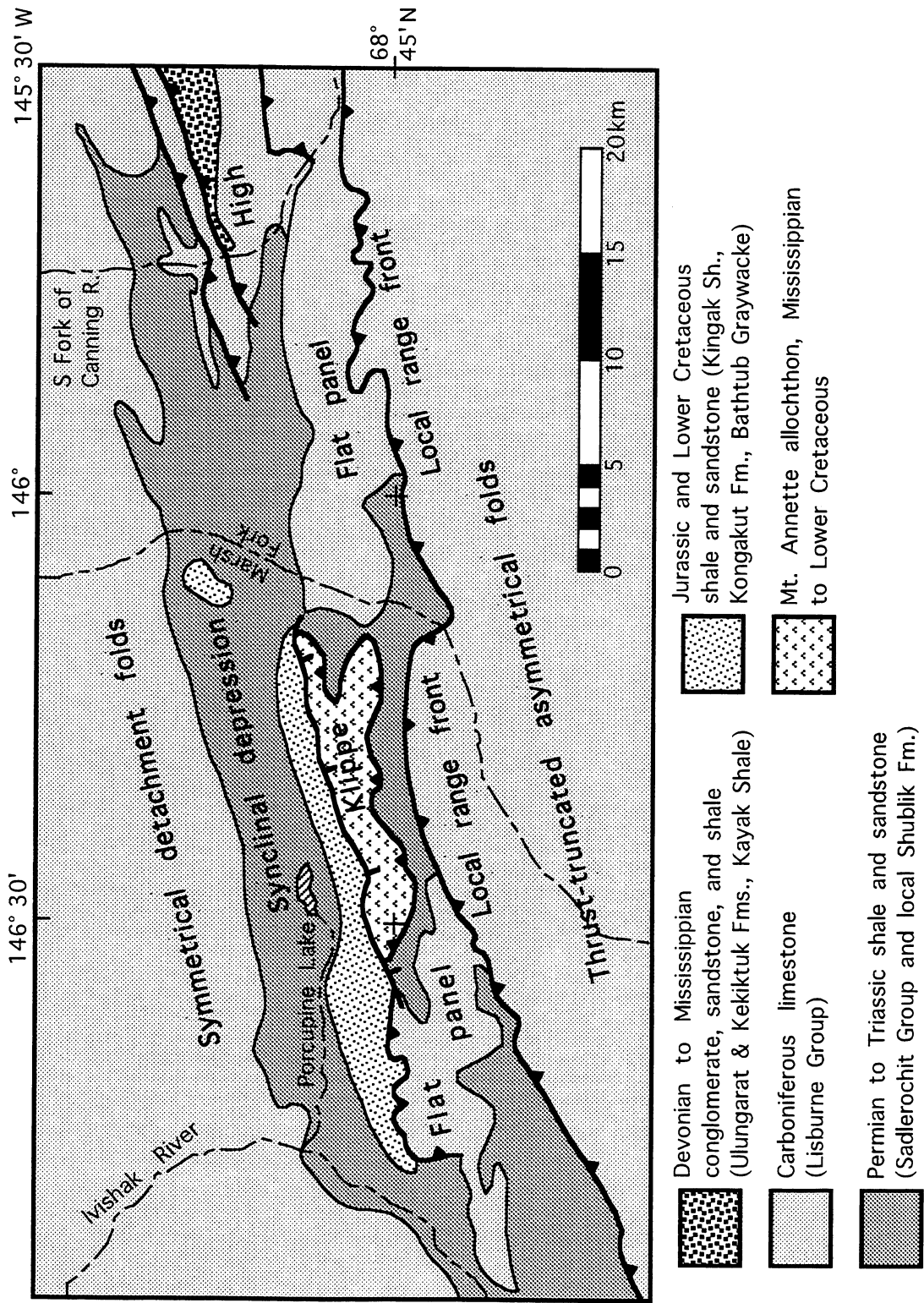


Figure 2. Generalized geologic map of the Porcupine Lake structural low showing the main structural domains and related structural features.

Baseline stratigraphy of the Lisburne Group

by Michelle M. McGee and Michael T. Whalen, Geophysical Institute and Department of Geology and Geophysics, University of Alaska, Fairbanks, Alaska 99775-5780

ABSTRACT

Significant progress has been made on establishing the baseline stratigraphy of the Lisburne Group, Porcupine Lake area, Philip Smith Mountains. Six partial sections in the Wachsmuth and Alapah Limestone were the focus of the 2000 field season. The Wachsmuth is poorly exposed and appears to be gradational with the underlying Kayak Shale and overlying lower Alapah Limestone. The lower Alapah is resistant and displays dark (chert) and light (limestone) banding. The middle Alapah is recessive and the upper Alapah is resistant and lithologically similar to the Wahoo Limestone in the north. Cycles in the Alapah, overall, shallow up from mudstones or wackestones to packstones, grainstones, or rudstones. Several parasequences were identified in the upper middle Alapah and upper Alapah. These packages are based on weathering profiles and may have an impact on the mechanical stratigraphy. Very little to no Wahoo was identified in the field areas. The thinness of the Wahoo maybe due to non-deposition or removal by erosion or tectonics.

The data collected will be used to identify depositional cycles and parasequences and provide criteria for correlations between Prudhoe Bay cores and Brooks Range outcrops. Subsurface and surface data will delineate package geometries, lateral changes of lithology and reservoir characteristics, and paleogeography across the broad carbonate platform. Seismic scale cross sections will eventually be constructed that will aid in sequence stratigraphic interpretations and delineation of major reservoir units.

OBJECTIVE

The goals of this phase of the research project are to establish a "baseline" for Lisburne reservoir characteristics in relatively undeformed rocks using surface and subsurface data. The goals of this portion of the project are being met through a multi-phase approach to stratigraphic data collection to insure the development of a comprehensive database for establishing the stratigraphic baseline. The multi-phase approach includes collection of high-resolution lithostratigraphic data, petrographic, mineralogic, and X-ray diffraction data, and outcrop spectral gamma ray profiles and comparable subsurface geophysical logs. Progress on the baseline stratigraphic study of the Lisburne Group includes acquisition of outcrop lithologic data from distal portions of the field area in the Philip Smith Mountains.

METHODS

During the summer of 2000, high-resolution lithostratigraphic data were collected from six partial sections in the south Porcupine Lake area, Philip Smith Mountains (Fig. 1) by Michelle McGee and Michael Whalen with assistance from Andrea Krumhardt, Sue Morgan and Rachael Pachter. Sections include Forks Canyon (FC), Forks Wahoo (FW), East Fork (EF), East Fork 2 (EF2), Marsh Fork (MF), and Marsh Fork 2 (MF2). The outcrop data is summarized in Table 1. Sections were measured at meter intervals using a jacob staff. One fist sized hand sample was collected at meter or smaller intervals. One four to five kilogram conodont sample was collected every ten to twenty meters. Detailed sedimentological descriptions included: depositional fabrics, identification of dolomitized intervals, sedimentary structures, bed thickness, lithologic contrasts, paleontologic content, porosity types and amounts, chert

content, fracture type and location, and ichnofabric. Outcrop gamma ray data was not collected this field season because no stratigraphically complete sections were identified.

All hand samples collected will be cut and select samples will be thin sectioned and stained for calcite (Alizarin Red S). X-ray diffraction will be completed on samples containing calcite and dolomite to determine percentages of each. Petrographic analysis will be completed to determine reservoir properties, such as primary and secondary porosity. Point counting will quantitatively identify skeletal and other sedimentary grains, matrix, pores, voids, cements, and compaction features. Cathodoluminescent analysis will further delineate diagenesis. Conodont samples will be crushed, processed in glacial acetic acid, subjected to heavy mineral separation, picked, and identified. Conodonts will be used in biostratigraphy and will aid in the identification of the Mississippian-Pennsylvanian boundary.

Data analysis will include identification of depositional cycles and parasequences, construction of cross-sections, and correlations between Prudhoe Bay cores and outcrop. Depositional cycles and unconformities will be used to classify units that are genetically similar. Cross-sections will be used to identify vertical variations of lithology and changes in reservoir properties. Correlations between subsurface and surface will delineate package geometries, lateral changes of lithology and reservoir characteristics, and paleogeography across the broad carbonate platform.

OBSERVATIONS AND INTERPRETATIONS

The first week of the 2000 field season was spent in Sunset Pass, Sadlerochit Mountains because of flight and weather delays. No stratigraphic sections were measured because most of the outcrops were very rubbly but several stratigraphic observations were made that will be incorporated into the study. Cave deposits were identified in the Lower Wahoo and uppermost Alapah Limestone. The cave deposits include breccias and laminated fine-grained carbonate sediment. These deposits may correlate to cave deposits found in the Shublik Mountains and Prudhoe Bay cores (Wallace et al., 2000). A paleosol was also identified in the Alapah Limestone along the northeast side of Sunset Pass. The paleosol was exposed laterally for approximately 4.5 m and then was covered by talus. At the base of the paleosol was a 2.5 cm thick green unit overlain by a several centimeter thick red unit with a blocky texture. A conodont sample was collected from the limestone directly below the paleosol. Conodont age dating indicates that the rocks are Upper Mississippian in age and part of the upper Alapah Limestone.

The remaining weeks of the 2000 field season were spent in the Porcupine Lake area where six partial stratigraphic sections were measured (Figure 1). An additional section from the Upper Kayak Shale through upper Alapah was discovered in the Forks area, but was difficult to reach because of ice in the creek. It will possibly be revisited next field season.

The lower Lisburne is approximately 700 meters thick and is overlain by a thin veneer of Wahoo in the south Porcupine Lake field area. The lower Lisburne can be subdivided into the Wachsmuth Limestone and informally lower, middle, and upper Alapah based on lithofacies and weathering profiles (Figure 2).

The Wachsmuth was first described by Bowsher and Dutro (1957) in the Shainin Lake area. Bowsher and Dutro (1957) subdivided the Wachsmuth into a shaly limestone member, crinoidal limestone member, dolomitic limestone member, and banded limestone member. Armstrong and Mamet (1975) and Brosgé et al. (1962) described the crinoidal limestone member, middle member (dolomitic limestone member) and the banded limestone member of the Wachsmuth in the eastern Brooks Range. The middle member and banded limestone member of the Wachsmuth is present in the East Fork and Marsh Fork field areas. The best exposure of the Wachsmuth was in the East Fork area (Figure 2).

The Wachsmuth is approximately 100 m thick and recessive weathering at the base and becomes more resistant with increasing chert content. The dark and light banding is gray wackestone alternating with dark gray to black chert.

The lower Alapah overlies the Wachsmuth and is approximately 250 m thick, relatively resistant. The unit consists of several packages of nodular or bedded chert and crinoid-bryozoan wackestone with large sub-horizontal, silicified burrows. These facies are overlain by meter-thick crinoid rudstones with reworked coral fragments. The cherty wackestones are interpreted to have been deposited below fairweather wave base in a deep ramp environment. Crinoid rudstones are interpreted as shoals.

The middle interval is 200 meters thick, cyclic, has a recessive weathering profile, and is darker colored than the lower unit. Cycles begin with greenish, calcareous shale that coarsens upward into crinoid-bryozoan-coral grainstone to rudstone and coral framestone. Basal shales drape over coral heads that form the top of the subjacent cycles. Progressively coarsening upward cycles indicate a progradational facies stacking pattern. Calcite replaced evaporites observed at the Middle-upper Alapah contact and the cycle stacking patterns are interpreted to indicate shallowing upward from deep ramp to shallow subtidal environments.

The upper 150 m thick package is relatively resistant, light in color, cyclic, and grainier than the middle interval. Cycles are a few meters to tens of meters thick. They coarsen upward from crinoid-bryozoan wackestone to crinoid-bryozoan packstone to grainstone. The cycles become muddier and bryozoan and chert abundance increases upward. The stratal stacking pattern and fauna indicate a change from open to restricted lagoonal environments on a shallow ramp.

The Lisburne Group in the Porcupine Lake Valley, Philip Smith Mountains records an initiation of deep-water carbonate ramp sedimentation atop the underlying Kayak Shale. Two major episodes of transgression and shallowing upward indicate significant relative changes in sea-level. The lower and middle interval appear to correlate to the middle and upper Alapah and the upper interval correlates to the Wahoo in the north.

STRATIGRAPHIC SECTIONS

SECTION FC

Section FC is located _ mile north of the Forks camp and is primarily middle Alapah with a few meters of upper Alapah (Figures 1, 3). Figure 4 is a key to the stratigraphic sections. The section is illustrated in Figure 5 and was recessive and complicated by normal faults. Lithofacies in the section overall were fine-grained, but commonly display a cyclic pattern that coarsened from calcareous shales or mudstones to wackestones. The calcareous shale beds ranged in thickness from a few mm to tens of cm. A few cycles were capped with packstone, grainstone or rudstone. Cycles were typically 0.25 to 0.5 m thick. Near the upper Alapah contact the cycle thickness increased to meter to several meters thick.

SECTION FW

Section FW is located approximately 800 m south of section FW (Figures 1, 3) and is illustrated in Figure 6. The FW section was originally thought to be in the Lower Wahoo. Lithologically section FW is similar to the Wahoo Limestone as described from localities further north. Conodont age dating however, indicates that it is Mississippian making it time equivalent to the Alapah Limestone in the north. This section is resistant and complicated by a minimum of three normal faults above 90 m. Displacement of these faults ranged between 0.5 to 1 m. The section was terminated at 120 m because the displacement of the normal fault could not be determined. The section was measured to

the last limestone outcrop at 178 m (not accounting for any displacement from normal faults above 120 m). The Sadlerochit Group overlies the limestone at this locality (Figure 3).

Facies identified represent a wide range of textures from mudstone to rudstone. Bed thickness is 0.25 to 0.5 m. The mudstones were typically devoid of fossils and were highly fractured. The wackestones have few crinoid, bryozoan, and coral fragments. The wackestones were less fractured than the mudstones and more fractured compared to the packstones. The packstones and grainstones were composed of crinoid, bryozoan, brachiopod, and coral fragments. The rudstones were composed almost entirely of crinoids with minor brachiopods and rare rugose corals. A typical cycle in this section fines from mudstone or wackestone to grainstone or rudstone. The rudstones displayed solution cleavage and were very brittle. Replaced evaporite nodules are present between 16 and 17 m.

SECTION EF

Section EF is located approximately 3 km to the S-SE of section FW (Figure 1). The section is illustrated in Figure 7. Section EF is within the middle Alapah and the outcrop is very recessive until 90.5 m. Corals are fist-sized, broken, and jumbled. Fragmented crinoids, bryozoans, brachiopods, and solitary rugose corals are often associated with the colonial coral beds. Non-shale-coral cycles consist of wackestone or packstone at the base and coarsen into packstones, grainstones, or rudstones. Shale beds form drapes over the coral heads. Below 90.5 m there are numerous _ to _ m thick cycles that have mm to several cm thick calcareous shale beds that are overlain by colonial coral beds. Above 90.5 m are several cycles of calcareous shale or wackestone to resistant grainstones to rudstones with planar laminations. A possible channel was identified to the east of the section (Figure 8).

SECTION EF2

The base of section EF2 is approximately 100 meters to the N-NE from the base of the EF section (Figure 1) and is illustrated in Figure 9. The base of the EF2 section is probably just above the top of the EF section. The section could not be completed due to time constraints, approximately 104 m of additional section are present above the top of section EF2 at 319 m. The Lisburne-Sadlerochit Group contact is at approximately 425 m. The Wahoo maybe present as a thin sliver above the end of section EF2, but is believed to be either eroded or possibly tectonically removed.

Typical cycles coarsen-upward from calcareous shale, mudstone, or wackestone to wackestone, packstone, or grainstone. A few cycles are capped with rudstone. Numerous cycles consist of mm to cm thick calcareous shale at the base and coarsen-up into fist-sized jumbled and broken corals and are similar to the shale-coral intervals in the EF section. Colonial rugose corals with a minimum diameter of 1 m were found at 170 m. The corals are underlain by calcareous shale and appear to be in growth position.

The middle Alapah-upper Alapah contact is at 214 m. A meter thick bed of mudstone with replaced evaporite nodules underlies this contact. Above the contact is a planar laminated very coarse-grained crinoid rudstone. The cycles above this contact are coarser-grained than those below. The cycles coarsen-upward from wackestone to grainstone or rudstone. Between 269.5 and 270 m is an iron-stained muddy dolomite. This dolomite is possibly the Mississippian-Pennsylvanian boundary. Conodont samples were collected above and below this bed for age analysis.

Four mechanical stratigraphic subdivisions were identified in the middle Alapah and an additional three in the upper Alapah in the EF2 section (Figure 10). These subdivisions are defined by their weathering profile. The mechanical subdivisions also correspond to parasequences sets. The parasequences have fine-grained recessive bases

and coarsen-upward. The parasequences internally contain the higher frequency cycles described above. Three additional parasequence were identified in the upper Alapah. The base of the first upper Alapah parasequence actually begins in the lower most upper Alapah. The upper Alapah parasequences were coarser-grained and thicker than the Middle Alapah parasequences. The parasequences of the upper Alapah were also slightly thicker than those in the middle Alapah.

SECTIONS MF AND MF2

Sections MF and MF2 are approximately 25 kilometers SE of EF2 (Figure 1) and are both within the Wachsmuth(?) and lower Alapah. The sections displayed light and dark banding similar to the Wachsmuth and lower Alapah in Figures 2, 11. The dark bands are chert-rich and the light bands are mostly limestone. The Kayak Shale was not identified in this field area. The MF section was terminated above 384 m because large boulders in the stream blocked access to the section. The MF2 outcrop became very recessive and rubbly and was terminated at 228 m.

The MF2 section is illustrated in Figure 12. The section overall is muddy below 120 m and coarser-grained above the covered interval at 135 m. Typical cycles below 120 m coarsen-upward from mudstone to wackestone. Few cycles are capped by packstone, grainstone, and rarely rudstone. A 10 cm thick bed of broken and jumbled solitary and colonial rugose corals occurs in a matrix of small crinoid and bryozoan fragments at 61 m. This interpreted as a small storm bed or debris. A wackestone with nodular chert exists between 61 m and 120 m. There is evidence that some of the chert, especially the nodular textured chert in the MF and MF2 sections may actually be silicified burrows (Figure 13). Above 135 m, bed thickness typically was 0.5 to 1 m. The wackestone-chert intervals were several to tens of meters thick. The bedding was typically obscured by the chert. The rudstone beds were typically 1 to 1.5 m thick.

Above 135 m, cycles coarsen-upward from mudstone or wackestone to rudstone and rarely grainstone. Chert nodules are very common in the mudstones and wackestones and rare in the grainstones and rudstones.

Section MF section is 60 m to the east of the base of the MF2 section (Figure 1). Section MF is illustrated in Figures 14 and 15. Sections MF and MF2 are very similar due to their close proximity. Each section has dark chert and light limestone bands, similar lithologies, bed thicknesses, and cherty mudstones-wackestone and crinoidal rudstone cycles. However, there are a few differences. Small cm thick normally graded beds at 18.25 m grade from a crinoid grainstone to wackestone or mudstone. Small scour surfaces between the mudstone-wackestone and grainstone were observed. These graded beds are interpreted to be storm beds. The MF section also has a thick unit of wackestone interbedded with chert. A possible fault exists in the MF section at 355 m. A calcite vein at 355 m is approximately 1 m thick and thins up and possibly down dip. The calcite vein is interpreted to be a thrust fault. The outcrop across the creek was very rubbly, but it appeared that beds were faulted at a very low angle. No obvious displacement was identified because the fault followed bedding planes.

DISCUSSION/CONCLUSIONS

Significant progress has been made on establishing the base-line stratigraphy of the Lisburne Group during the summer of 2000. Six partial sections were described in detail from the Porcupine Lake area, Philip Smith Mountains. The focus of this field season was on the Lower Lisburne. Detailed lithostratigraphic outcrop data identified several shallowing-upward cycles or parasequences section EF. These parasequences may have implications for the mechanical stratigraphy.

Several generic conclusions can be made from the sections described. First, The Lower and upper Alapah were resistant and the middle Alapah was recessive. The upper

Alapah overall is the coarsest-grained and lithologically similar to the Wahoo identified in the north (Watts, 1995). Secondly, the mudstones are typically highly fractured and the wackestones, packstones, and grainstones, and rudstones are not. The exception is a few rudstones displayed solution cleavage and were very brittle. These brittle units tended to be less than 1 m thick. Chert may affect the competency of a unit. Several cycles, especially in the Lower Lisburne, have cherty units several tens of meters thick. The coral abundance, especially colonial rugose corals, increases through the lower Alapah, reaches a maximum in the middle Alapah, and become rarer in the upper Alapah.

RESEARCH PLAN FOR PROJECT COMPLETION

Fieldwork during 2000 has permitted identification of priorities for research during the next field season. The ultimate goal of this portion of the project is to develop a stratigraphic baseline along a proximal-to-distal transect. This necessitates visiting the best-exposed outcrop sections to refine the stratigraphic data base. One priority is to revisit the well-exposed section at "Mosquito Bee Creek" in the Fourth Range to help document small-scale stratigraphic cycles and to collect gamma ray data. This section is exposed in the creek drainage and will provide some of the most continuous exposure of the Alapah in a mid-ramp paleogeographic setting. Other well-exposed sections in the Philip Smith Mountains in the north and south Porcupine Lake areas will also be examined to provide detailed stratigraphic data from the distal portion of the field area. The boundary between parautochthonous rocks of the northeastern Brooks Range and the Endicott Mountains allochthon appears to be between the north and south Porcupine Lake areas. These areas display markedly different structural styles. Documentation of the sedimentology and stratigraphy of the north Porcupine Lake area during summer 2001 will be crucial to unraveling the paleogeography and controls on deformation of the Lisburne Carbonate ramp. Analysis of subsurface core and log data is also an integral part of this study. At least two entire cores of the Lisburne Group from Prudhoe Bay will be logged in detail. Cores targeted for analysis include: L2-06, L4-15, and possibly L5-13. Core L2-06 is on loan from Philips Petroleum and additional work on that core will be completed by the end of 2001.

Most field and subsurface stratigraphic data has been drafted as stratigraphic sections and important mechanical and sequence stratigraphic subdivisions have been identified. Detailed petrographic analysis will help refine the high-resolution lithostratigraphy and aid in identification of sedimentary cycles or parasequences (Van Wagoner and others, 1988) that might influence reservoir characteristics. Identification of different phases of diagenesis will also lend insight into variations in reservoir characteristics. Petrographic analysis will be used to identify microscopic variations in lithofacies important to determining reservoir properties. X-ray diffraction will be employed to quantify the percentage of calcite and dolomite in lithologic samples collected from outcrop and core. These data, along with quantitative porosity and fracture-related data, will allow us to gauge the importance of differing patterns of dolomitization on reservoir development.

Seismic-scale outcrop and subsurface analysis will permit the identification of large-scale (tens to hundreds of meters) lithologic variations that might influence reservoir characteristics. Because the Lisburne represents a broad carbonate ramp (Gruzlovic, 1991; Watts and others, 1995), lateral facies variations may not be apparent in single outcrops or cores. Analysis of facies variations along a transect from paleogeographically proximal cores in the subsurface at Prudhoe Bay to more distal outcrop localities in the northeastern Brooks Range will help identify lithologic trends that produce lateral reservoir heterogeneities. Seismic-scale analyses in conjunction with high-resolution lithostratigraphy will also aid in the identification of larger-scale

depositional sequences, the boundaries of which may be related to subaerial exposure surfaces or other stratal discontinuities with reservoir or mechanical significance.

RECOMMENDED APPROACH FOR FUTURE SIMILAR RESEARCH

The Lisburne Group presents significant challenges to obtaining high-resolution stratigraphic data in outcrop. The lateral (along both strike and dip) of the Lisburne ramp necessitates correlation of spatially distant sections. Outcrop gamma ray profiles of well-exposed sections also appear to be a useful correlation tool although nearly continuous exposure is necessary for this tool to be used effectively. Large-scale weathering patterns that define outcrop exposure are related to the overall mechanical stratigraphy (Figs 2, 8, 10). A fruitful approach to determining overall mechanical stratigraphy involves relating sections measured in the field to outcrop photos or photomosaics (Figs. 2, 3, 7-10). Relating the weathering patterns to lithology will permit further evaluation of the lithologic controls on mechanical stratigraphy. Application of these methods to future studies in the Brooks Range and correlation of outcrop exposures with the subsurface will enhance our understanding of the geologic history of Arctic Alaska and improve our ability to predict the reservoir potential of folded and fractured carbonates.

REFERENCES

- Armstrong, A. K., and Mamet, B. L., 1975, Carboniferous biostratigraphy, northeastern Brooks Range, Arctic Alaska: U. S. Geological Survey Professional Paper 884, 29 p.
- Bowsher, A. L., and Dutro, J. T., Jr., 1957, The Paleozoic section in the Shainin Lake area, central Brooks Range, Alaska, Exploration of Naval Petroleum Reserve No. 4 and Adjacent Areas, Northern Alaska, 1944-53: Part 3, Areal Geology, U. S. Geological Survey Professional Paper 303 A, B, p. 1-39.
- Brosgé, W. P., Dutro, J. T., Mangus, M. D., and Reiser, H. N., 1962, Paleozoic sequence in eastern Brooks Range, Alaska: American Association of Petroleum Geologists Bulletin, v. 46, p. 2174-2198.
- Watts, K. F., Harris, A. G., Carlson, R. C., Eckstein, M. K. Gruzlovic, P. D., Imm, T. A., Krumhardt, A. P., Lasota, D. K., Morgan, S. K., Dumoulin, J. A., Enos, P., Goldstein, R. H., and Mamet, B. L., 1995, Analysis of reservoir heterogeneities due to shallowing-upward cycles in carbonate rocks of the Pennsylvanian Wahoo Limestone of northeastern Alaska: United States Department of Energy, final Report for 1989-1992 (DOE/BC/14471-19), Bartlesville, CA Project Office, 433 p.

Table 1

Section	Section Measured	Thickness/ Stratigraphic Interval	# Lithologic Samples
FC	Summer 2000	135 m, middle Alapah, upper Alapah	94
FW	Summer 2000	120 m, upper Alapah	108
EF	Summer 2000	99 m, middle Alapah	81
EF2	Summer 2000	319 m, Middle and upper Alapah	219
MF	Summer 2000	384 m, lower Alapah	295
MF2	Summer 2000	228 m, lower Alapah	164
TOTALS:			961

Table 1. Summary of outcrop data collected in the northeastern Brooks Range during summer 2000.

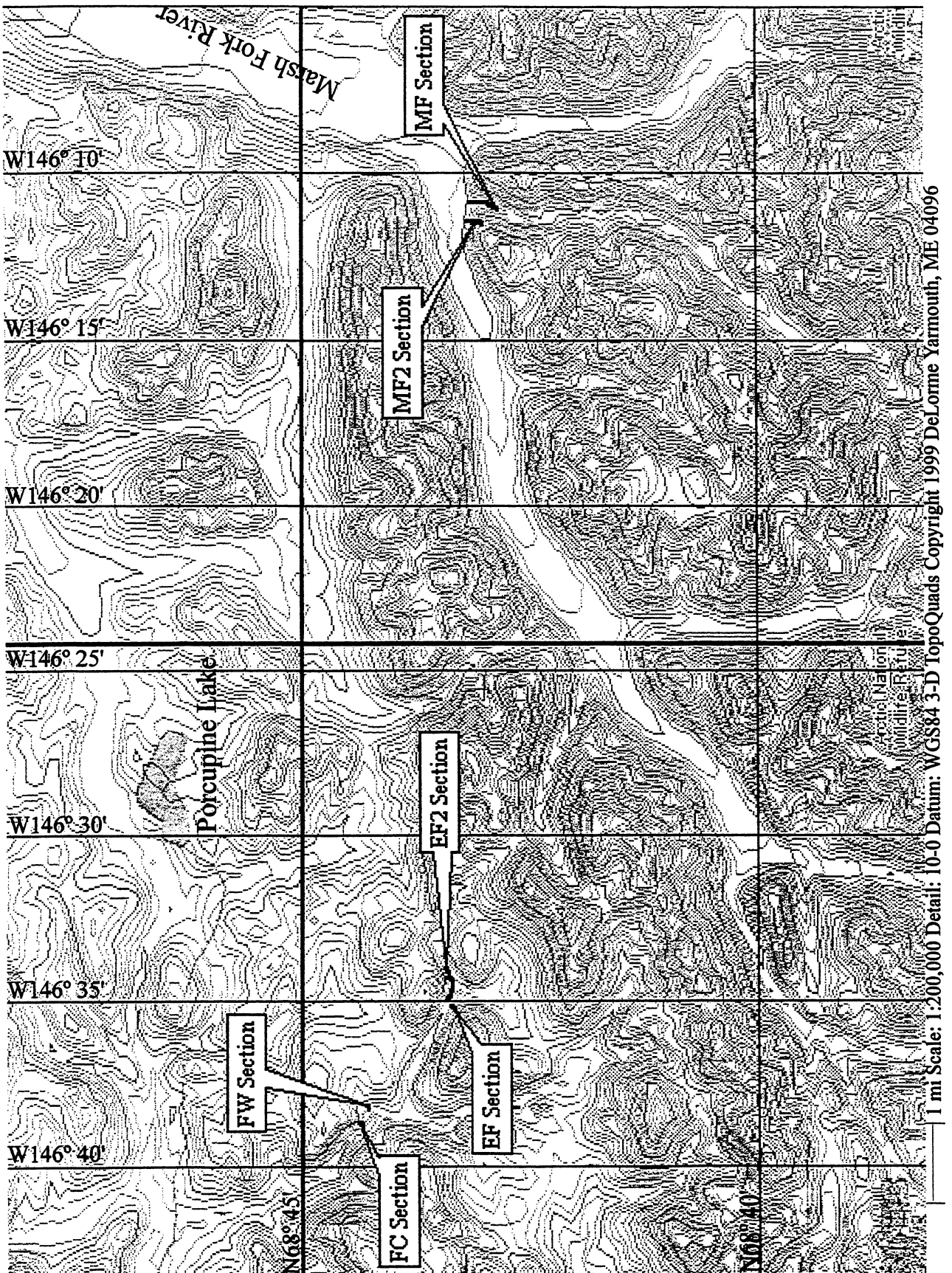


Figure 1. Map illustrating locations of stratigraphic sections.

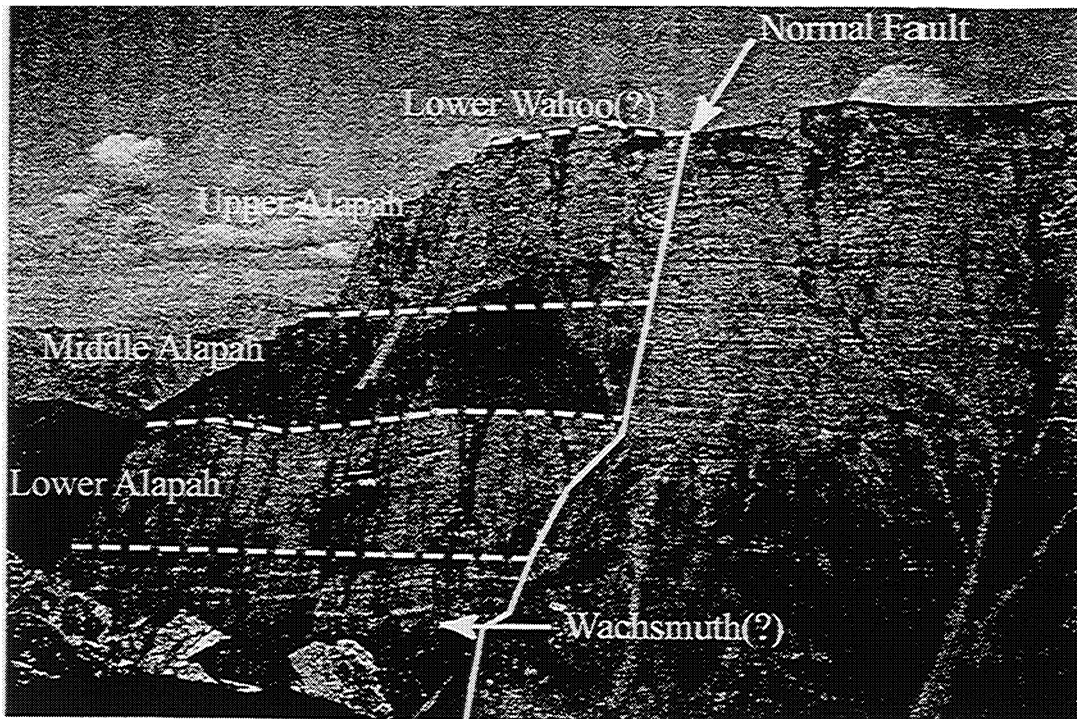


Figure 2. Generalized section through the Wachsmuth (?) and Alapah Limestone. This section was inaccessible during the 2000 field season and will possibly be examined during the 2001 field season.

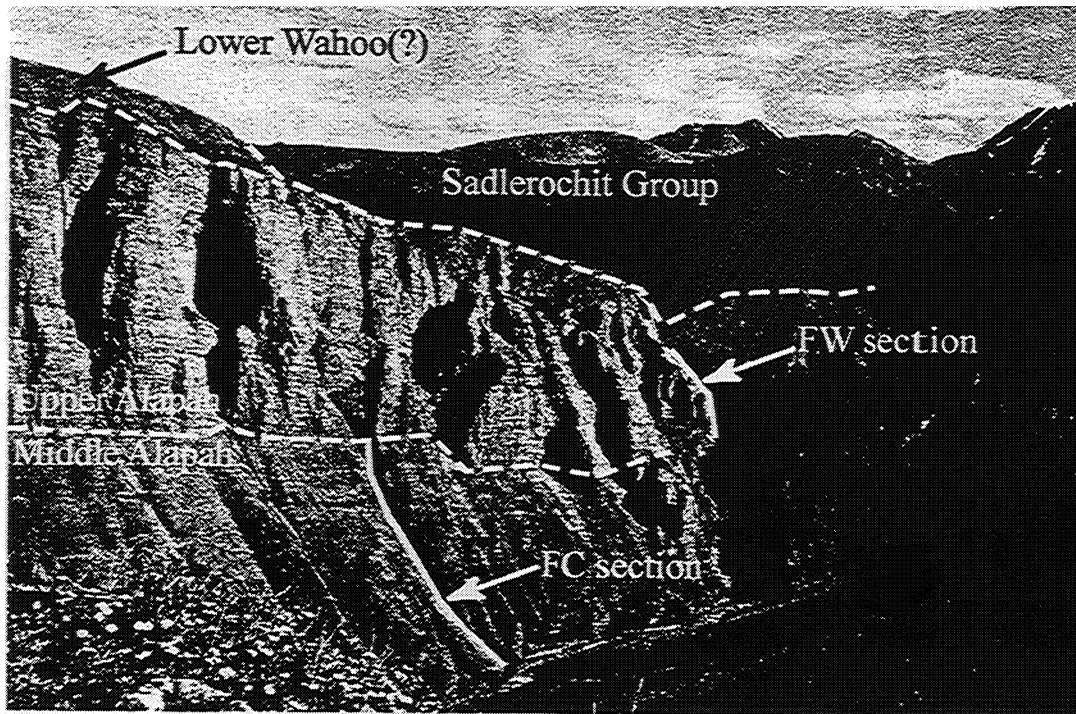


Figure 3. Illustrates the locations of sections FC and FW. Figure 2 was taken approximately 400 meters to the north (left) of this photo.

☆	Crinoids	=	Flat Laminations
γ	Branching Bryozoan	~	Wispy Laminations
	Fenestrae Bryozoan	∩	Crinkly Laminations
	Brachiopod	∧	Ripples
	Rugose Coral		Herringbone X-bed.
	Colonial Coral	∴	Graded Bed
	Gastropod	□	Breccia
	Bivalve	∞	Scour
\	Sponge Spicules	v	Vug
∩	Burrow	Δ	Sparite Zone
•	Pellets	⊙	Ooids
	Chert Nodule	p	Pyrite
	Replaced Evaporite		Stylolite
	Fenestral Fabric		Normal Fault
		┌ — ┐	Calcareous Shale

Figure 4. Key to symbols used in stratigraphic sections.

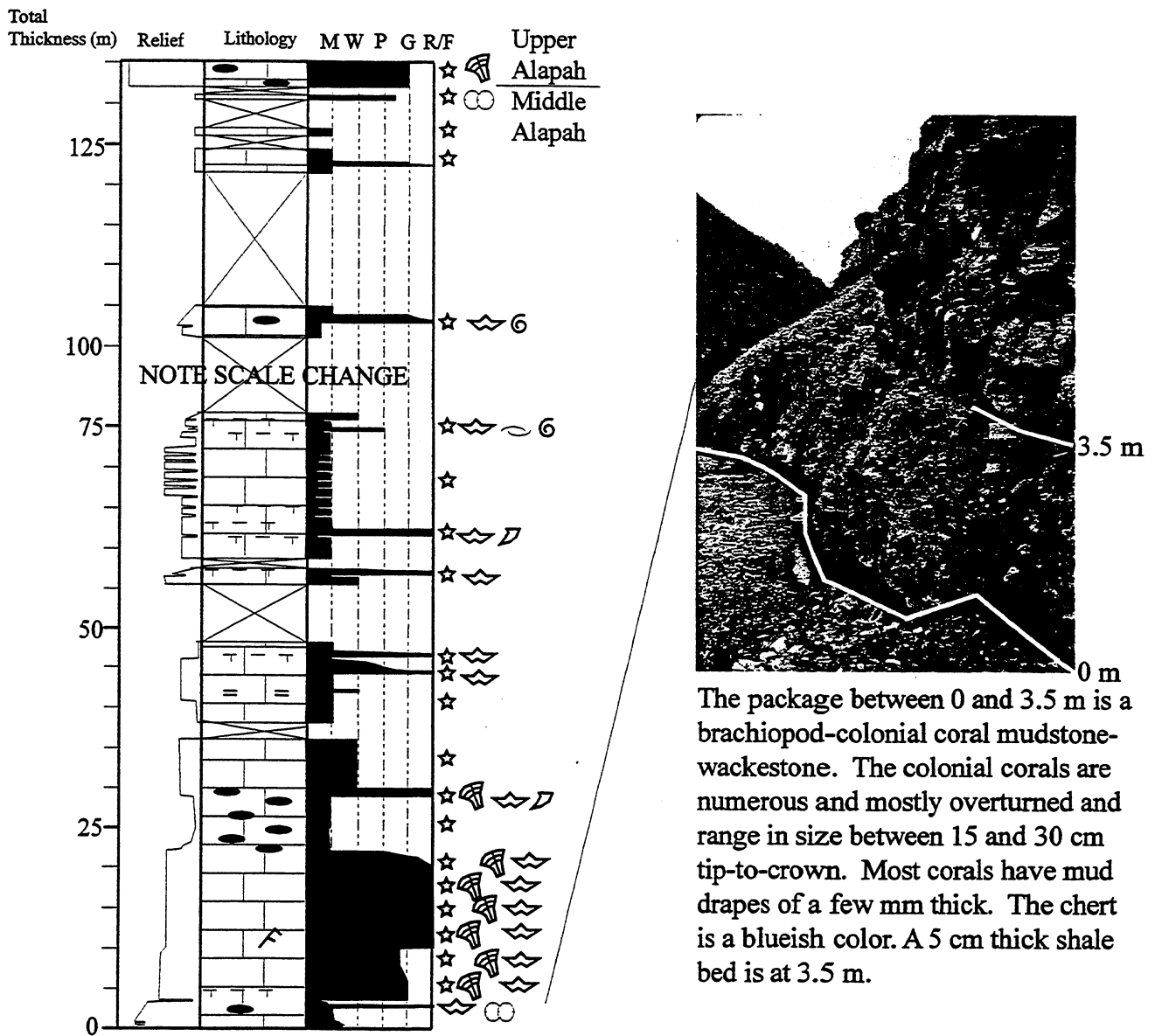
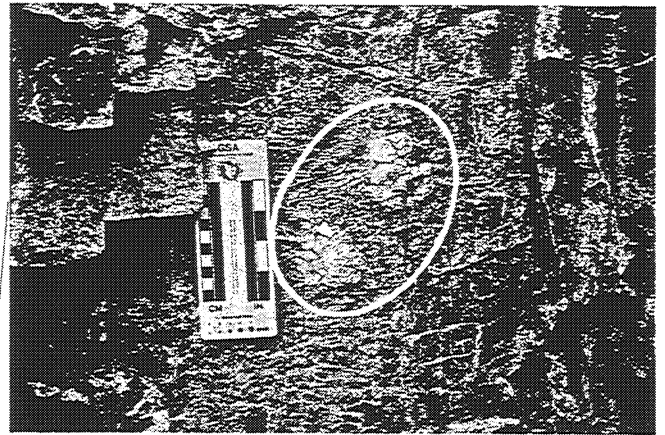
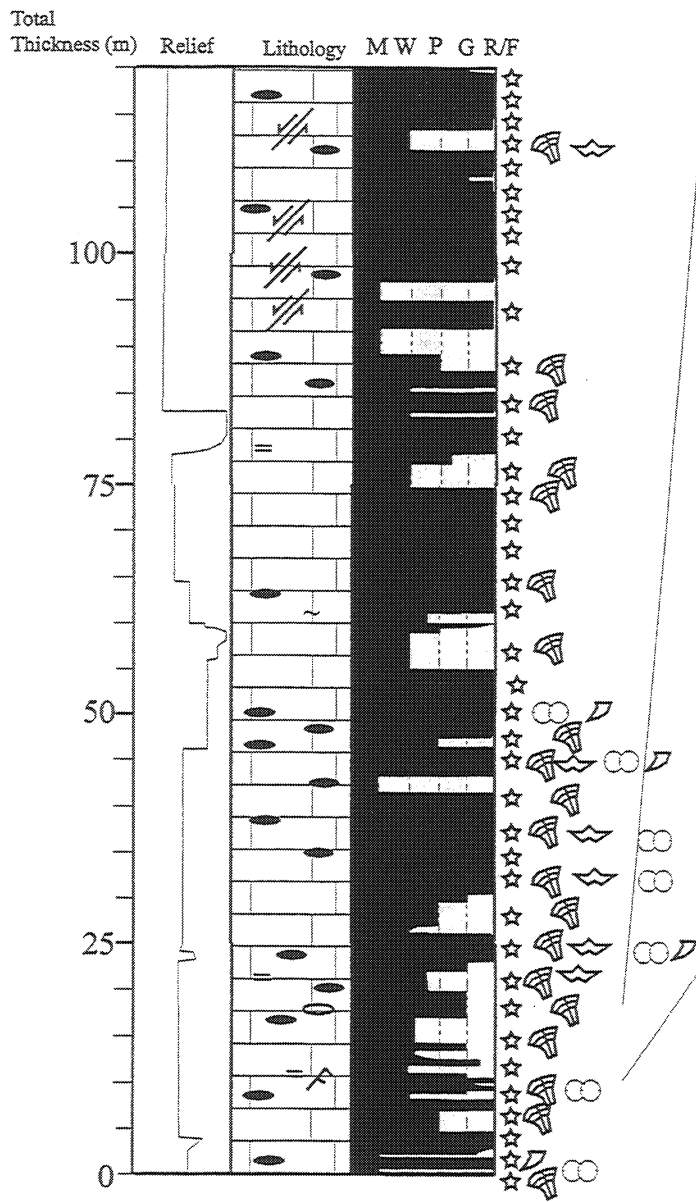
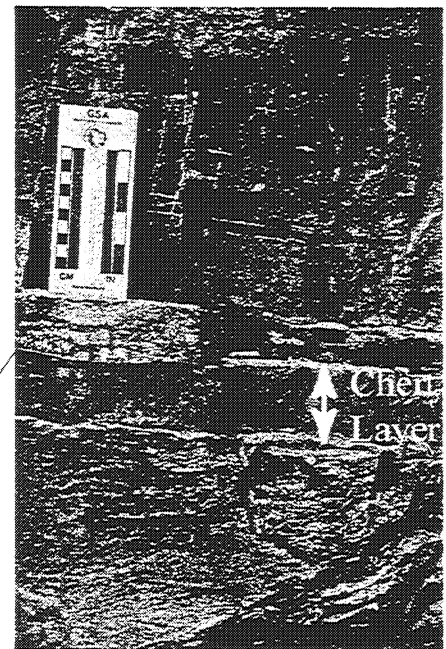


Figure 5. Measured stratigraphic section FC. Section illustrates thickness, weathering profile (relief), lithology, sedimentary and diagenetic features, and faunal elements. Middle-Upper Alapah contact at 132 m.

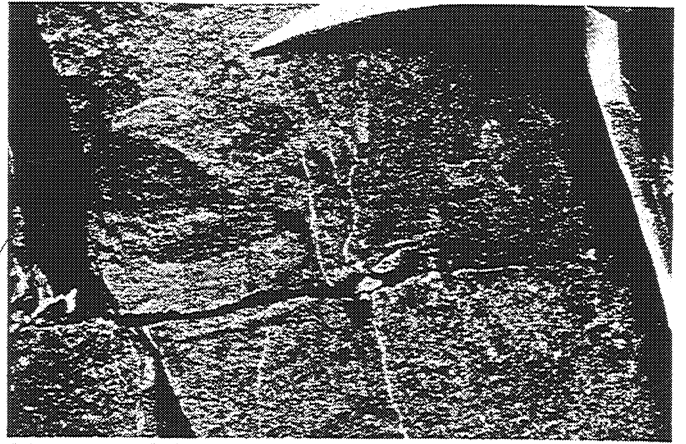
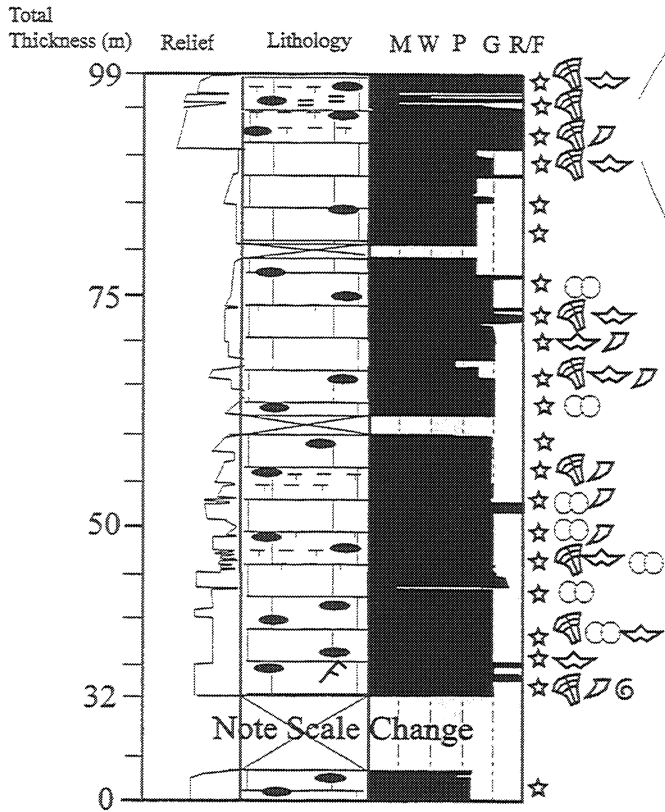


Calcite replaced evaporite nodules between 16 and 17 m.

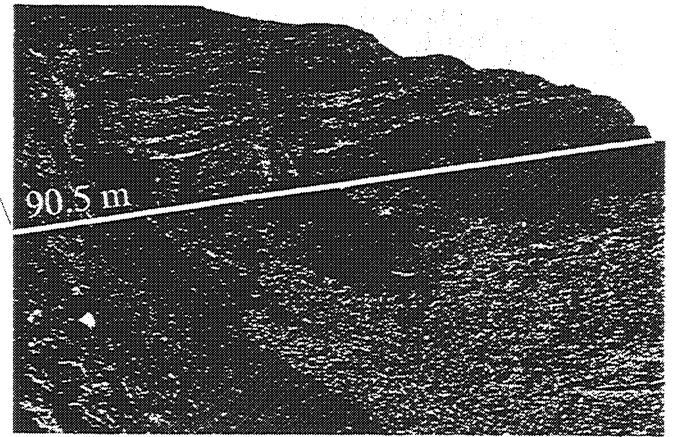


A 15 cm thick bed of planar laminations at 10.75 m. A 5 cm thick chert bed is below the laminations.

Figure 6. Measured stratigraphic section FW. Section illustrates thickness, weathering profile (relief), lithology, sedimentary and diagenetic features, and faunal elements. Section is complicated by several normal faults. Sadlerochit Group contact with Lisburne is at approximately 178 m.



Close-up of the parallel to wavy laminations in a crinoid-bryozoan-brachiopod rudstone at 96.3 m.



Major lithologic change from recessive weathering crinoid-bryozoan packstone-grainstone to a resistant crinoid-bryozoan-brachiopod rudstone at 90.5 m.



Shale drapes above and below a colonial rugose coral head (behind hammer) at 45 m.

Figure 7. Measured stratigraphic section EF. Section illustrates thickness, weathering profile (relief), lithology, sedimentary and diagenetic features, and faunal elements.

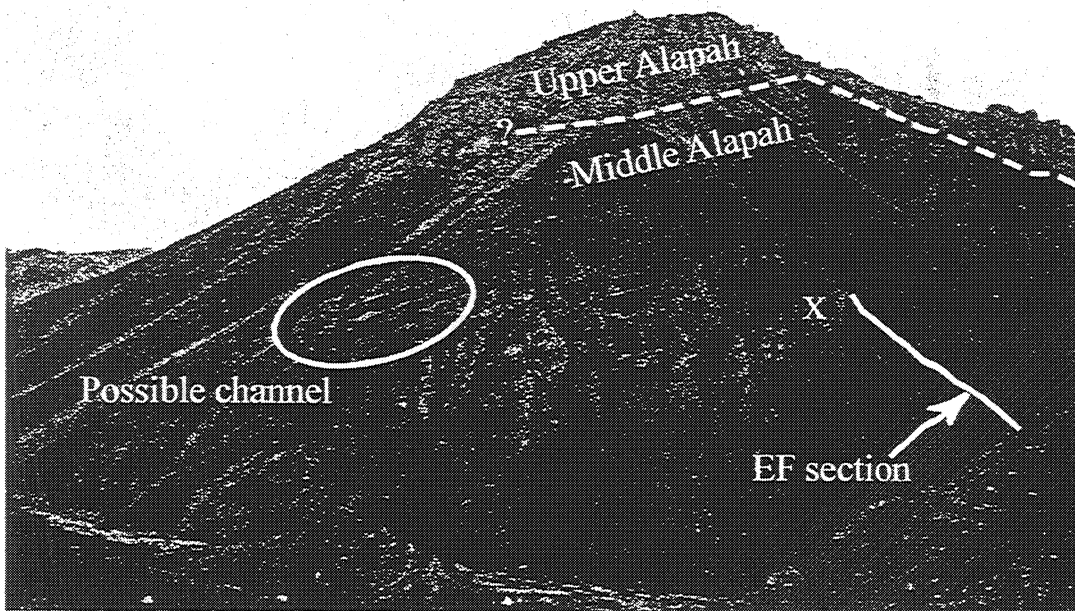


Figure 8. Photo showing location of EF section. Location of possible channel is outlined in the circle. If this is indeed a channel, there may be implications for environmental interpretations. The X indicates the approximate stratigraphic position of the base of the EF2 section.

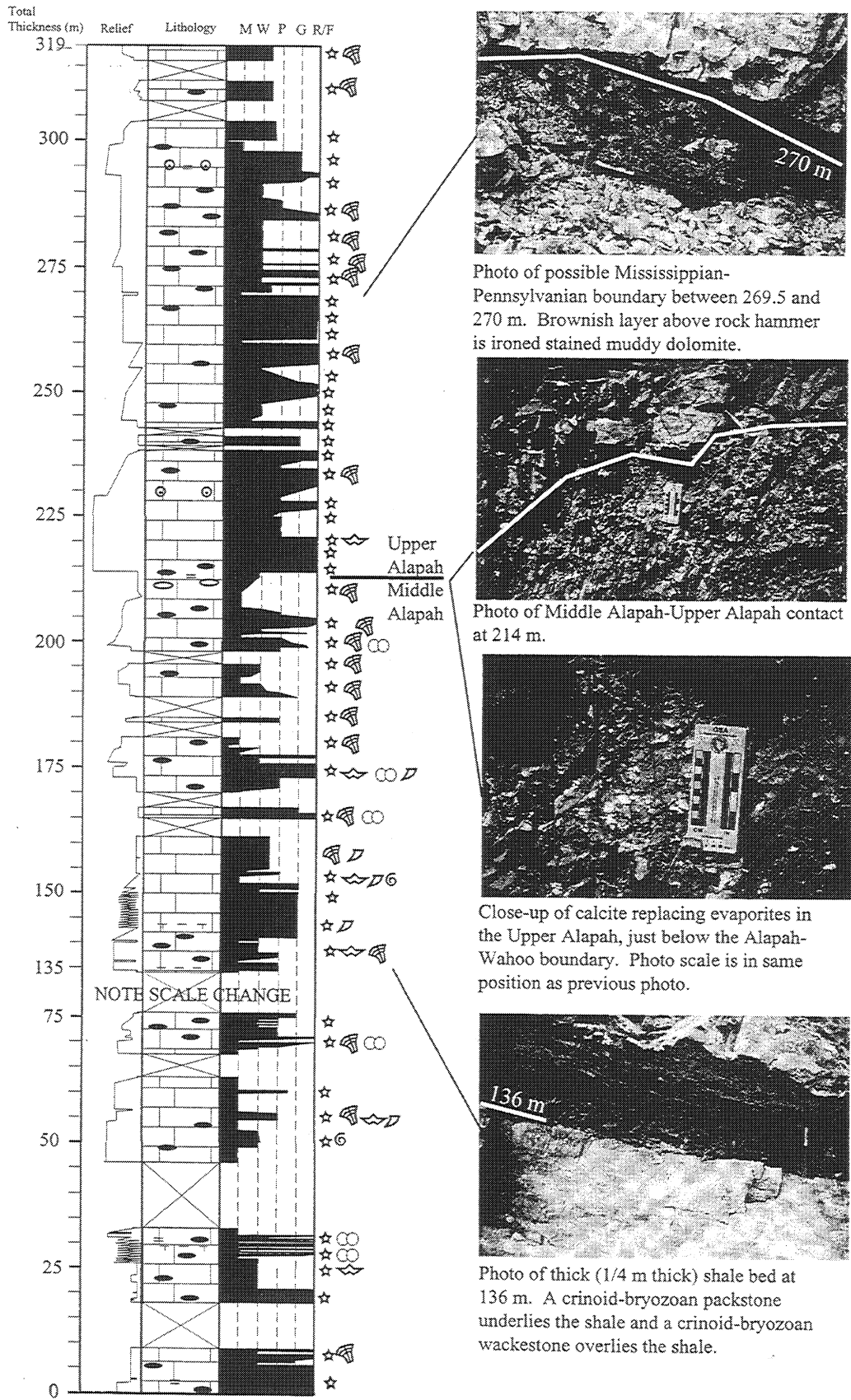


Figure 9 Measured stratigraphic section from EF2. Section illustrates thickness, weathering profile (relief), lithology, sedimentary and diagenetic features, and faunal elements. Middle-Upper Alapah-contact at 214 m.

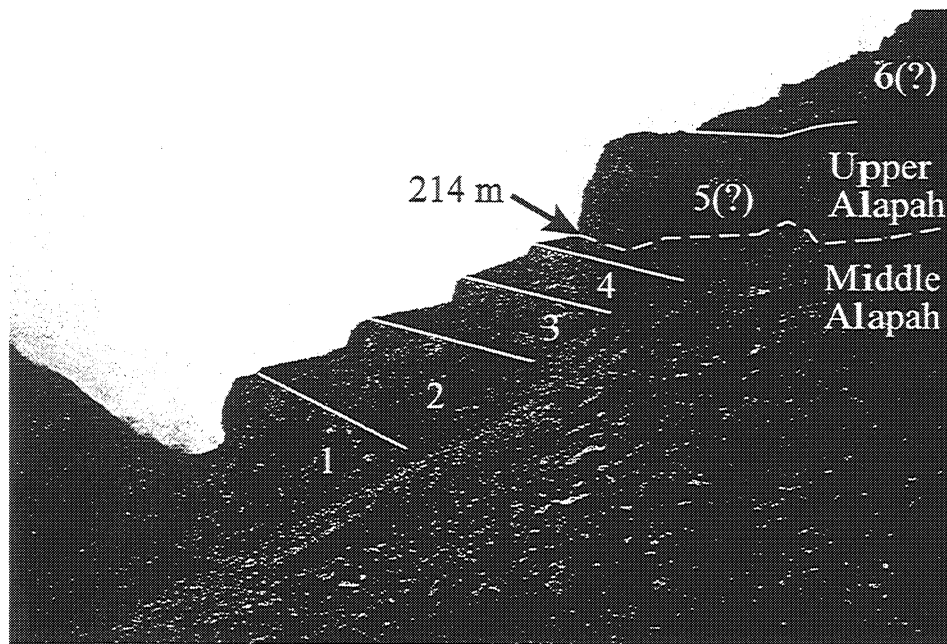


Figure 10. Photo illustrating Middle Alapah-Upper Alapah contact in EF2 section at 214 m. The Middle Alapah can be subdivided into four parasequence sets. A fifth parasequence set begins in the upper-most Middle Alapah and continues into the Upper Alapah. The Upper Alapah also contains several parasequence sets. These parasequence sets have recessive fine-grained bases and coarsen upward. Each parasequence set internally contains several 1/4 to 1/2 meter thick cycles that coarsen upward from mudstones and wackestones to packstones, grainstones, and rarely rudstones. These parasequence sets may influence the mechanical stratigraphy of the Lisburne.



Figure 11. Photo illustrates the dark and light banding in the Lower Alapah. The dark bands are chert-rich beds and the light are mostly limestone. The dark and light bands are similar to those observed in the Lower Alapah in Figure 3. Base of cliff is at 134 m in the MF2 section.

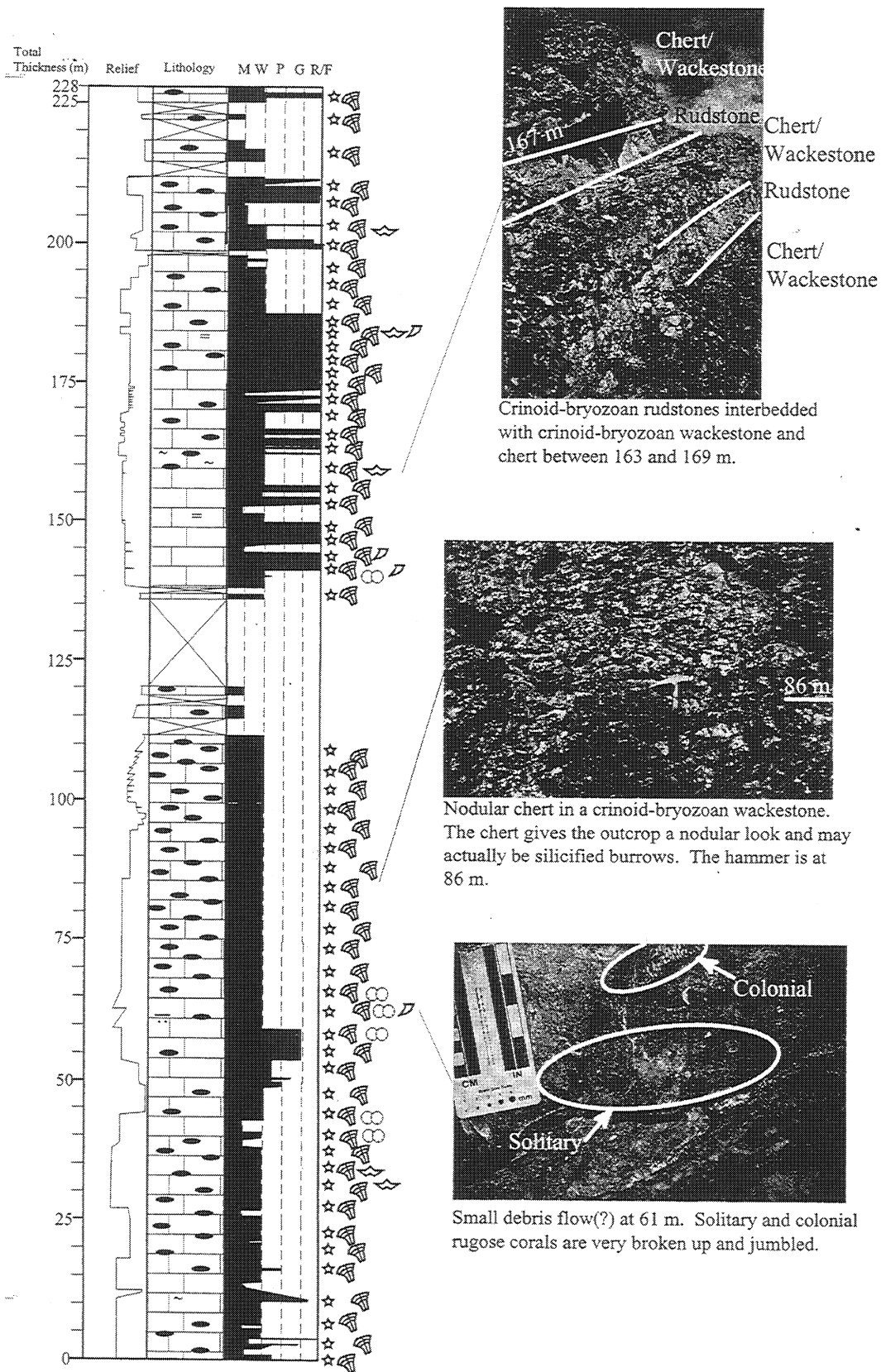


Figure 12. Measured stratigraphic section from MF2. Section illustrates thickness, weathering profile (relief), lithology, sedimentary and diagenetic features, and faunal elements.

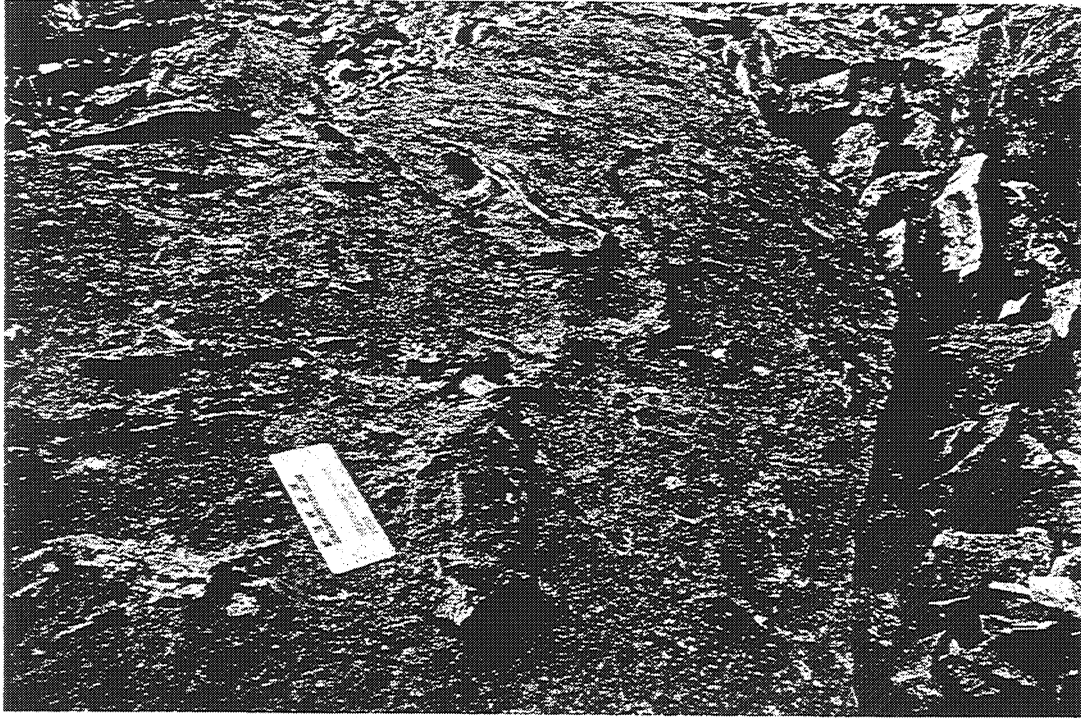


Figure 13. Silicified burrows on a large block of talus between sections MF and MF2. Approximately 10 feet to the south-west (upper left) of this photo is a block attached to the outcrop with similar structures.

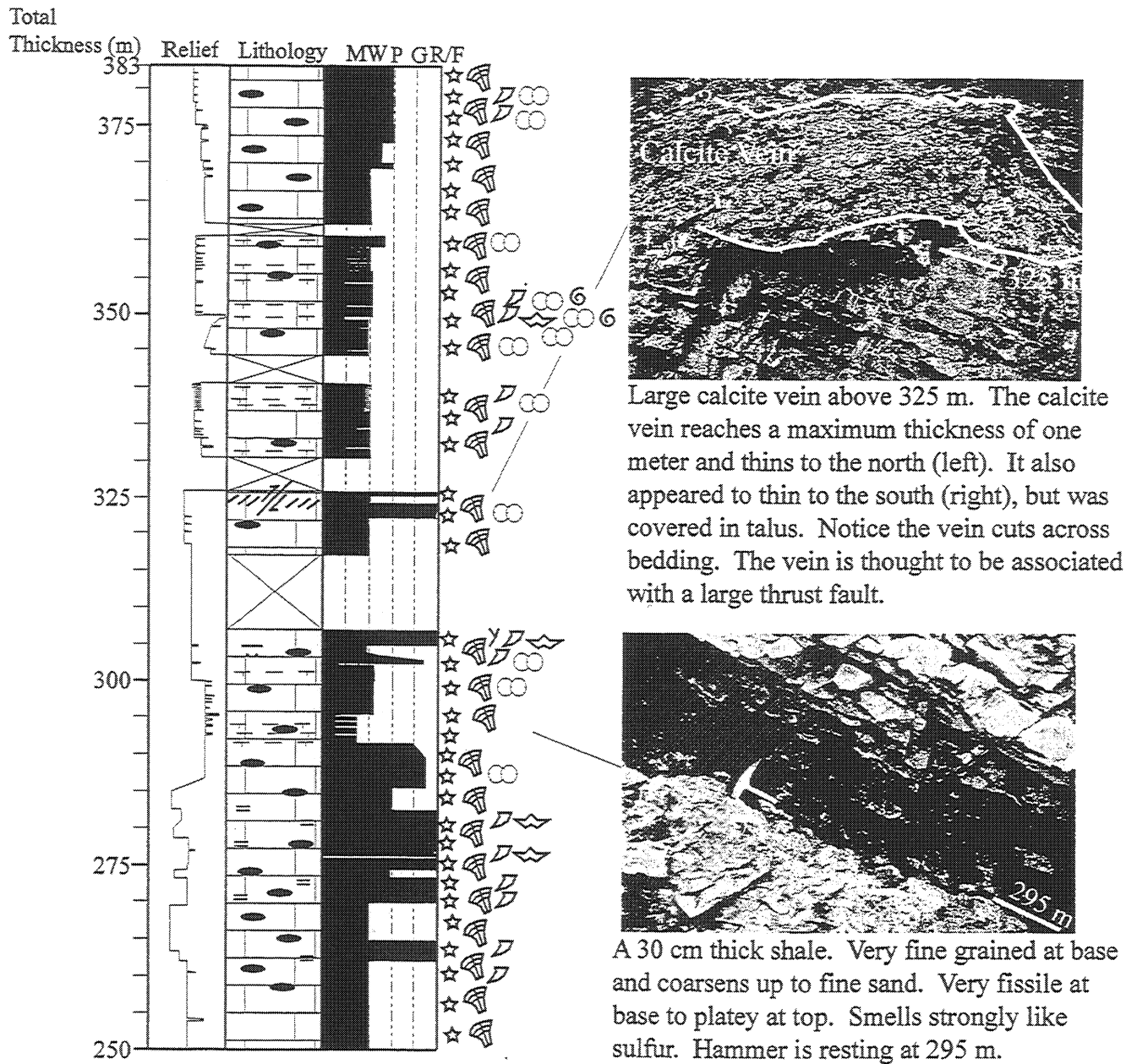
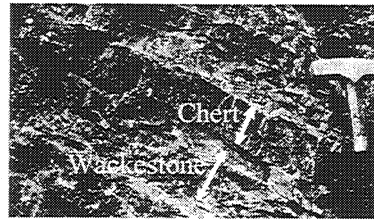
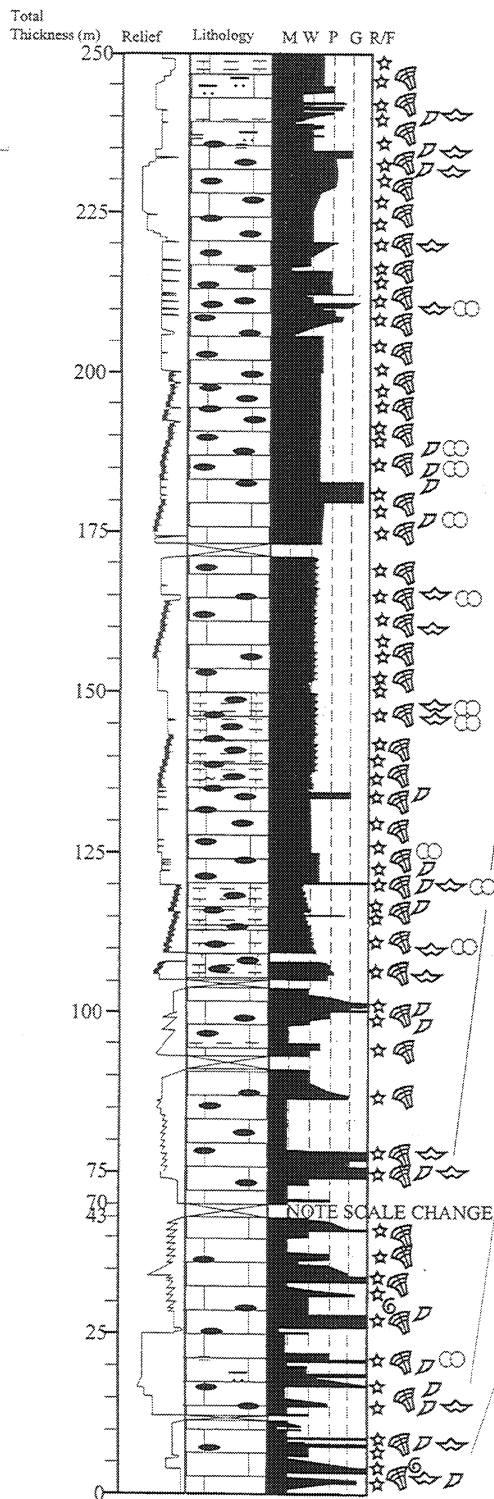
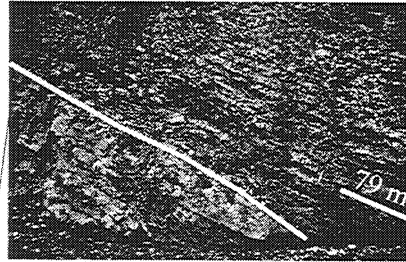


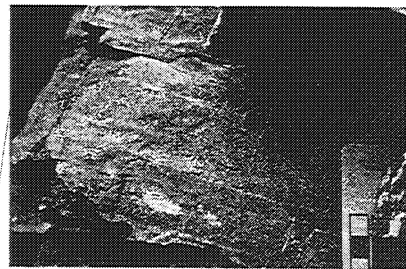
Figure 14. Measured stratigraphic section from MF2. Section illustrates thickness, weathering profile (relief), lithology, sedimentary and diagenetic features, and faunal elements.



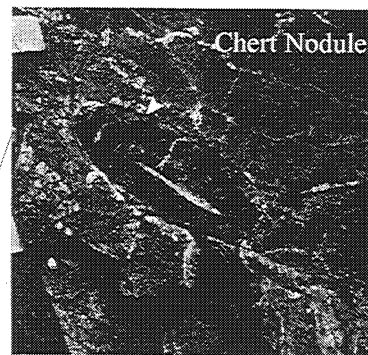
Close up of the wackestone interbedded with chert from photo below. Hammer is resting at 79 m.



Contact between a crinoidal rudstone (below line) and a wackestone interbedded with chert (above line) in section MF. Hammer is resting at 79 m.



Storm beds at 18.25 m. Each bed was approximately one centimeter thick and graded from a crinoid grainstone or rudstone to a mudstone or wackestone.



Small chert nodule that is similar to silicified burrows identified on bedding planes between sections MF and MF2 (Figure 13). Chert nodule is at 10.25 m.

Figure 15. Measured stratigraphic section from MF. Section illustrates thickness, weathering profile (relief), lithology, sedimentary and diagenetic features, and faunal elements. Remaining 133 m of section MF is illustrated in Figure 14.

Kinematic evolution of thrust-truncated folds

by M. A. Jadamec, Geophysical Institute and Department of Geology and Geophysics,
University of Alaska, Fairbanks, Alaska, 99775. ftmaj@uaf.edu

Abstract

Geometric analyses of the map-scale folds and thrust sheets in the eastern Brooks Range, south of the continental divide thrust front, suggest that asymmetric detachment folds in this region kinematically evolved into thrust-truncated folds. The three-dimensional character of the map-scale folds and faults is well constrained because of the excellent outcrop exposure and the implementation of surveying methods for the collection of data on fold geometry.

The overall structural style south of the continental divide thrust front is defined by a series of map-scale hangingwall anticlines imbricately stacked via south-dipping thrusts. More specifically, the thrust sheets strike east-northeast and dip gently to moderately towards the south-southeast. Each thrust sheet typically contains a map-scale, truncated anticline at its leading edge and consists of the Lisburne Group (limestone) and the stratigraphically overlying Sadlerochit Group (shale/sandstone). In addition, each thrust sheet includes a transition from a hangingwall flat at the base of the anticline backlimb to a hangingwall ramp near the anticline hinge. The hangingwall anticlines trend east-northeast and typically possess a parasitically folded, overturned, and truncated forelimb and a long and planar upright backlimb. Fold vergence is to the north, and the axial surfaces are inclined moderately to gently to the south. North vergent, asymmetric parasitic folds in the Lisburne Group suggest that the map-scale folds are also asymmetric, although this cannot be determined explicitly for the anticlines with the thrust-truncated forelimbs.

The hangingwall anticlines are interpreted as detachment folds that were truncated by thrust faults. The following evidence supports this hypothesis: (1) the competency contrast between the Lisburne Group (competent unit) and the stratigraphically underlying Mississippian Kayak Shale (incompetent unit) favors detachment folding, although the Kayak Shale is not exposed, (2) detachment folds composed of the Lisburne Group and Kayak Shale are prevalent to the north of the study area, and (3) both footwall synclines in the Lisburne Group as well as Kayak Shale in the cores of anticlines are exposed along strike to the east and west.

The thrust faults appear preferentially to breach the folds in the anticline forelimb and/or adjacent syncline hinge. This is indicated by the prevalence of truncated forelimbs in contrast to long, flat, relatively undeformed backlimbs. In general, the forelimbs appear to have accumulated more strain during deformation because they are either visibly truncated by thrust faults or deformed by numerous parasitic folds. The overall structural character of the truncated anticlines appears to reflect the superposition of a fault-bend-fold that formed as a result of their translation over the upper footwall flat. In addition, steeply southwest-dipping normal faults truncate the thrust sheets and associated hangingwall anticlines. The normal faults may be a consequence of late-stage extension associated with the general north-northeast shortening responsible for thrust-emplacement and fold truncation.

A different structural style occurs locally south of the range front. Here an unbroken, asymmetric anticline in the Lisburne Group contains numerous parasitic folds in the backlimb, and the axial surface dips steeply to the south. Adjacent to and north of this fold, several minor thrusts, including one that ends in a syncline, may represent the core of a fault-propagation anticline.

Introduction

The Brooks Range in northeastern Alaska contains spectacularly exposed map-scale foreland fold-and-thrust belt structures. The Carboniferous limestone units that best display these deformation features are divided into two general structural domains: (1) the symmetric, upright, east-northeast-trending detachment folded Paleozoic strata of the northeastern Brooks Range, and (2) the east-northeast-trending asymmetrically folded and thrust-faulted Paleozoic strata of the central Brooks Range. These two structural domains meet along the locally east-west trending continental divide thrust front. Field-based research was conducted just south of the thrust front in domain 2 where both asymmetric truncated and untruncated map-scale folds are exposed.

Numerous models have been proposed to quantify the geometry and kinematic development of foreland fold-and-thrust belt structures such as fault-bend, fault-propagation, and detachment folds (Suppe, 1983; Jamison, 1987; Mitra, 1990; Suppe and Medwedeff, 1990; McNaught and Mitra, 1993; Homza and Wallace, 1995, 1997; Poblet and McClay, 1996). Less emphasis has been placed, however, on the documentation and analysis of the truncation of existing folds by thrust faults. South of the Continental Divide thrust front in the eastern Brooks Range, both truncated and untruncated map-scale folds in the Lisburne Limestone were studied in order to address the question of how asymmetric detachment folds evolve into thrust-truncated folds (figures 1 & 2).

Methods

The rugged topography of the eastern Brooks Range lent itself perfectly to two distinct methods of field analyses. First, the traditional method of field mapping at 1:25,000 scale was facilitated by excellent and spatially extensive exposures. This method involved measuring the orientations of structures, sketching/photographing folds and faults, and collecting oriented hand samples. The second field method enabled the acquisition of quantitative fold and fault geometry data via the use of a T-16 theodolite and a Viper laser range finder. The T-16 theodolite measures two angles: (1) the horizontal angle from a reference line to a specified point on a distinctive bedding horizon and (2) the angle from zenith to that same point. The T-16 theodolite resolves an angle to the nearest 10 seconds. The Viper laser range finder transmits a wave to a specified point on a bed and uses the reflection of that wave to determine the distance to that specified point. The combination of the data acquired from the T-16 theodolite and Viper laser range finder yields the three-dimensional location of a particular point on a bedding horizon or fault surface. Combining the data for the many points that describe a particular fold or fault will provide a quantitative description of the three-dimensional geometry of the map-scale fold or fault.

Preliminary Results

Field Mapping

The area of detailed study, outlined in figure 1, is subdivided on the basis of the local geographic features into three sub-areas: (1) SPLV- south of Porcupine Lake valley, (2) MFS - Marsh Fork strip, and (3) UMF - upper Marsh Fork. The fieldwork in SPLV focused on traditional field mapping; the results of which are described here. In contrast, the map-scale structures in MFS and UMF were analyzed via the aforementioned surveying method, with less emphasis placed on field mapping. The character of MFS and UMF structures is described subsequently in the surveying section.

A preliminary field map depicts the key structures observed along the range front in SPLV (figure 3), namely a north-vergent anticline in the Lisburne Limestone that can be traced along strike for approximately 8 km. This anticline displays a south-dipping axial plane, a long planar south-dipping backlimb, and a parasitically folded forelimb (figure 4). Table 1 outlines the geometric properties of this frontal anticline at intervals referred to as Dr. -1N, Dr. 0N, Dr. +1N, Dr. +2N, and Dr. +3N according to the river drainage in which the fold was exposed from west to east.

To the south, a map-scale hangingwall anticline structurally overlies the long, planar backlimb of the frontal anticline (figures 3 & 5). The axial plane of the hangingwall anticline dips gently to moderately to the south; the overturned forelimb dips steeply to the south, and the relatively long and planar backlimb dips moderately to the south. The forelimb of the hangingwall anticline is cut by a thrust fault. This thrust fault that separates the hangingwall anticline from the frontal anticline dips approximately 30° to the southeast. In the footwall, the thrust fault consistently parallels bedding in the underlying Sadlerochit Group. The geometric properties of the hangingwall anticline, at intervals referred to as Dr. +2S and Dr. +3S from west to east, are listed in Table 1. In addition, three transverse normal faults, spaced approximately 1.5 km apart along the strike of the folds, appear to cut the anticlines and interlying thrust fault. The apparent displacement on these northwest-striking normal faults is southwest side down.

Surveying

Two map-scale folds in MFS and three map-scale structures in UMF were surveyed (figures 6, 7 & 8). The two map-scale anticlines in MFS are referred to as the west fold and east fold (figures 6 & 7). The west fold in MFS is interpreted as an eastward continuation along strike of the hangingwall anticline described in SPLV. The west fold is characterized by a south-dipping axial plane, a steeply south-dipping overturned forelimb that is cut by a thrust fault, and a moderately to steeply north-dipping backlimb (figure 6 and Table 1). Much of the backlimb has been eroded. Nonetheless, both limbs of this anticline are planar, with the exception of the decimeter scale curvature in the forelimb fault panel (figure 6). The east fold in MFS is characterized by a south-dipping axial plane, a long planar southeast-dipping backlimb, and a north- to overturned south-dipping forelimb that is cut by a thrust fault (figure 7 and Table 1). The hinge area of the east fold contains a prominent calcite (?) vein that is near and sub-parallel to the axial trace. The thrust fault is exposed across the entire width of the exposed anticline and lies along a hangingwall flat in the anticline backlimb and forms a hangingwall ramp forward of the anticline hinge.

The anticline-syncline-fault system in UMF differs in structural character from the other folds observed in this area. For example in UMF, the southern most anticline is nearly upright and the axial-plane dips very steeply to the south. The anticline backlimb dips moderately to the south and is parasitically folded rather than planar (figures 8A & 8B, Table 1). The adjacent syncline north of the anticline is more open than the forelimb synclines in SPLV (figures 8A & 8C). Adjacent and to the north of the syncline, several reverse splays and associated splays cut the Lisburne (figures 8A & 8C). One of the fault splays appears to tip out in the syncline in the upper Lisburne above the fault (figure 8C).

Discussion

The anticlines in SPLV, MFS, and UMF are north vergent and asymmetric. Some of these anticlines are visibly cut by thrust faults, and other anticlines may have been cut by thrust faults but lack the fault exposure. Whether or not a fault is exposed, a common pattern is displayed by the anticlines in SPLV and MFS: the anticlines contain a shortened and thickened forelimb and a relatively long and flat backlimb.

What, then, is the relationship between anticline forelimb deformation and fault break-through of anticlines? More specifically, is shortening and thickening of the forelimb a prerequisite to fault break-through? Where a thrust fault is exposed in an anticline composed of the Lisburne Group, the thrust tends to cut parallel to bedding beneath the backlimb. However, forward of the anticline hinge, the thrust fault is discordant with bedding in the Lisburne Group. Thus, the thrust fault appears to breach the fold in the anticline forelimb. Alternatively, the fault may breach the fold along an adjacent syncline hinge, however, no footwall ramps or synclines are exposed to test this possibility. Nonetheless, the region of fault breakthrough can be narrowed down to the anticline forelimb and/or the adjacent syncline hinge.

There is one notable outlier in terms of fold geometry in SPLV. The anticline named Dr. +3N in Table 1 is a nearly upright, open fold. This fold appears in the last exposure of the frontal anticline to the west of where it plunges beneath the surface (figure 3). The open character of this fold could be attributed to the mechanically competent character of the upper Lisburne Group, or more likely, to that fact that it is only the crest of a tighter structure at depth.

The occurrence of transverse normal faults with a down-to-the-southwest sense of displacement was an unexpected result. The normal faults appear to cut the hangingwall anticlines and thrust faults and thus postdate these structures. The normal faulting could have occurred as a result of the stress regime associated with fold and thrust fault formation; the folds trend to the northeast, and the normal faults strike northwest. Therefore, the normal faults may be a response to extension oriented perpendicular to the shortening that caused the fold and thrust formation. In addition, the normal faulting may have been facilitated by late extension resulting from an increase in the vertical stress component due to an increase in the load from the overlying mountain belt.

A speculative summary of deformation events is (1) folding of the Lisburne Group, via detachment (?) folding, (2) stacking of the hangingwall anticlines, via northward translation on

moderately- to gently-dipping thrust faults, and (3) extension of the mountain belt along northwest-striking normal faults.

Future Work

The immediate objectives of this research are to construct at least one balanced cross section and four scaled cross sections across the range front in the vicinity SPLV, MFS, and UMF. In addition, the field map of SPLV will be refined, and the field maps from MFS and UMF will be completed. These data will be essential in order to describe the kinematic evolution of the thrust-truncated folds. The fortunate exposures in SPLV allowed enough data to be collected so that cross sections can potentially be interlinked to provide a three-dimensional view of the structural character of this region.

Samples collected for conodont analysis are currently being processed. These analyses aim to constrain the age and maximum paleotemperature of the Lisburne Group in the MFS and UMF regions.

Processing of the surveying data will be completed. Early analyses suggest good agreement between the surveying data and the data gathered by traditional field mapping methods. The surveying data will be displayed in plan and cross-section view using RockWorks software. In addition, the surveying data will be imported into the GeoSec cross section balancing program where a three-dimensional view of the structures will be constructed.

After the geometry of the folds has been reconstructed, forward modeling will be used to further analyze the data and develop a kinematic model for the evolution truncated anticlines in the eastern Brooks Range.

During the summer of 2001, I will return to the field to complete the field mapping of the region between SPLV and MFS. In addition, I will survey the frontal anticline in SPLV. Acquisition of these data will complete the data set collected during the 2000 field season.

Two additional general questions will be explored, although they probably cannot be answered with the data currently available. The majority of the anticline forelimbs display extensive deformation, i.e., faulting and parasitic folding. Whether the relation between this style of deformation and fold truncation is a coincidence, a common effect, or a cause and effect is an important question. An additional point of interest to explore is the extent to which fold asymmetry plays a genetic role in the fault breakthrough of anticlines.

References

- Homza, T.X., and Wallace, W.K., 1995, Geometric and kinematic models for detachment folds with fixed and variable detachment depths: *Journal of Structural Geology*, v. 17, no. 4, p. 475-588.
- Homza, T.X., and Wallace, W.K., 1997, Detachment folds with fixed hinges and variable

- detachment depth, northeastern Brooks Range, Alaska: *Journal of Structural Geology*, v. 19, nos. 3-4 (special issue on fault-related folding), p. 337-354.
- Jamison, W.R., 1987, Geometric analysis of fold development in overthrust terranes: *Journal of Structural Geology*, v. 9, p. 207-219.
- McNaught, M. A., and Mitra, G., 1993, A kinematic model for the origin of footwall synclines: *Journal of Structural geology*, v. 15, n. 6, p. 805-808.
- Mitra, S., 1990, Fault-propagation folds: geometry, kinematic evolution, and hydrocarbon traps: *American Association of Petroleum Geologists Bulletin*, v. 74, p. 921-945.
- Poblet, J., and McClay, K., 1996, Geometry and kinematics of single-layer detachment folds: *American Association of Petroleum Geologists Bulletin*, v. 80, p. 1085-1109.
- Suppe, J., 1983, Geometry and kinematics of fault-bend folding: *American Journal of Science*, v. 283, p. 684-721.
- Suppe, J., and Medwedeff, D.A., 1990, Geometry and kinematics of fault-propagation folding: *Ecolgae Geologicae Helvetiae*, v. 83, p. 409-454.
- Wallace, W.K. and Homza, T., In press, Detachment folds vs. fault propagation folds, and their truncation by thrust faults: in McClay, K.R., editor, *Thrust tectonics and Petroleum Systems: American Association of Petroleum Geologists memoir*.

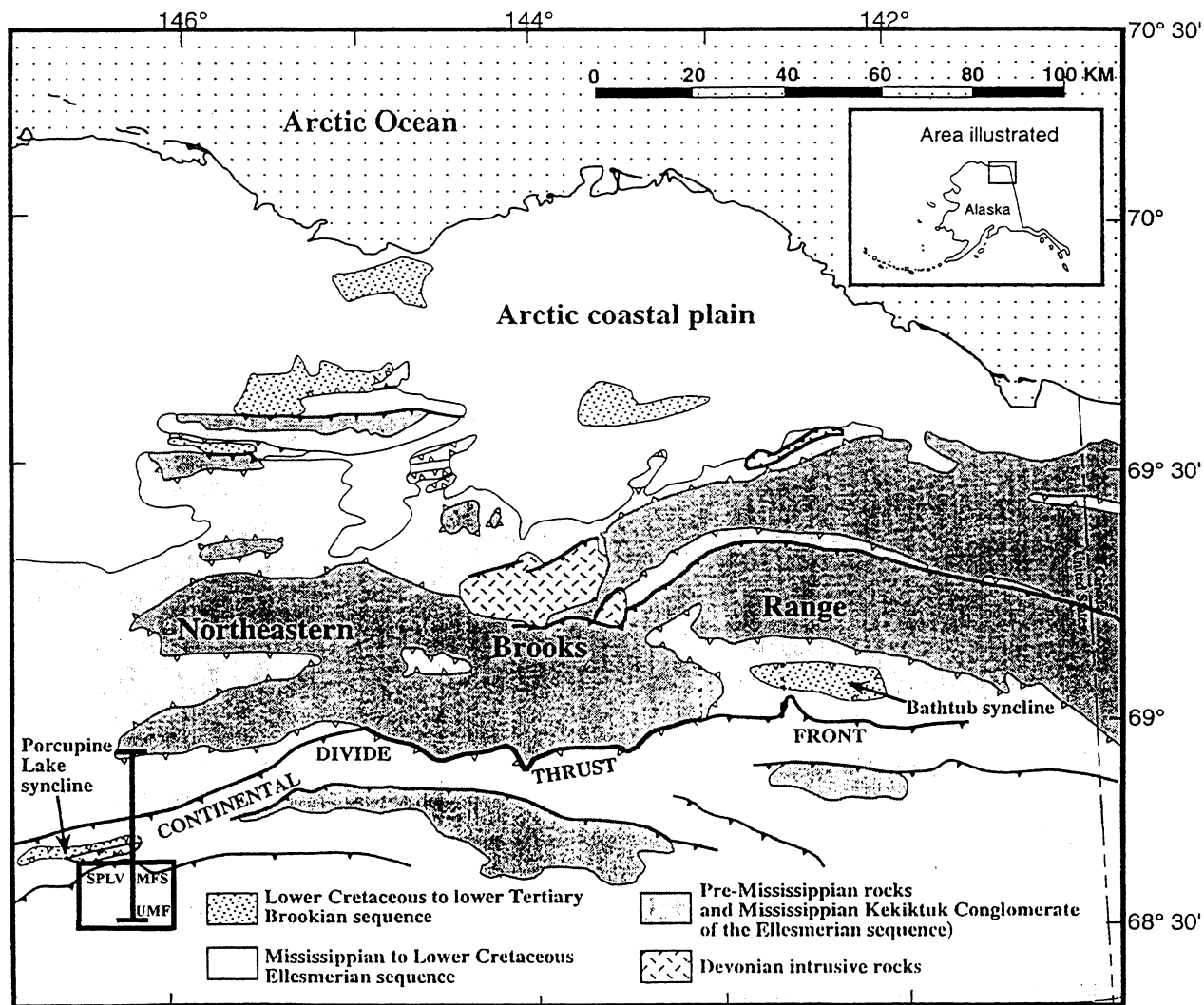


Figure 1. Map of the northeastern Brooks Range (modified from Wallace and Homza, in press, 2001). The continental divide thrust front generally separates symmetric detachment folds in the Lisburne Group to the north from thrust-truncated folds in the Lisburne Group to the south. Line in lower left depicts location of cross section (figure 2). Lower left box outlines approximate location of field areas. MFS - Marsh Fork strip; UMF- upper Marsh Fork; SPLV - south of Porcupine Lake Valley.

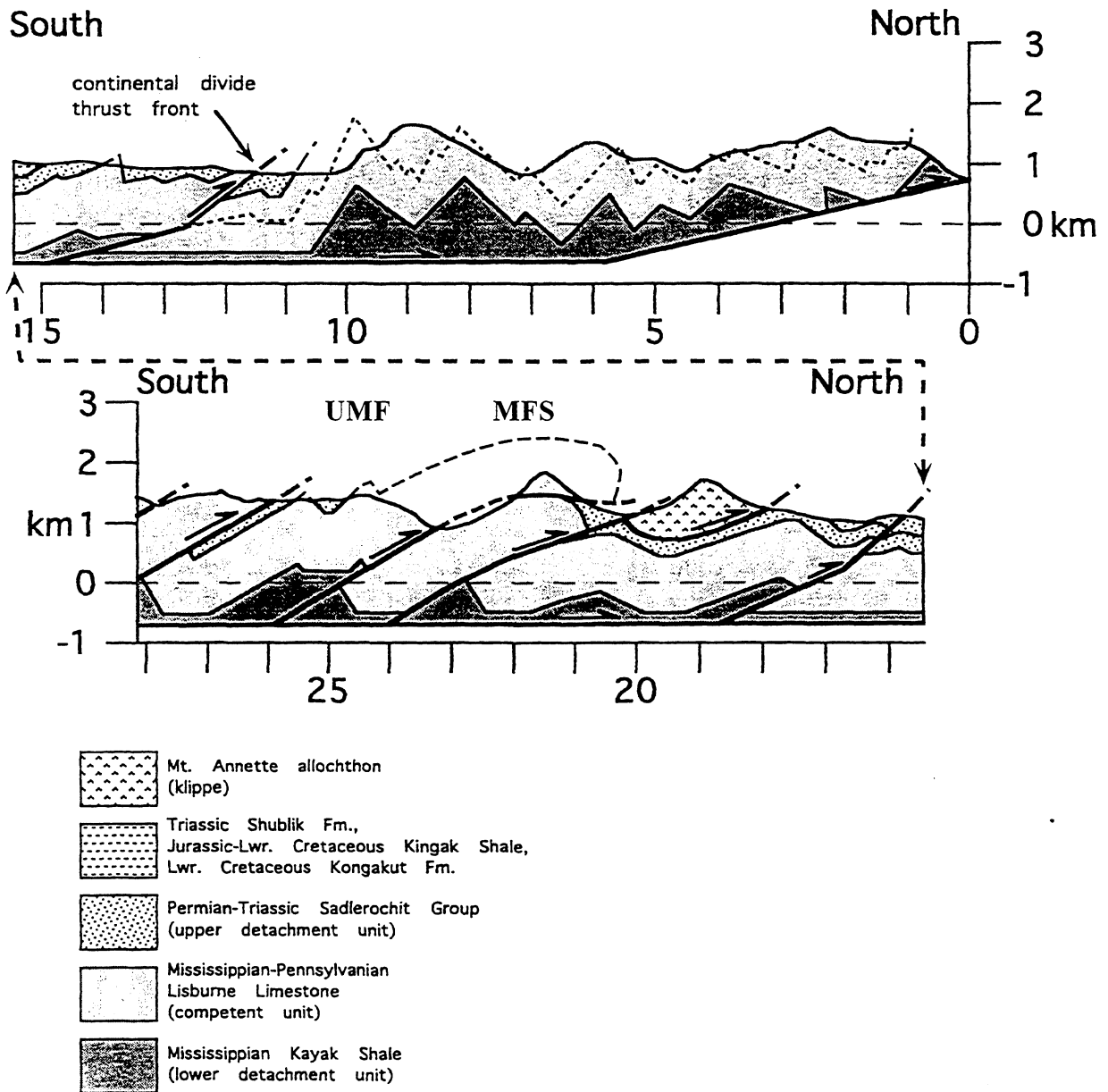
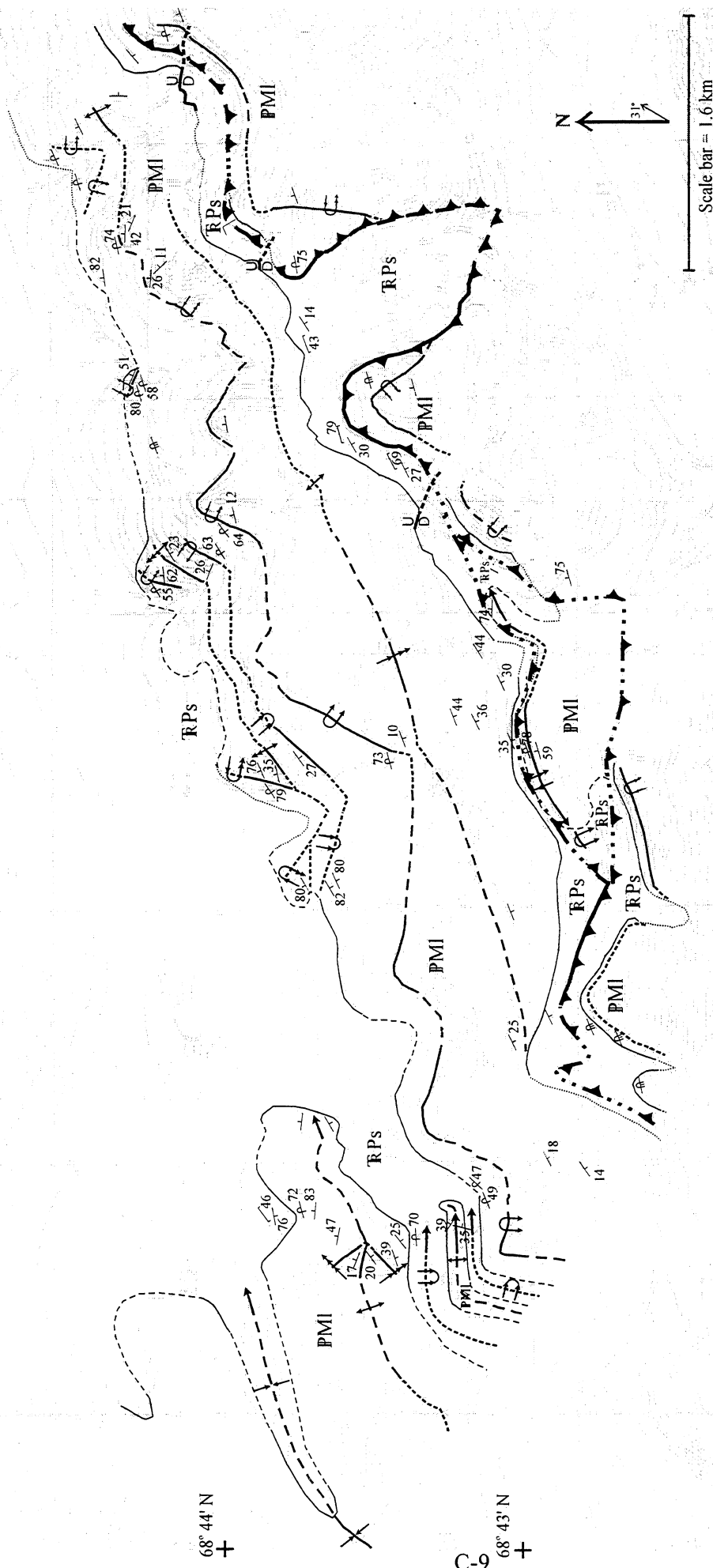


Figure 2. Scaled cross section across the continental divide thrust-front (modified from Wallace and Homza, in press, 2001). Location of cross section is shown in Figure 1. MFS denotes the Marsh Fork strip field area. UMF denotes the upper Marsh Fork field area.

146° 30' W

146° 24' W



Lithologic Units

- PMI Mississippian to Pennsylvanian Lisburne Limestone
- RPs Permian to Triassic shale/sandstone

Geologic Symbols

- 14 Strike and dip of bedding
- 78 Strike and dip of overturned bedding
- Estimated strike and dip of bedding: one, two, three dip bars indicate shallow, moderate, steep dips, respectively
- Estimated strike and dip of overturned bedding, magnitude of dip as indicated above
- 49 Strike and dip of cleavage

- Contact (solid where observed, dashed where approximated, dotted where covered)
- Axial trace and plunge of anticline (solid where observed, dashed where approximated, dotted where covered)
- Axial trace and plunge of syncline (solid where observed, dashed where approximated, dotted where covered)
- Overturned anticline
- Overturned syncline

- Overturned fold, arrows indicate dip, double arrows for steeper dip
- Anticline, double arrows for steeper dip
- Anticline, limbs dip in same direction, double arrows for steeper dip
- Normal fault, D and U for downthrown and upthrown blocks, respectively (dotted where covered)
- Thrust fault (solid where observed, dashed where covered, dotted where speculated)

Figure 3. Preliminary map of field area south of Porcupine Lake Valley, Arctic National Wildlife Refuge, Alaska. The overall structural style of this region, which is located south of the continental divide thrust front, is defined by a series of map-scale hangingwall anticlines imbricately stacked via southeast dipping thrust sheets. Topography is from Arctic C-4 and Arctic C-5 Quadrangles.

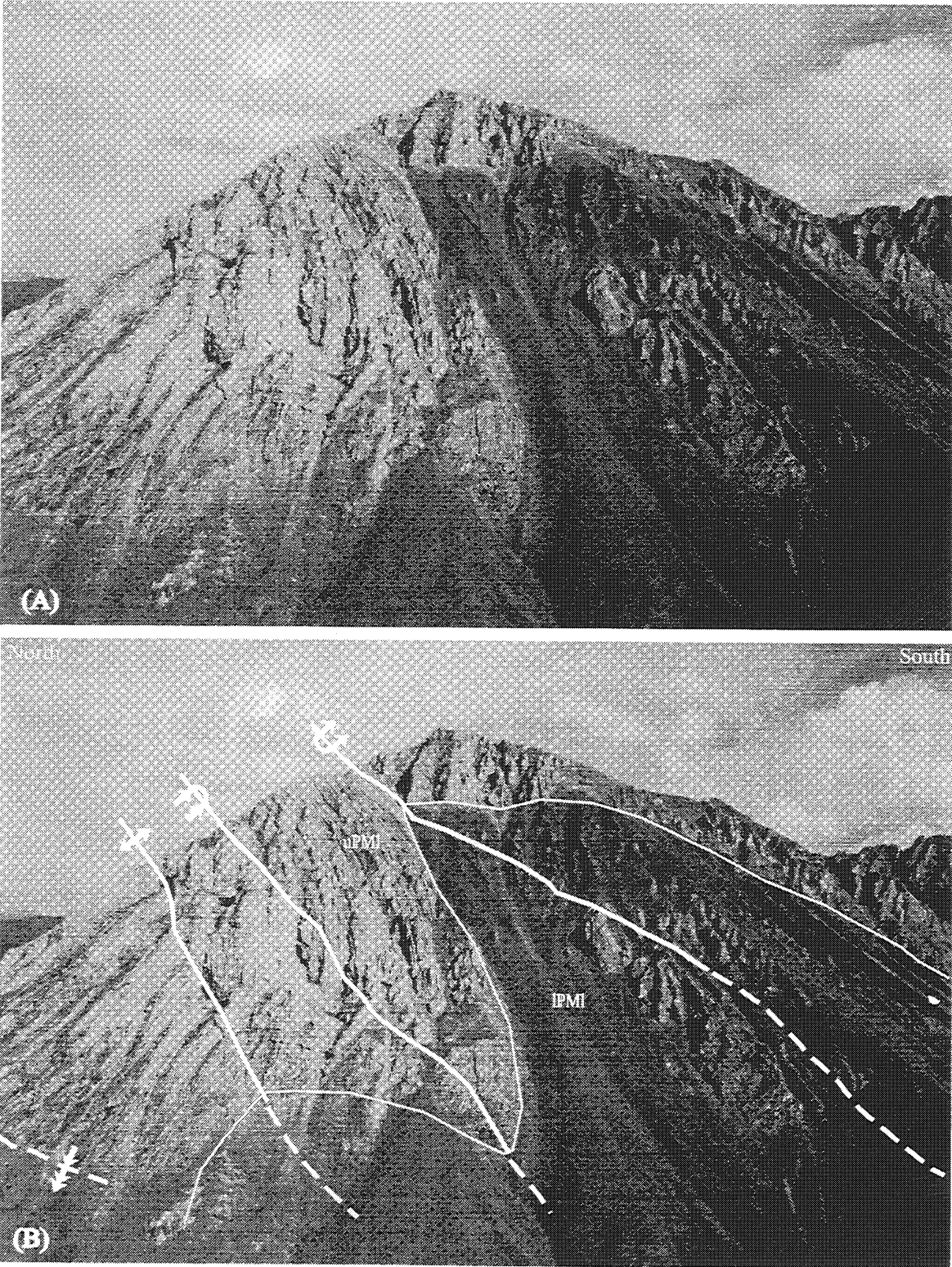


Figure 4. (A) Structural character of frontal anticline in SPLV. (B) Fold with interpretations. Thin white line divides upper and lower Lisburne. Heavy white lines: fold hinges observed; dashed: covered. Arrows toward hinge: syncline; away: anticline; with u: overturned. uPMI and IPMI: upper and lower Mississippian to Pennsylvanian Lisburne Group, respectively.

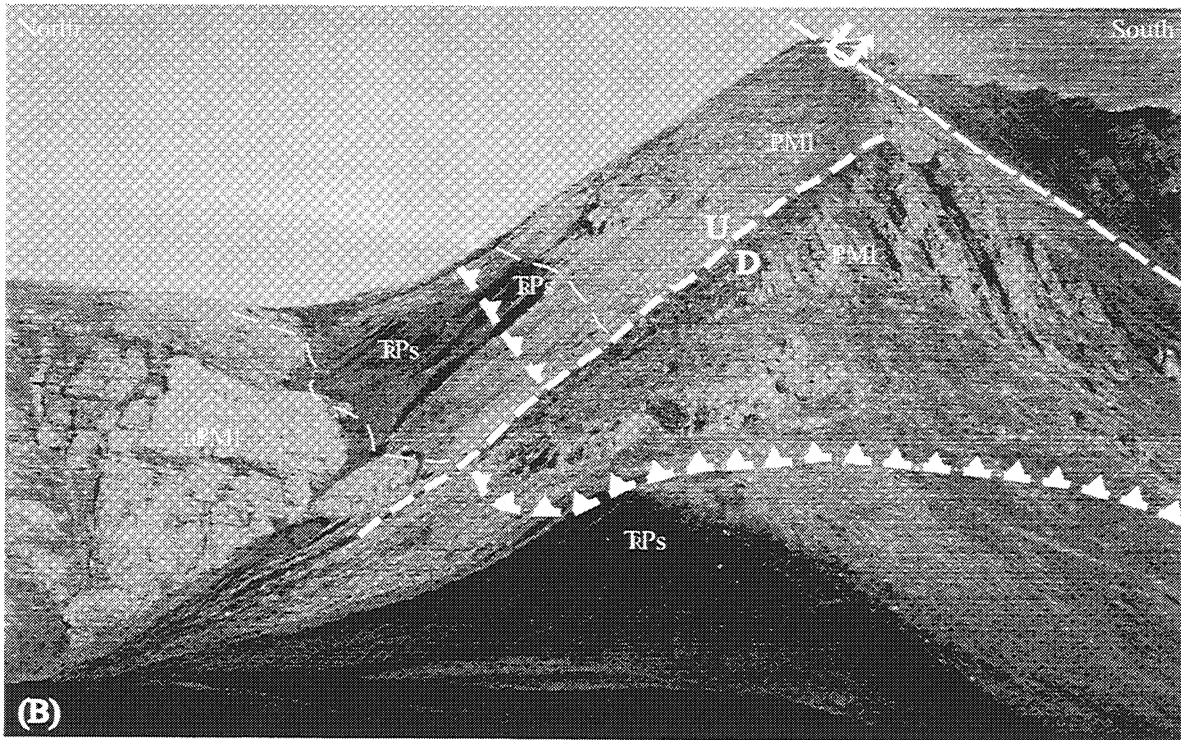
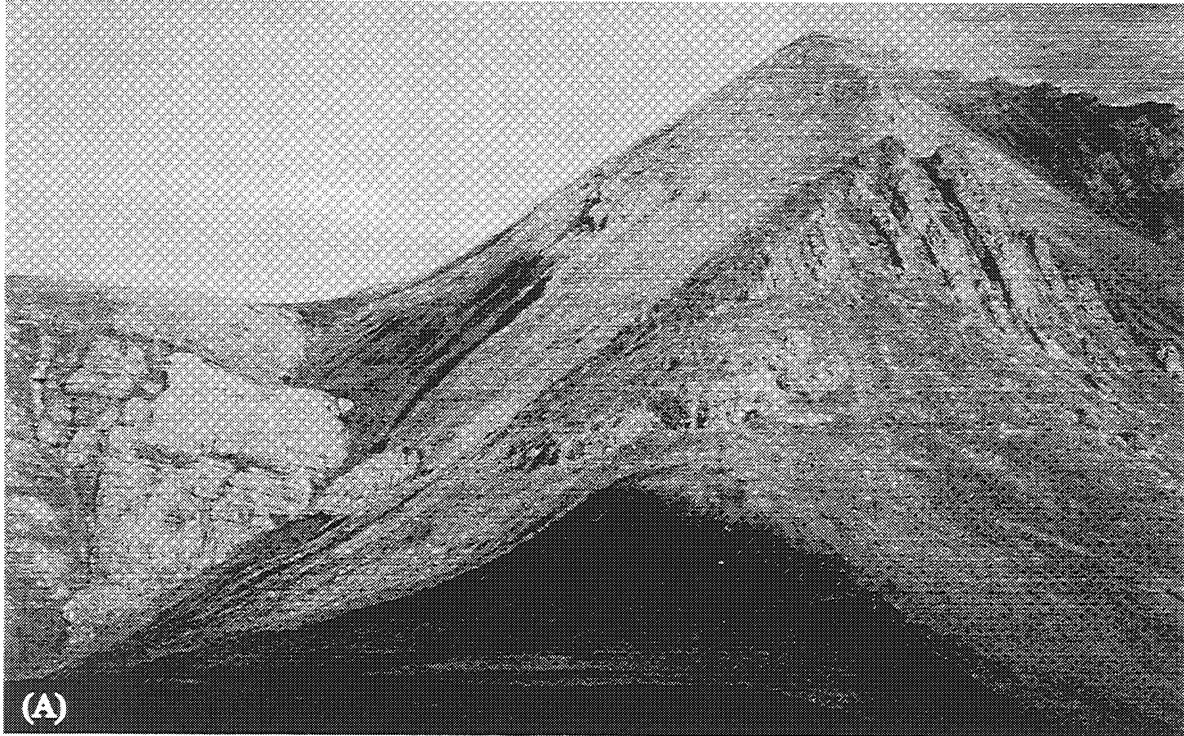


Figure 5. (A) Structural style of hangingwall anticline south of the frontal anticline in SPLV. (B) Fold with interpretations. Thin dashed lines: covered bedding contacts. Heavy dashed lines: covered structural traces; fold symbol: overturned anticline; teeth on upper plate of thrust fault; U/D: apparent displacement on normal(?) fault. PMI: Mississippian to Pennsylvanian Lisburne Group. RP's: Permian to Triassic Sadlerochit shale to sandstone.

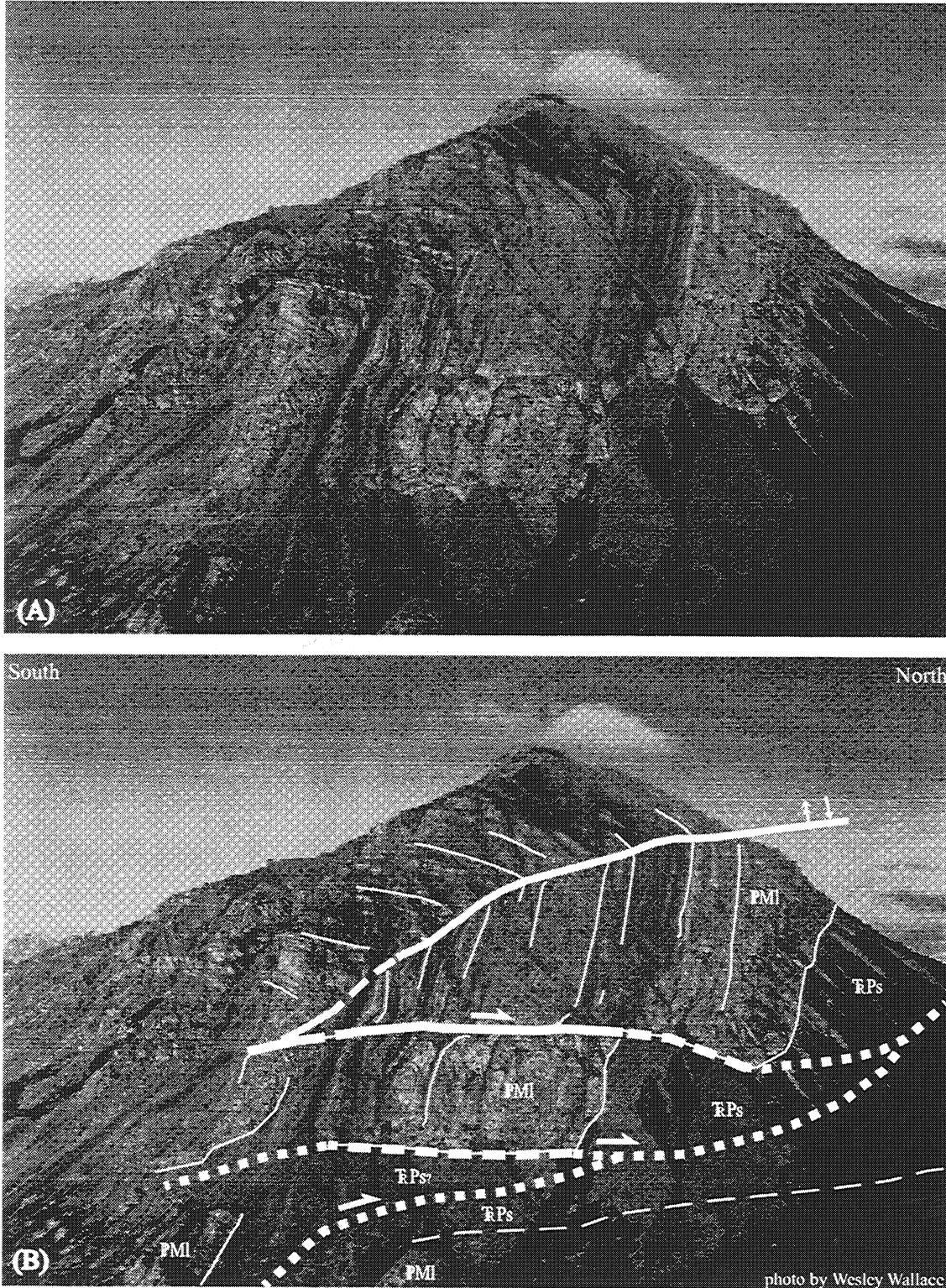


Figure 6. (A) West fold in MFS. (B) Fold with interpretations. Thin white lines: surveyed fold elements; dashed: inferred contact. Medium white lines: fold hinges observed; dashed: covered. Heavy white lines: thrust fault; dashed: covered; dotted: inferred. Fold symbol: overturned anticline. **PMI**: Mississippian to Pennsylvanian Lisburne Group. **RPs**: Permian to Triassic Sadlerochit shale to sandstone.

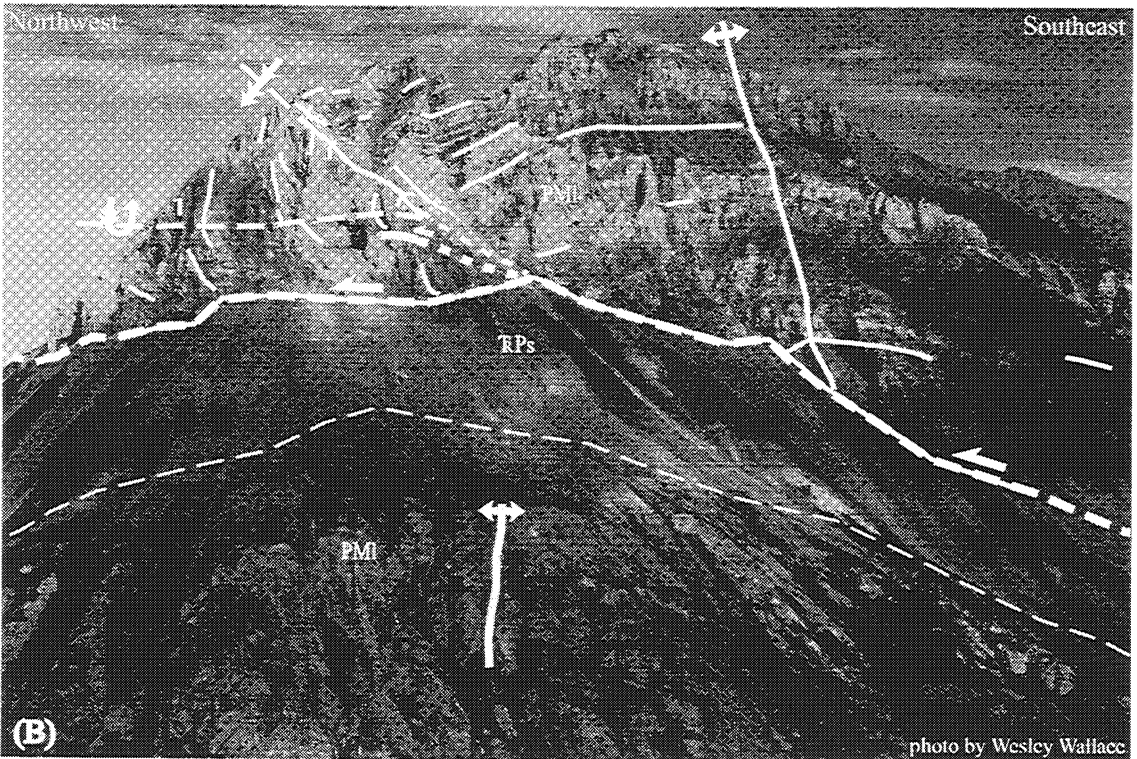
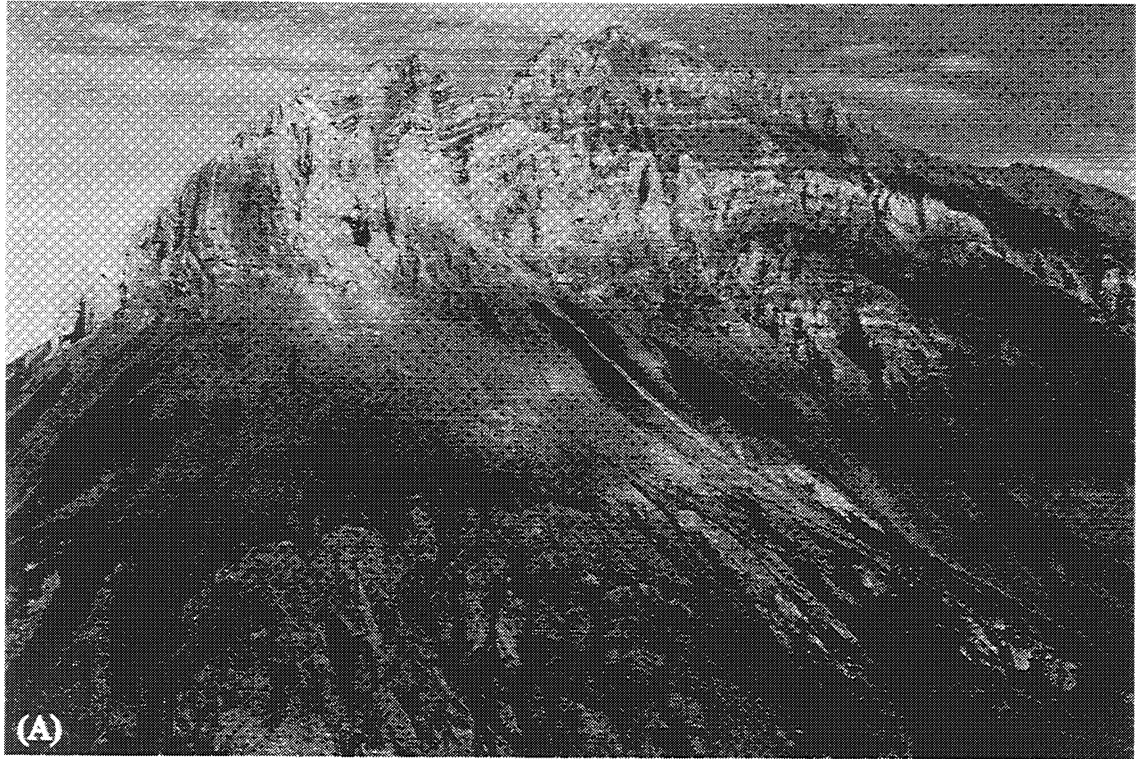


Figure 7. (A) East fold in MFS. (B) Fold with interpretations. Thin white lines: surveyed fold elements; dashed: covered contact. Medium white lines: fold hinges observed; dashed: covered. Heavy white lines: thrust fault; dashed: covered; dotted: inferred. Fold symbols with arrows away from hinge: anticline; with u: overturned anticline; double arrow: steeper limb dip. PMI: Mississippian to Pennsylvanian Lisburne Group. RPs: Permian to Triassic Sadlerochit shale to sandstone.

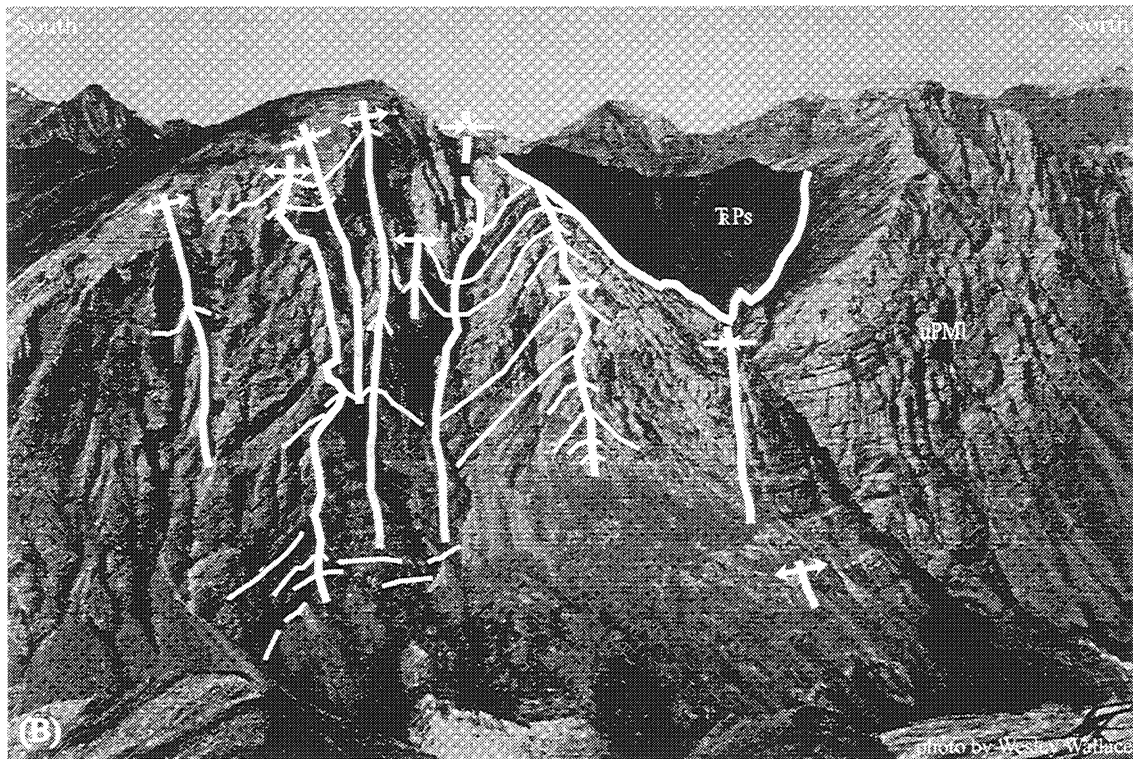


Figure 8. (A) Structures in UMF. (B) UMF anticline with interpretations. Thin white lines: surveyed fold elements. Heavy white lines: fold hinges; dashed: covered. Arrows toward hinge: syncline; away: anticline. PMI: Mississippian to Pennsylvanian Lisburne Group. RPs: Permian to Triassic Sadlerochit shale to sandstone.

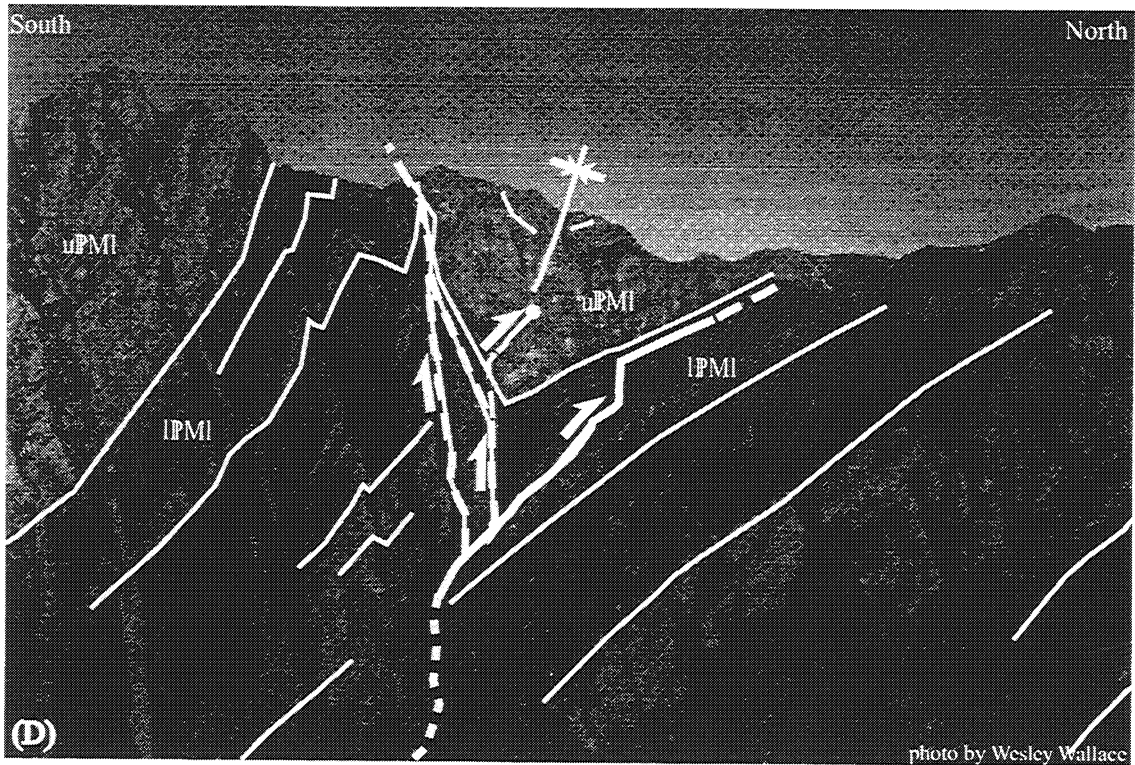
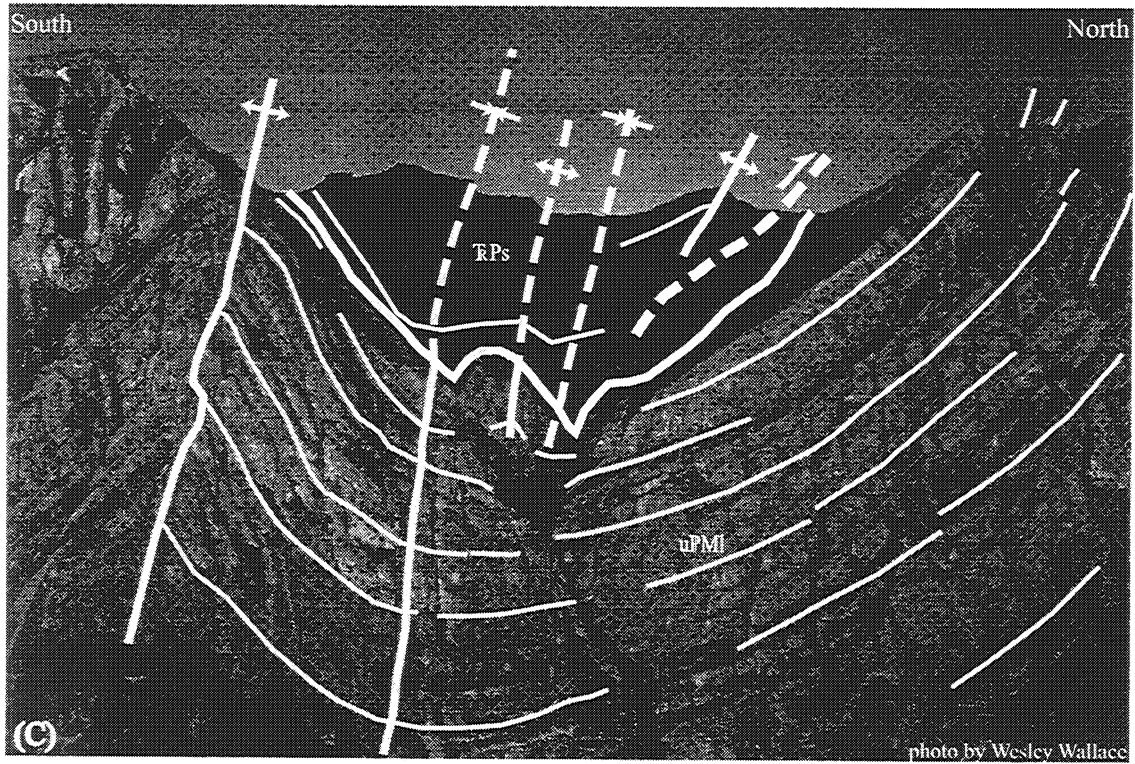


Figure 8. (C) UMF syncline. (D) UMF fault. Thin white lines: surveyed fold elements. Medium white lines: fold hinges observed; dashed: covered. Heavy white lines: thrust fault; dashed: covered; dotted: inferred. Fold symbols with arrows toward hinge: syncline; away: anticline. PMI: Mississippian to Pennsylvanian Lisburne Group. RP's: Permian to Triassic Sadlerochit shale to sandstone.

A. MFS fold properties. See figures 6 & 7 for fold illustrations.

Fold name	Interlimb angle (°)	Axial plane dip (°)	Forelimb dip (°)	Backlimb dip (°)	Minimum forelimb length (m)	Minimum backlimb length (m)	Forelimb character	Backlimb character	Distinctive properties
West anticline	~ 100	~ 20 S	~ 60 S overturned	~ 50 N	~ 270	~ 300	planar; cut by thrust faults	planar	chevron fold
East anticline	~ 95 multiple axial surfaces	~ 25 S	~ 80 NNW to overturned ~ 60 S	~ 45 SE	~ 120	~ 975	planar; cut by thrust fault	planar; few north-vergent parasitic folds (decimeter scale)	main hinge filled with calcite (?) vein

B. UMF fold properties. See figures 8A & 8B for fold illustrations.

anticline	~100 widens to ~120 downward	~ 80 S	60 NW	45 S	~ 105	~ 490	planar to gently curved; continuous into map-scale syncline to the north	contains numerous parasitic folds	folded backlimb
-----------	------------------------------------	--------	-------	------	-------	-------	--	-----------------------------------	-----------------

C-16

C. SPLV fold properties. Dr. refers to number of river drainage in which the anticline is exposed. See figures 4 & 5 for fold illustrations.

Dr. -1 N anticline	~ 40	~ 35 S	49 SE overturned	20 SE	~ 110	~ 710	planar; folds to the north may be parasitic to forelimb	planar	plunges NE ~ 20°
Dr. 0 N anticline	~ 50	39 SE	73 SE overturned	35 SE	~ 260	~ 750	contains map-scale parasitic folds	planar	
Dr. +1 N anticline	~ 40	~ 10 S	60 S overturned	12 N	~ 375	~ 475	contains map-scale parasitic folds	planar	minor faulting in forelimb
Dr. +2 N anticline	~ 4	~ 40 S	74 SE overturned	25 NE	~ 300	~ 375	contains map-scale parasitic folds	planar	
Dr. +3 N anticline	~ 150	~ 80 S	~ 45 N to overturned	~ 20 S	~ 330	~ 300	planar to gently curved	planar; cut by transverse fault	plunges NE
Dr. +2 S anticline	~ 60	~ 30 S	75 S overturned	~ 30 N	~ 90	~ 580	planar; cut by thrust fault	planar	
Dr. +3 S anticline	~ 80	~ 10 S	~ 20 S overturned	~ 30 N	~ 180	~ 375	planar; cut by thrust fault	planar	

Table 1. Preliminary summary of MFS, UMF, and SPLV fold properties. Column headings in A apply to fold properties listed in parts B and C of this table. Limb lengths are rough field estimates.

**The relationship between fracturing, asymmetric folding, and normal faulting in
Lisburne Group carbonates:
West Porcupine Lake Valley, northeastern Brooks Range, Alaska**

J.R. Shackleton, C.L. Hanks, and W.K. Wallace
Geophysical Institute and Department of Geology and Geophysics
University of Alaska Fairbanks

Abstract

The area of Porcupine Lake Valley in the northeastern Brooks Range (NEBR) is at a major structural transition between symmetric detachment folds that are characteristic of the NEBR proper, and asymmetric thrust truncated folds resembling those along the main axis of the Brooks Range. Lisburne Group carbonates in the western end of Porcupine Lake Valley are locally folded into strongly asymmetric NE striking and plunging (detachment?) folds characterized by short, steep to overturned forelimbs, and long (up to 1 km) gently dipping backlimbs. Only one thrust fault was documented in the NW end of the field area that places a long, relatively flat panel of Lisburne Group carbonates above the Sadlerochit Group. NE and NW striking normal faults with relatively small displacements cut folds in West Porcupine Lake Valley.

Four major sets of extension fractures were documented in West Porcupine Lake valley, the majority of which dip steeply between 60°-90° in both directions: 1) a N-S striking set; 2) an E-W striking set; 3) a N-S to NW striking set; and 4) a NE striking set. While the relative timing of each of these fracture sets is unclear, some generalities can be made. The NW set appears to be younger than the N-S and E-W sets. E-W fractures terminate against N-S fractures at most sample locations. However, the opposite relationship was documented elsewhere in the field area, possibly suggesting multiple generations of N-S and E-W fracturing. All three fracture sets were found in en echelon sets of extension fractures, which indicate a component of shear during formation. Shear sense on these sets was commonly normal or strike-slip, suggesting that many fractures are related to normal faulting in the area. The N-S and NW striking fractures were often found in 3-5 meter wide swarms of en echelon fractures, each swarm spaced approximately 10-20 meters apart. NE striking fractures were well developed in the lower portions of one of the major synclines in the area, although the timing of these fractures is unclear. Other major mesoscopic-scale structures indicate some period of penetrative semi-ductile deformation, including dissolution cleavage, deformed crinoid stems, sheared stylolites, and elongated and transposed chert nodules.

Normal faulting in West Porcupine Lake Valley is atypical for the NEBR, and may have influenced fracture character and distribution. Cross cutting relationships suggest that NE striking faults occurred after thrusting, whereas folds truncated by hinge sub-parallel normal faults suggest that normal faulting may have occurred during folding, or may have significantly modified fold geometries after a previous phase of compressional deformation. Changes in fold geometry were observed across NW striking normal faults, suggesting that either the normal faulting modified fold geometries, or that these faults

originated as transverse structures and developed a normal sense of shear during or after folding.

The goal of this project is to understand the relationship between fracturing, faulting and folding in West Porcupine Lake Valley. Some important questions to be addressed are: did folds in the field area form as detachment folds or fault propagation folds, and how does each of these fold models influence fracturing? Conversely, can we use fracture distribution to understand the kinematics of fold formation? Another important question is how normal faulting has affected fracturing and folding in the area, and whether or not fractures related to folding can be distinguished from those related to faulting. In order to answer these previous questions, it will be important to understand how lithology and bed thickness affect fracturing, since changes in these two variables affect fracture spacing within the stratigraphy.

Future work includes: 1) completion of data compilation and production of mechanical stratigraphic sections; 2) construction of balanced, restored cross-sections; 3) statistical analysis of fracture data in order to understand the relationship between fracture density, folding, bed thickness, and lithology; 4) integration of fracture data into a three-dimensional fold model in order to understand the relationship between fracturing and folding; and 5) detailed statistical and geometric analysis to distinguish between fractures and fracture sets related to faulting vs. folding.

Introduction

Fractures in flat lying rocks in advance of fold and thrust belts have been studied by numerous authors (eg. Hanks et al., 1997, Lorenz et al, 1991, Hancock and Engelder, 1989, Narr and Suppe, 1991, Ladeira and Price, 1981). However, few models exist for the distribution and/or character of fracturing and strain indicators in folded rocks of specific fold geometries (Hennings et al., 2000, Homza and Wallace, 1997, Stearns and Friedman, 1969, Stearns, 1968). Understanding the distribution and character of fractures in folds is important for hydrocarbon exploration because fractures may enhance certain reservoir characteristics such as porosity and permeability in certain regions of folds such as the hinges or near bed surfaces. Since there are a variety of fold geometries found in the natural world, it is important to understand the relationship between fracturing and folding for each type of fold.

This report summarizes the preliminary field results of research on Lisburne group carbonates located at a major structural transition between symmetric detachment folds that are characteristic of the northeastern Brooks Range (NEBR) proper, and asymmetric thrust truncated folds resembling those along the main axis of the Brooks Range (figure 1). The field area is structurally bounded to the NW by a large displacement thrust fault that places Lisburne Group carbonates above Sadlerochit Group siltstones and sandstones, and to the SW by range front thrusts that stack Lisburne carbonates to form duplexes in the Phillip Smith Mountains. The study area in West Porcupine Lake Valley consists of NE striking and plunging asymmetrically folded Lisburne Group carbonates with short, steep to overturned forelimbs and long backlimbs. NE and NW striking normal faults with relatively small displacements cut folds in West Porcupine Lake

Valley. The relatively subdued topography in the area provides easy access to outcrops, making the study area an excellent location for close examination of fracturing in asymmetric folds. The purpose of this research is to understand the relationship between fracturing, normal faulting and asymmetric folding in Lisburne Group carbonates in order to develop a predictive model for fracture density and distribution in asymmetric folds in the northeastern Brooks Range.

Fractures and Folds

Models for fracturing in flat-lying and folded rocks are derived from a few important experimental and field observations. A summary of one set of early rock deformation experiments is shown in figure 2A (Griggs and Handin, 1960). Stage 1 shows that at low differential stresses, mode I (extensional) fractures develop parallel to σ_1 . Lorenz et al. (1991) used the results of this laboratory experiment to explain regional extension fractures in front of an advancing mountain belt. According to this model, high pore pressures and low differential stresses created by far field compression of an advancing mountain belt create regional extension fractures perpendicular to the strike of the advancing mountain belt.

Figure 2A (stages 2-4) shows that with increasing differential stresses, shear fractures develop at an oblique orientation (usually between 30° and 60° relative to σ_1). This experimental observation is applicable in models of fracturing in folds, such as that of Stearns and Friedman (1969) (figure 2B). Most models for fracturing in folds are based on Stearns and Friedman's (1969) model, which is not only very generalized, but does not take into account fold geometry or kinematics. Since Stearns and Friedman (1969) published their model, different fold types have been recognized, necessitating further studies of fractures in various fold types. The major types of fault related folds are detachment folds (figure 3)(Jamison, 1987, Poblet and McClay, 1996, Homza and Wallace, 1997), fault propagation folds (figure 4)(Suppe and Medwedeff, 1990, Mitra, 1990), and fault-bend folds (figure 5)(Suppe, 1983). Very little detailed work has been done on fracture distributions within each type of fault related fold. Homza and Wallace (1997) showed that fractures and other strain indicators tend to be localized in the hinge regions of upright detachment folds in the Franklin Mountains, but little work has been published on fracture distributions in other types of folds. In general, it has been hypothesized that fixed hinge folding tends to localize fractures in the hinge regions (Homza and Wallace, 1997). Migrating hinge folding has been hypothesized to produce uniform fracture distributions throughout the hinges and limbs, since the limbs of a fold must pass through the hinges (Homza and Wallace, 1997). These distributions of fracture density in a fold can be strongly influenced by the kinematics of folding. Conversely, the distribution of fractures may yield clues to the kinematic history of fold formation.

Mechanical Stratigraphy and Fracture Development

The term “mechanical stratigraphy” or “mechanical layering” has been used to describe the way in which a given package of lithologically heterogeneous rocks responds to deformation (Erickson, 1996, Narr and Suppe, 1991.) A description of mechanical

stratigraphy usually takes into account 1) the rheology of each lithologic unit and how rheology changes during deformation, 2) the relative thicknesses and nature of interfaces between rock layers, 3) boundary conditions on the stratigraphic section, and 4) the scale of the deformed layers (Ramsay & Huber, 1987). Fracturing is one particular mechanical or rheological response of the stratigraphy to deformation. Understanding the mechanical stratigraphy of a package of rocks is important for studies of fracture density since laboratory experiments as well as field research have shown that there is a general relationship between fracture spacing, lithology, and bed thickness. In its simplest form, that relationship states that higher densities of fractures tend to be found in finer grained lithologies and/or in thinner beds (Hanks, et al, 1997, Narr and Suppe, 1991, Hancock and Engelder, 1989, Ladeira and Price, 1981). Therefore, in order to study the distribution of fracture density throughout a given fold, one must have an understanding of both the mechanical stratigraphy and the distribution of fracturing within that stratigraphy.

Geologic Setting

The Brooks Range is the northernmost part of the Rocky Mountain fold-and-thrust belt. The majority of shortening in the fold-and-thrust belt occurred in Late Jurassic to Early Cretaceous time when a wide, south-facing late Paleozoic to early Mesozoic passive continental margin collapsed in response to the collision of an intra-oceanic arc (Mayfield and others, 1988; Moore and others, 1994). The Colville basin formed in advance of, and was filled with sediment shed from, the growing fold-and-thrust belt (Mull, 1985; Bird and Molenaar, 1992). Shortly after the main phase of compressional collapse of the continental margin, rifting led to the eventual formation of the Canada basin to the north (present geographic coordinates) in Early Cretaceous time (Grantz and May, 1983; Moore and others, 1994). Post-collisional contraction in the Brooks Range increases eastward along strike and has resulted in progradation of fold-and-thrust deformation northward toward, and locally across, the Barrow arch and the Cretaceous rifted margin (figure 1, Grantz and others, 1990).

The stratigraphy of the northeastern Brooks Range consists of three major depositional sequences (figure 6). The Franklinian basement sequence is Proterozoic to middle-Devonian in age and consists of weakly metamorphosed sedimentary and volcanic rocks that were eroded prior to deposition of the Ellsmerian sequence. The Ellsmerian sequence is a Mississippian to Lower Cretaceous sequence of marine clastics, carbonates, and shales deposited on a south facing passive continental margin. The uppermost sequence in the northeastern Brooks Range is the Brookian sequence, a Cretaceous to Cenozoic sequence which consists of sediments derived from the early forming Brooks Range to the south (Wallace and Hanks, 1990). The structural style of the main axis of the Brooks Range is characterized by north vergent, thrust-truncated asymmetric folds, duplexes and allochthons that were shortened by hundreds of kilometers during the Middle Jurassic to Early Cretaceous (Wallace and Hanks, 1990). The northeastern Brooks Range, however, is characterized by a passive roof duplex that has been shortened by less than 100 kilometers (Wallace and Hanks, 1990).

This research focuses on folds within the Carboniferous Lisburne Carbonate Group of the Ellsmerian sequence in the Phillip Smith Mountains near an important structural transition between the Franklin Mountains and the Phillip Smith Mountains. The structural style of the Franklin Mountains Domain is characteristic of the structural style of the northeastern Brooks Range, consisting of upright detachment folded Lisburne Limestone and younger rocks that developed above the roof of a passive roof duplex cored by sub-Mississippian basement horses (figures 7 & 8) (Wallace and Hanks, 1990). The Phillip Smith Mountains Domain lies directly south of the Franklin Mountains Domain and the continental divide thrust front. The Phillip Smith Mountains domain has a structural style more characteristic of the main axis of the Brooks Range, and consists of asymmetric, north vergent, thrust-truncated folds that have been interpreted as thrust-truncated detachment folds (Wallace, 1993).

Lisburne Group Stratigraphy

The stratigraphy of the Lisburne Group has been well studied both in the subsurface on the north slope of Alaska and in the front ranges of the northeastern Brooks Range (Watts, et al., 1995, Krumhardt, et al., 1996). An unconformity truncates the uppermost Lisburne Group, which is overlain by the Sadlerochit Group, a clastic unit of variable composition ranging from quartz sandstone to shales and siltstones (figure 9). Previous studies have grouped the Lisburne into two separate units: the Wahoo Limestone, which is a cliff forming unit consisting primarily of grainstones and packstones, and the Alapah Limestone, which is generally more recessive and consists of a variety of carbonate lithologies. The lower contact of the Lisburne Group with the Kayak shale is often gradational and sometimes contains a discontinuous layer of sandy limestone (figure 9).

Methodology

This project was broken down into five major tasks:

- 1) Construct a 1:25,000 scale map of the chosen field area in order to document the fold geometries and sequence of deformation that may have affected fracture development. This includes detailed photographic documentation and sketches of fold geometries in order to produce balanced cross-sections of the field area, as well as to locate fracture sample locations relative to hinges and limbs of each fold.
- 2) Characterization of fracture patterns within a relatively undeformed section of Lisburne Group carbonates in order to understand the “background” fracture patterns and the relationship between fracturing, lithology and bed thickness. Since the chosen field area contained asymmetric folds with long, flat backlimbs, these backlimbs could be used to examine a relatively undeformed section of Lisburne.
- 3) Characterization of the fractures in a variety of folds with various interlimb angles in order to understand the relationship between fracturing and folding. Due to exposure limitations in the field area, a single stratigraphic horizon was sampled in detail throughout a fold. This method normalizes the effects of bed thickness and lithology on fracturing, and is aimed at understanding the relationship between fracturing and folding for a single bed.

- 4) Qualitatively define the mechanical stratigraphy of the Lisburne Group carbonates in the area.
- 5) Characterization of fracturing within the entire mechanical stratigraphic section in order to compare fracture patterns in folded and relatively unfolded Lisburne group carbonates. Synclines tended to be better exposed in the area, and were therefore preferentially sampled.

Measurement and description of fractures followed three major strategies: detailed fracture sampling, generalized characterization of fracturing, and surveys of fractures within the stratigraphic section. Each of these methods is described below.

- 1) Detailed fracture sampling. This method of sampling was employed both along a single stratigraphic horizon (as described in #3 above) and for selected representative lithologies in the mechanical sections (as described in #4 above). The following information was collected about the outcrop itself:
 - a. location (on map, within the stratigraphy, and on a photograph of each fold)
 - b. type of outcrop (pavement or cross-section)
 - c. collection of oriented samples of representative lithologies for thin section identification of lithology and/or strain analysis
 - d. photograph/sketch of relevant aspects of the outcrop
 - e. lithology
 - f. bed thickness
 - g. nature of contacts between layers
 - h. major diagenetic features (presence/shape of cherts, dolomitization, etc.)
 - i. orientation/characteristics of strain indicators

After the characteristics of the outcrop were examined, characteristics of each fracture set were recorded. A measuring tape was placed along each fracture set and the orientation of the measuring tape was recorded in order to determine the true spacing of each fracture. Where it was possible, the measuring tape was placed orthogonal to the fracture set to record the true spacing directly. The following information was recorded at each fracture:

- a. orientation of fractures
- b. spacing between fractures
- c. aperture (size of the opening of the fracture)
- d. fill (any mineral fillings of the aperture such as calcite)
- e. height perpendicular to bedding
- f. width parallel to bedding
- g. terminations (how the fracture interacts with bed surfaces or other fractures)
- h. mode (type of fracture: extensional or shear) where observable

Where possible, 25 fractures in each set were measured in order to obtain statistically significant sample at outcrop. In addition, any en echelon sets were noted along with their direction of shear. Conjugate sets were noted when

observed. Other features that were often recorded were timing relationships between fractures, slickenlines and slickensides, dissolution cleavages, strained fossils, folded veins, and sheared stylolites.

- 2) Generalized fracture sampling. This method was very similar to the detailed method of sampling in that all of the aspects of the outcrop were recorded, but the detailed characteristics of each fracture set (spacing, aperture, fill, etc.) were not measured. Instead, the orientations of the major fracture sets were recorded, as well as any additional features such as slickenlines and slickensides, dissolution cleavages, strained fossils, etc. were recorded.
- 3) Surveys of fracture characteristics in the stratigraphic section in order to determine the mechanical behavior of the stratigraphic section. This method was often employed where UAF Department of Geology stratigraphers (Mike Whalen, Michelle McGee, and Andy Krumhardt) had measured stratigraphic section. Lithology and other stratigraphic information were sampled (by the UAF stratigraphers or myself and field assistant) at a given interval (usually 1 meter.) In order to understand how fracture density changed throughout the section, the orientations of major fracture sets were measured, in addition to a rough estimate of their spacing. This estimate was obtained by counting the number of fractures in a 0.5 meter interval. These data were generally collected every meter or every 0.5 meter within the stratigraphic section. Approximate bed thicknesses and presence/absence of diagenetic features or strain indicators were also noted.

Preliminary Observations

Mechanical Stratigraphy of the Lisburne Group

The general stratigraphy of the Lisburne is somewhat different from that previously studied in the Franklin Mountains and front ranges of the northeastern Brooks Range. Since work on the stratigraphic section is still in progress and the temporal boundaries within the stratigraphy are still being explored, the more traditional divisions of “Wahoo” and “Alapah” limestone will not be used. The generalized lithostratigraphy can be divided into mechanical packages as shown in figure 10. The mechanical behavior of each unit is shown in figure 11.

A. Upper Lisburne

This unit is approximately 500 meters thick (McGee, this volume) consisting primarily of massively bedded, light gray colored grainstones and packstones. The upper Lisburne tends to be the most structurally competent unit in the section, and defines the map scale fold geometry in the area.

B. Lower Lisburne

The overall thickness of the lower Lisburne is approximately 400-500 meters. This unit can be divided into three major mechanical packages as follows.

1. Lower Lisburne, upper portion

This unit is composed primarily of recessively weathering, relatively thinly bedded, dark colored floatstones and shales that tend to behave slightly less

competently than the upper Lisburne. Little bed parallel shear was observed within this unit in the northwestern end of the field area, but minor parasitic folding and/or bed parallel shear within this unit was observed in folds in the southwestern end of the field area (E and W fork box folds).

2. Lower Lisburne, middle portion

Composed primarily of massively bedded floatstone units that behave mechanically like the upper Lisburne. Bed parallel slip and duplexing were documented within this unit in the flat panel in the northwest end of the field area.

3. Lower Lisburne, lower portion

A dark colored, recessive unit that appears similar in outcrop to the upper portion of the lower Lisburne. This unit is also less competent than the Upper Lisburne or the middle portion of the Lower Lisburne. Bed parallel shear along bed contacts, duplexing, parasitic folding, and well developed dissolution cleavage were observed in the flat panel in the northwest end of the field area near the thrust.

The contact between the lower portion of the lower Lisburne and the Kayak shale below appears to be gradational.

Map Scale and Mesoscopic Scale Structures

The general structure of West Porcupine Lake Valley is characterized by strongly asymmetric, NE striking, NE plunging folds that involve Sadlerochit siltstones, Lisburne Group carbonates, and probably Kayak Shale. These are map scale (300-1000 m high in outcrop) folds with interlimb angles between approximately 130° and 30°. Some of the folds in the southeast side of the field area are overturned (figures 12 & 13). One major fold in the field area (East Fork Box Fold on figures 12 & 13) deviates from the geometry of the majority of other folds in the field area. This particular fold lies in the southeastern end of the field area and, while still asymmetrical, is characterized by a box fold geometry. The geometry of this fold changes dramatically along strike, both in the general fold shape, and in the location of normal faults in the fold. Detailed geometric analysis of this fold may reveal important information about timing relationships that can be compared to fracture timing relationships in order to understand the tectonic history of the area.

In the northwest end of the field area, a major thrust fault places Lisburne Group carbonates on top of siltstones, shales and sandstones of the Sadlerochit Group. This is the only major thrust fault that was found in the field area.

Mesoscopic scale structures in the field area suggest a predominance of “top-to-northwest” oriented layer parallel shear in West Porcupine Lake Valley, especially in the northwestern end of the field area in the relatively flat panel of Lisburne carbonates near the thrust. Numerous en echelon fractures and veins, shear planes along bed surfaces, as well as bed scale duplex structures indicate that top to north oriented layer parallel shear occurred during the structural history of the area. These north vergent structures were found throughout the field area, in both the flat backlimbs of folds and more tightly folded rocks to the southeast.

Three major sets of normal faults were documented in the area: Set 1) a NE striking, predominantly SE dipping set; Set 2) a NW striking, SW dipping set; and Set 3) an E striking; S dipping fault (figures 12 & 13). Normal faults of Set 1 were sub-parallel to the regional strike, and appeared to be concentrated both in the relatively gently folded flat panel in the northwestern end of the field area and near the hinges of some of the major anticlines in the area. Set 2 was sub-perpendicular to the regional strike and was best exposed in the southeast end of the field area, although many of these faults likely continue to the northwest. Changes in fold geometry were documented across this set of normal faults. Set 3 is actually only composed of one normal fault, but is included as a major “set” because of its anomalous orientation, large displacement and lateral extent. This fault is oriented obliquely to the regional strike and has arguably the largest displacement of any of the faults in the area, with a down-to-the-south sense of displacement.

Fracturing

A. General Character

Four major sets of extension fractures were documented in West Porcupine Lake valley, the majority of which dip steeply between 60°-90° in both directions: 1) a N-S striking set; 2) an E-W striking set; 3) a N-S to NW striking set; and 4) a NE striking set. While the relative timing of each of these fracture sets is unclear, some generalities can be made. The NW set appears to be younger than the N-S and E-W sets. E-W fractures terminate against N-S fractures at most sample locations. However, the opposite relationship was documented elsewhere in the field area, possibly suggesting multiple generations of N-S and E-W fracturing. All three fracture sets were found in en echelon sets of extension fractures, which indicate a component of shear during formation. Shear sense on these sets was commonly normal or strike slip, suggesting that many fractures are related to normal faulting in the area. The N-S and NW striking fractures were often found in 3-5 meter wide swarms of en echelon fractures, each swarm spaced approximately 10-20 meters apart. NE striking fractures were well developed in the lower portions of one of the major synclines in the area (Camp Syncline, figures 12&13), although the timing of these fractures is unclear. Other major mesoscopic-scale structures indicate some period of penetrative semi-ductile deformation, including dissolution cleavage, deformed crinoid stems, sheared stylolites, and elongated and transposed chert nodules.

B. Distribution within the stratigraphy

General surveys of fracture distribution in a relatively complete stratigraphic section were conducted in three areas; A) in the upper Lisburne and part of the lower Lisburne in a long, relatively flat backlimb in the northwestern end of the field area (see figures 12, 13), B) in the upper Lisburne in the backlimb of “Camp Syncline” (figure 14), C) and in the upper Lisburne in the backlimb of “Open Syncline” (figures 12,13,15). Detailed sampling of representative lithologies in each stratigraphic section was also conducted. In general, finer grained lithologies such as dark colored wackestones tended to have higher fracture densities than light gray colored packstones and grainstones. Higher fracture densities seemed to be found in thinner beds, although further analysis of

fracturing within the stratigraphic sections may help quantify this relationship. The lower Lisburne seemed to have higher fracture densities than the upper Lisburne, although many wackestones in the upper Lisburne were highly fractured.

C. Distribution of fracturing within folds

The upper Lisburne of three major folds was sampled in detail at: 1) "Camp Syncline", where two stratigraphic horizons were sampled (figures 12,13,14), 2) "Open Anticline", and 3) "Open Syncline" (figures 12,13,15). The lower Lisburne was not exposed in any of these folds and was therefore not sampled. Within Camp Syncline, the "Upper Camp Syncline" sample locations (UCS1-1 through UCS-7 on figure 14) tended to have higher fracture densities than the "Lower Camp Syncline" (F3-F12 on figure 14). No obvious change in fracture density was observed between limbs and hinges, although further analysis may elucidate more subtle trends in fracture distribution.

Preliminary Interpretations

Mechanism of folding

Since the mechanism by which the folds in West Porcupine Lake Valley formed has important implications for fracture distribution and character within the folds, it is important to understand their kinematic history. No definitive evidence was found as to whether the West Porcupine Lake Valley folds are detachment folds or fault propagation folds, but current research (Jadamec, this volume) may help to answer this question. Future construction of balanced cross sections of the field area may also provide constraints on the kinematic history of these folds.

Influence of mechanical stratigraphy on folds in the area

Preliminary observations indicate that the mechanical stratigraphy of the Lisburne in West Porcupine Lake Valley is different from the Lisburne in the front ranges. In the Franklin Mountains and front ranges, the lower Lisburne (Alapah) tends to behave as a relatively weak unit, often containing numerous parasitic folds that thicken the unit, commonly in the cores of detachment folds. In West Porcupine Lake Valley, very few parasitic folds were seen in the lower Lisburne. This suggests that either a change in the mechanical stratigraphy prevented this type of thickening, or another factor (such as an increased tectonic overburden?) prevented parasitic folding from occurring. Although the relationship is unclear, the absence of thickening in the Alapah may favor asymmetric detachment folding.

Alternatively, the mechanical stratigraphy described above may have favored the propagation of a fault ramp, leading to fault propagation folding. In the study area the middle portion of the lower Lisburne was observed to be more competent than the upper or lower portions of the lower Lisburne. This mechanically rigid layer buttressing the lower Lisburne might favor the propagation of a ramp, leading to fault propagation folding. Fault propagation folding would also explain the fold asymmetry in the area since the leading models on fault propagation folding (Suppe and Medwedeff, 1990,

Mitra, 1990) require asymmetric folds due to the geometry of the ramp. Further detailed geometric analysis and cross section balancing may aid in understanding the effect of the change in mechanical stratigraphy on fold kinematics.

Normal Faulting

Preliminary results suggest that at least one stage of normal faulting post-dated, or was possibly concurrent with folding and/or thrusting. This is suggested by a cross cutting relationship between the major thrust fault and one of the NE striking, SE dipping normal faults in the northwestern end of the field area. Another possible line of evidence for folding concurrent with normal faulting lies in one fold in the southeast side of the field area ("East Fork Box Fold"). This fold has two different hinges separated by a normal fault. The geometry of this particular fold may suggest concurrent folding and normal faulting. Future analysis will address this question.

While the timing of each set of normal faults relative to the other is somewhat unclear at this point, many of the NW oriented normal faults (of set 2) appear to be the sites of major changes in fold geometry along strike. This suggests that these faults may have originated as accommodation structures that formed concurrent with folding and/or thrusting, and were activated as normal faults during or after folding had occurred.

The numerous normal faults found in the Porcupine Lake structural low are atypical for the Brooks Range and may be related to the origin of the structural low. Several hypotheses were developed over the course of the summer to explain the presence of both the Porcupine Lake structural low itself and the normal faults associated with it. These included some combination of the following: 1) extension above the trailing edge of the basement thrust sheets that form the major structures of the northeastern Brooks Range; 2) extension of the Mississippian and younger rocks over the buried edge of a rifted Devonian continental margin; 3) normal faulting in the west associated with inversion of an isolated Devonian basin in the east; and 4) segmentation of the thrust front by transverse normal faults due to a combination of a complex basement topography and lateral variations in the amount and distribution of shortening.

Fracturing

Preliminary observations of fracturing in the field area suggest a complicated history of fracturing related to pre-folding processes, folding processes and normal faulting. Numerous fractures were documented that strike both sub-parallel (NE striking) and sub-perpendicular (NW striking) to regional trends, which are sub-parallel and perpendicular to the orientations of normal faults in the area. Models and field observations for fracturing in advance of a developing fold and thrust belt, (Hanks, et al, 1997, Lorenz, et al, 1997, Lorenz et al, 1991, Hancock and Engelder, 1989), as well as models for fractures related to folding (Stearns, 1968, Stearns and Friedman, 1969) commonly have two major fracture orientations that strike parallel and perpendicular to regional trends. The N-S, and E-W striking trends seem to fit the model for fracturing in advance of a developing fold and thrust belt. Since many of these fractures exhibit a sense of shear,

very often with a strike slip component, they don't fit particularly well with the models described above. In addition, many N-S striking fractures were found in en echelon sets with a given sense of shear, which can be compared to senses of shear on normal faults in the area. This is one method of distinguishing which sets of fractures are related to normal faulting vs. folding. However, since normal faulting in the area may have produced an "overprint" of fractures in the field area, any analysis of the distribution of fracturing in folds will be ambiguous. Since fractures with similar orientation may be produced by multiple mechanisms through time, further statistical and three-dimensional analysis will be conducted to attempt to distinguish each generation of fracturing.

Future research:

Future research will include the following:

- 1) Completion of data compilation.
- 2) Production of mechanical stratigraphic sections with integrated fracture data.
- 3) Construction of balanced, restored cross-sections. Balanced and restored cross sections will help constrain the relevant structural history in the area, as well as accurately place fracture sample locations.
- 4) Statistical and three-dimensional analysis of fracture data. The relationship between fracture density, folding, bed thickness, and lithology is important when developing a predictive model for fracture density within a folded stratigraphic section. Statistical analysis will focus on fracture spacing as a measure of fracture density and the distribution of fracture density throughout a given fold. This analysis will enable comparison of relatively unfolded sample locations to open folds and tight folds in order to understanding the kinematic history of fracturing and folding. In addition, statistical analysis and restoration techniques may aid in distinguishing between fractures related to folding and normal faulting.
- 4) Integration of fracture data into a three-dimensional fold model. Since folds and fractures are three-dimensional structures, the third dimension is critical to understanding the relationship between fracturing and folding, highlighting areas of higher fracture density, and understanding the kinematic history of folding and fracturing.

References

- Bird, K.J., and Mollenaar, C.M., 1992, The North Slope foreland basin, *in* MacQueen, R.W., and Leckie, D.A., eds., Foreland basins and foldbelts: American Association of Petroleum Geologists Memoir 55, p. 363-393.
- Chester, J.S., Logan, J.M., Spang, J.H., 1991, Influence of layering and boundary conditions on fault-bend and fault-propagation folding: Geological Society of America Bulletin, v. 103, p. 1059-1072.
- Erickson, S.G., 1996, Influence of mechanical stratigraphy on folding vs. faulting: Journal of Structural Geology, v. 18, no. 4, p. 443-450.
- Fischer, M.W., and Coward, M.P., 1982, Strains and folds within thrust sheets: an analysis of the Helium sheet, Northwest Scotland: Tectonophysics v. 88, p. 291-312.
- Grantz, A., and May, S.D., 1983, Rifting history and structural development of the continental margin of north Alaska, in Watkins, J.S., and Drake, C.L., eds., Studies in continental margin geology: AAPG Memoir 34, p. 77-100.
- Grantz, A., May, S.D., and Hart, P.E., 1990, Geology of the Arctic continental margin of Alaska, in Grantz, A., Johnson, L., and Sweeney, J.F., eds., The Arctic Ocean region: Boulder Colorado, GSA, The Geology of North America, v.L., p. 257-288.
- Hancock, P.L., and Engelder, T., 1989, Neotectonic Joints: Geological Society of America Bulletin, v. 101, p. 1197-1028.
- Hanks, C.L., Lorenz, J.C., Teufel, L.W., and Krumhardt, A.P., 1997, Lithologic and Structural Controls on Natural Fracture Distribution and Behavior within the Lisburne Group, Northeastern Brooks Range and North Slope Subsurface, Alaska: American Association of Petroleum Geologists Bulletin, v. 81, no. 10, p. 1700-1720.
- Hennings, Peter H., Olson, Jon E., and Thompson, Laird B., 2000, Combining Outcrop Data and Three-Dimensional Structural Models to Characterize Fractured Reservoirs: An Example from Wyoming. AAPG Bulletin v. 84, no. 6, p. 830-849.
- Homza, T.X., and Wallace, W.K., 1997, Detachment folds with fixed hinges and variable detachment depth, northeastern Brooks Range, Alaska: Journal of Structural Geology, v. 19, nos. 3-4, p. 337-354.
- Jamison, W.R., 1987, Geometric analysis of fold development in overthrust terranes: Journal of Structural Geology, v. 9, p. 207-219.

- Krumhardt, A.P., Harris, A.H., and Watts, K.F., 1996, Lithostratigraphy, Microlithofacies, and Condodont Biostratigraphy and Biofacies of the Wahoo Limestone (Carboniferous), Eastern Sadlerochit Mountains, Northeast Brooks Range, Alaska: U.S. Geological Survey Professional Paper 1568, 70 p.
- Ladeira, F.L., and Price, N.J., 1981, Relationship between fracture spacing and bed thickness: *Journal of Structural Geology*, v. 3, p.179-183.
- Lorenz, J.C., Farrell, H.E., Hanks, C.L., Rizer, W.C., and Sonnenfield, M.D., 1997, The Characteristics of Natural Fractures in Carbonate Strata: *in* Palaz, I., and Markfurt, K, eds., *Carbonate Seismology: Society of Exploration Geophysics Publication*, p. 179-201.
- Lorenz, J.C., Teufel, L.W., and Warpinski, N.R., 1991, Regional Fractures I: A Mechanism for the Formation of Regional Fractures at Depth on Flatlying Reservoirs: *American Association of Petroleum Geologists Bulletin*, v. 75, no. 11, p. 1714-1737.
- Mayfield, C.F., Tailleur, I.L., and Ellersieck, I., 1988, Stratigraphy, structure, and palinspatic synthesis of the western Brooks Range, northwest Alaska: *in* Gryc, G. ed., *Geology and Exploration of the National Petroleum Reserve in Alaska, 1974 to 1982: U.S. Geological Survey Professional Paper 1399*, p.143-186.
- McClay, Ken, 1987, *The mapping of geological structures*, Geological Society of London handbook series, Open Univ. Press, Milton Keynes, United Kingdom, Halsted Press, New York, NY, United States, 161 p.
- Moore, T.E., Wallace, W.K., Bird, K.J., Karl, S.M., Mull, C.G., and Dillon, J.T., 1994, Geology of northern Alaska, *in* Tailleur, I.L., and Weimer, P., eds., *Alaskan North Slope geology: Pacific Section, SEPM and Alaska Geological Society, Book 50*, p. 513-528.
- Mull, C.G., 1985, Cretaceous tectonics, depositional cycles, and the Nanushuk Group, Brooks Range and Arctic Slope, Alaska, *in* Huffman, A.C., Jr., ed., *Geology of the Nanushuk Group and related rocks, North Slope, Alaska: U.S. Geological Survey Bulletin 1614*, p. 7-36.
- Narr, W., and Suppe, J., 1991, Joint spacing in sedimentary rocks: *Journal of Structural Geology*, v. 13, no. 9, p. 1037-1048.
- Mitra, S., 1990, Fault propagation folds: geometry, kinematic evolution, and hydrocarbon traps: *American Association of Petroleum Geologists Bulletin*, v. 74, p. 921-945.
- Poblet, J., and McClay, K., 1996, Geometry and kinematics of single-layer detachment folds: *American Association of Petroleum Geologists Bulletin*, v. 80, p. 1085-1109.

- Ramsay, J.G., and Huber, M.I., 1987, Techniques of Modern Structural Geology, Volume 2: Folds and Fractures, Session 20: Fold Mechanics 2: Multilayers, p. 405-444, Academic Press Inc, San Diego CA.
- Stearns, D.W., 1968, Certain aspects of fracture in naturally deformed rocks *in* Riecker, R.E., ed., NSF Advanced Science Seminar in Rock Mechanics: Bedford, Massachusetts, Air Force Cambridge Research Lab. Special Report, p. 97-118.
- Stearns, D.W., and Friedman, M., 1969, Reservoirs in Fractured Rock *in* Stratigraphic oil and gas fields: Classification, exploration methods, and case histories: American Association of Petroleum Geologists Memoir 16, p. 82-106.
- Suppe, J., 1983, Geometry and kinematics of fault-bend folding: American Journal of Science, v. 283, p. 684-721.
- Suppe, J., and Medwedeff, D.A., 1990, Geometry and kinematics of fault-propagation folding: *Ecolgae Geologicae Helvetiae*, v. 83, p. 409-454.
- Wallace, W.K., 1993, Detachment fold and a passive roof duplex: Examples from the northeastern Brooks Range, Alaska *in* Solie, D.N., and Tannian, F., eds., Short Notes on Alaskan Geology 1993: Alaska Division of Geological and Geophysical Surveys Geologic Report 113, p. 81-99.
- Wallace, W.K., and Hanks, C.L., 1990, Structural Provinces of the northeastern Brooks Range, Arctic National Wildlife Refuge, Alaska: American Association of Petroleum Geologists Bulletin, v. 74, no. 7, p. 1100-1118.
- Watts, K.F., Harris, A.G., Carlson, R.C., Eckstein, M.K., Gruslovic, P.D., Imm, T.A., Krumhardt, A.P., Lasota, D.K., Morgan, S.K., Dumoulin, J.A., Enos, P., Goldstein, R.H., and Mamet, B.L., 1995, Analysis of reservoir heterogeneities due to shallowing upward cycles in carbonate rocks of the Pennsylvanian Wahoo Limestone of northeastern Alaska: United States Department of Energy, Final Report for 1989-1992 (DOE/BC/14471-19), Bartlesville Project Office, 433

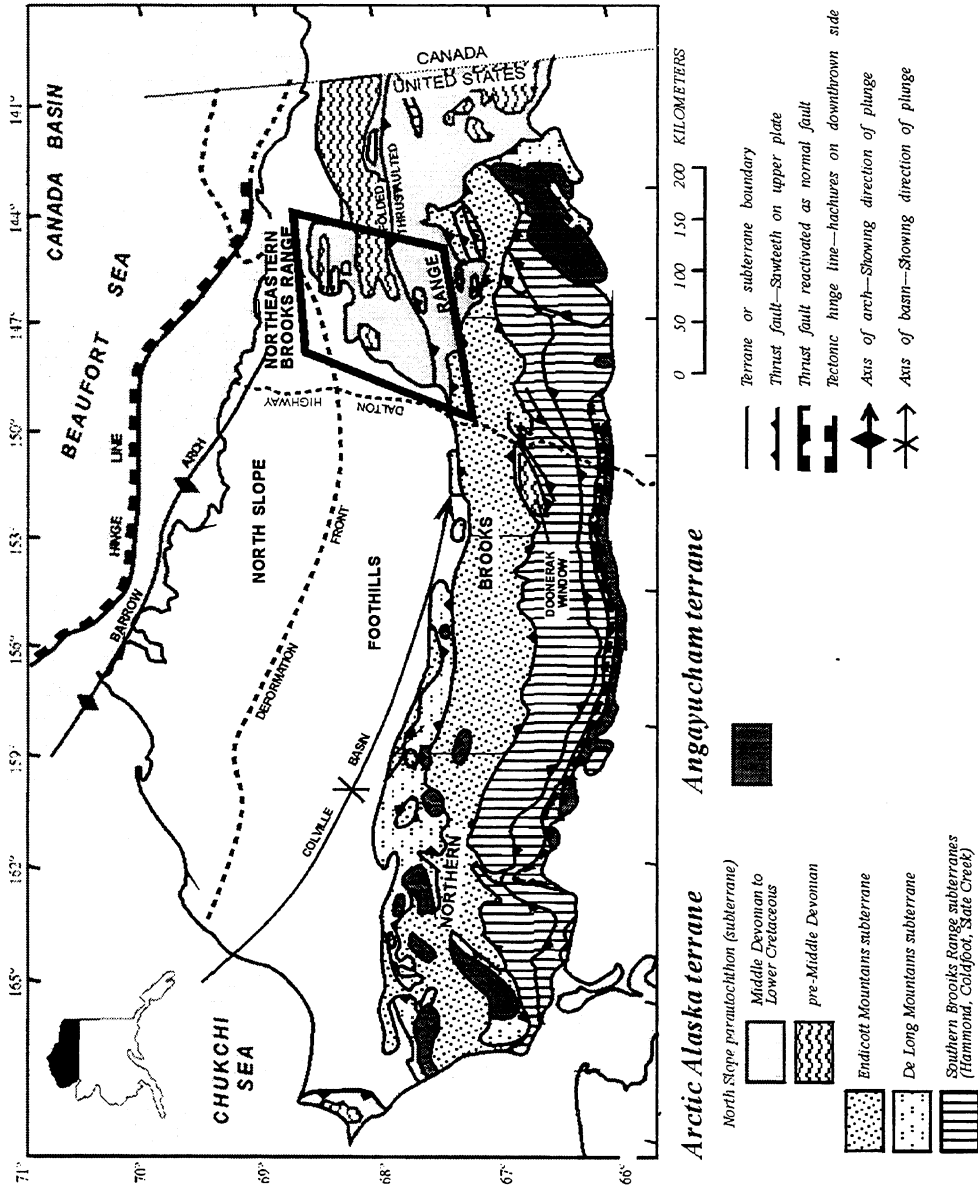
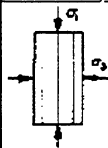
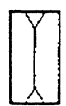


Figure 1: Regional Structure and tectonic map of the Brooks Range and North Slope of Alaska. Outline area is illustrated in more detail in figure 7. (modified from Wallace and others, 1997).

A

STAGE	1	2	3	4	5
TYPICAL STRAIN BEFORE FRACTURE OR FAULTING (PERCENT)	<1	1-5	2-8	5-10	>10
$\sigma_1 > \sigma_2 = \sigma_3$					
TYPICAL STRESS-STRAIN CURVES					

B

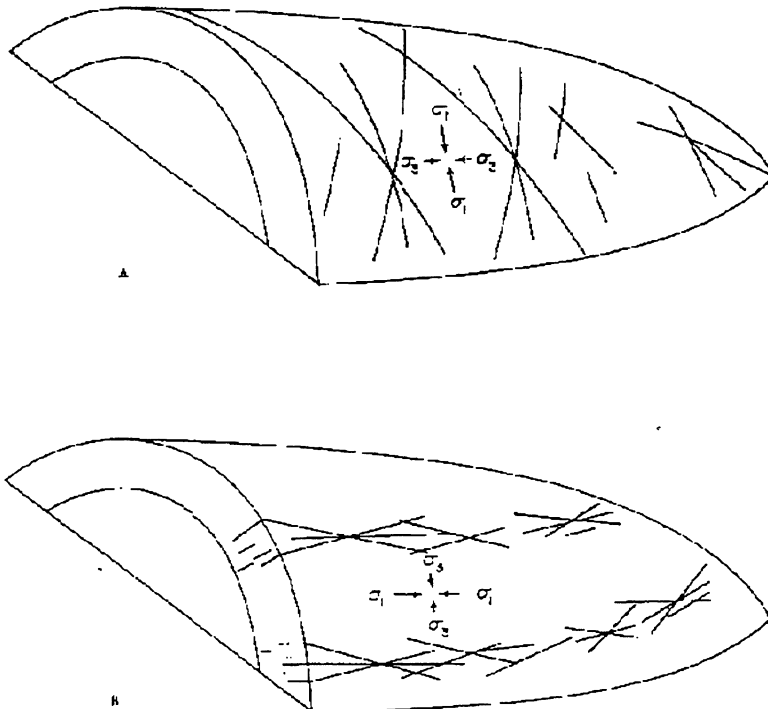
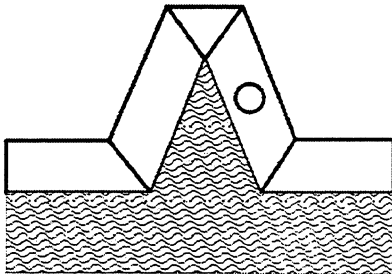
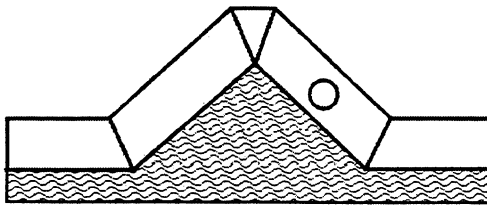
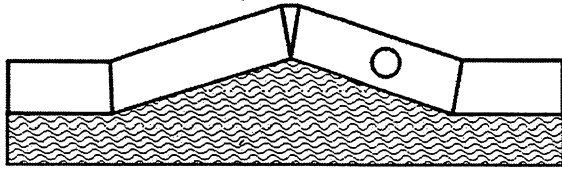
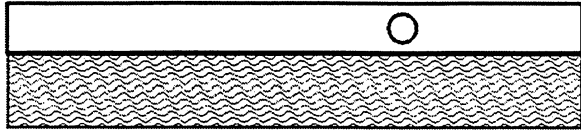


Figure 2: Part A: Diagram showing fracture orientation with increasing strain (from: Griggs and Handin, 1960), Part B: Stearns and Friedman's (1969) model for fractures related to folds. Note the different orientations of fractures with respect to σ_1 , σ_2 , and σ_3 .

Fixed Hinge Detachment Folding



Migrating Hinge Detachment Folding

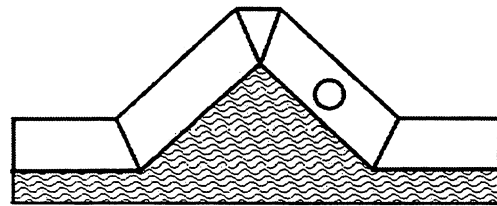
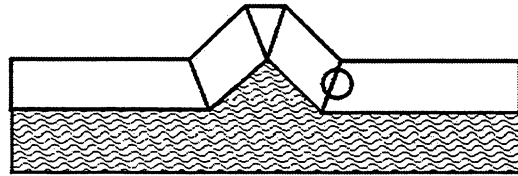
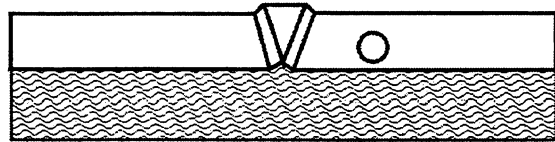
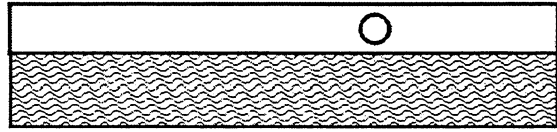


Figure 3: Simplified models for detachment folds. Detachment unit is stippled. Fixed hinge folding requires that the limbs rotate with respect to relatively fixed hinges. Migrating hinge folding requires that the hinges migrate through the upper unit (circle shows a single point in the competent unit). Note that the detachment volume must migrate to fill the core of the fold in both cases. (Modified from: Homza and Wallace, 1995)

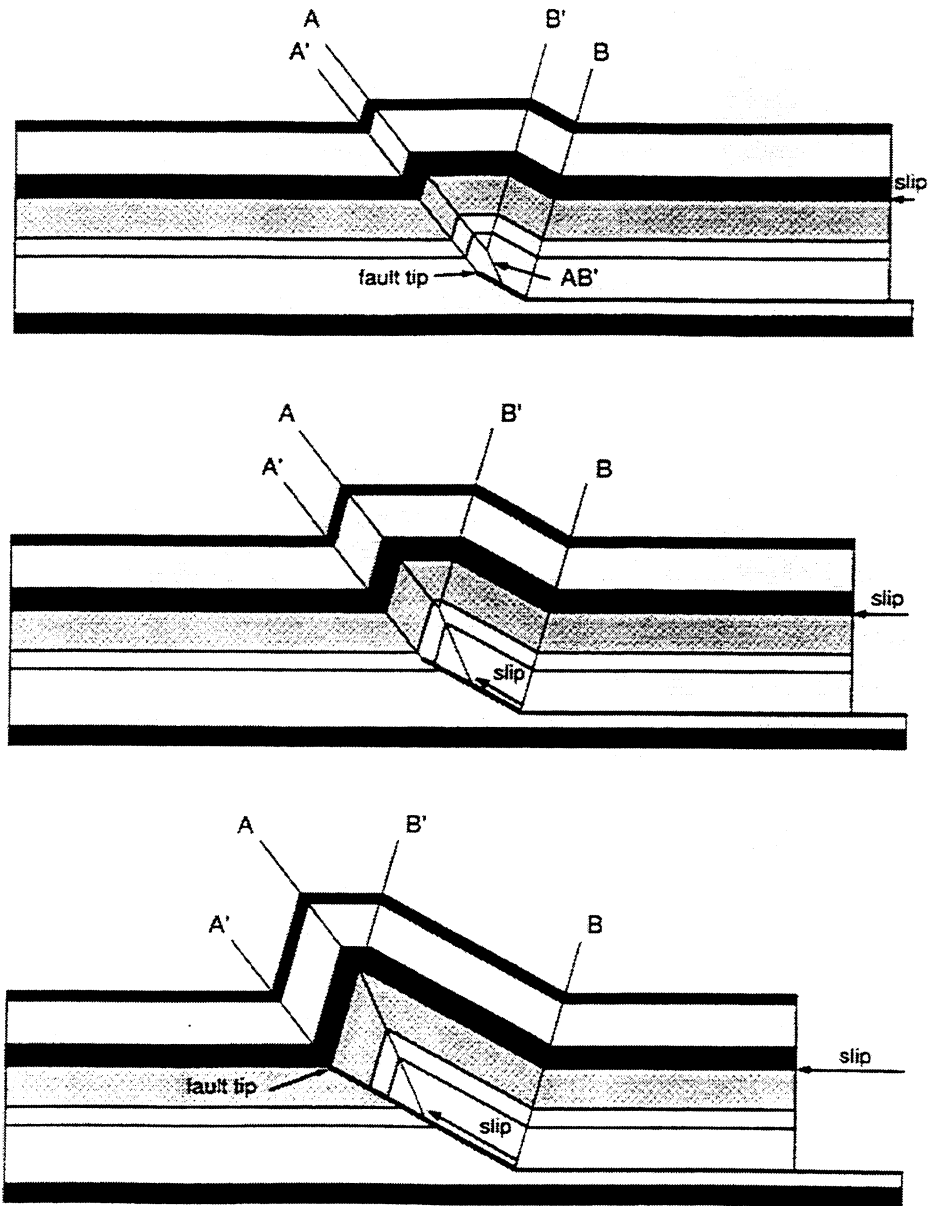


Figure 4: Suppe and Medwedeff's (1990) model for fault propagation folding.

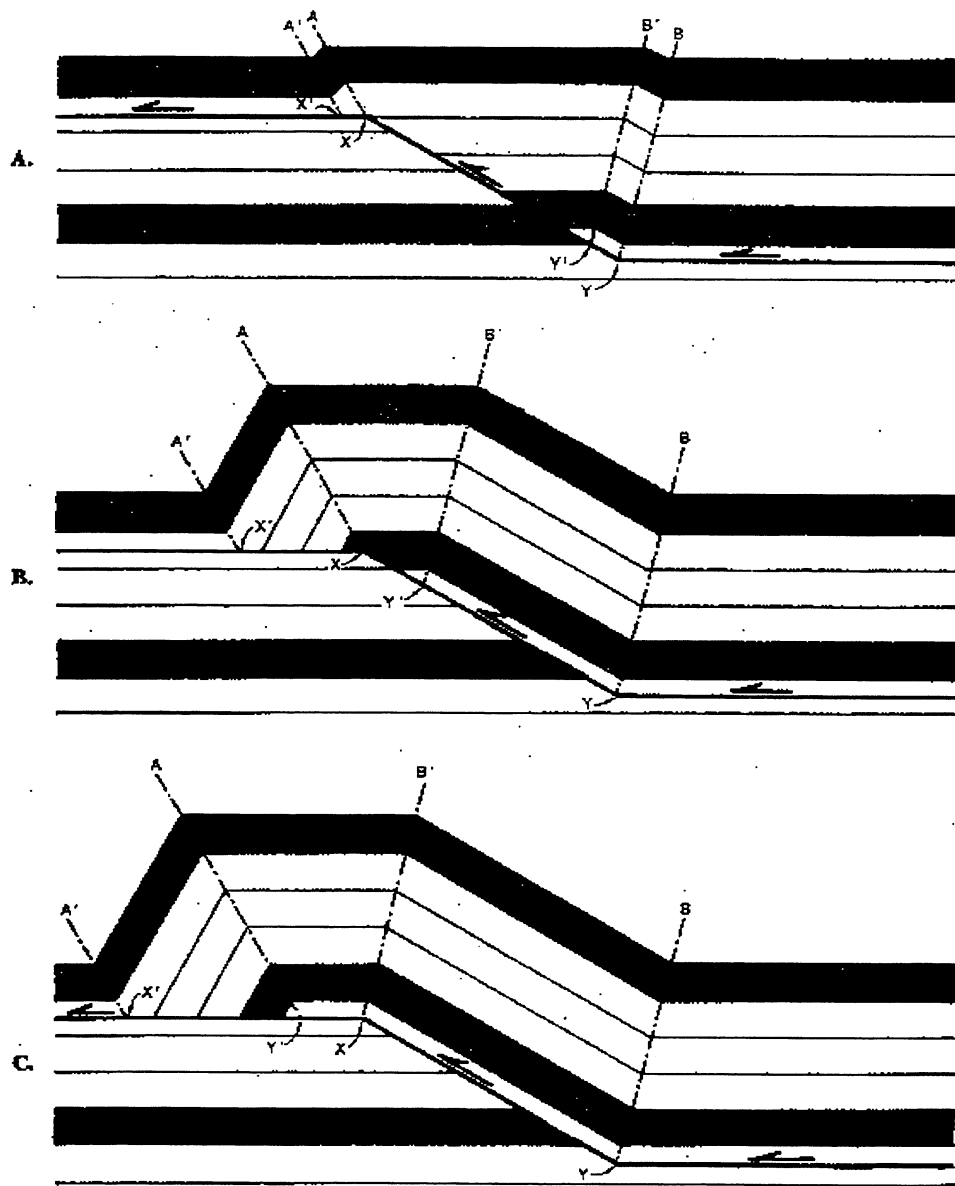


Figure 5: Model for fault bend folding (from Suppe, 1983).

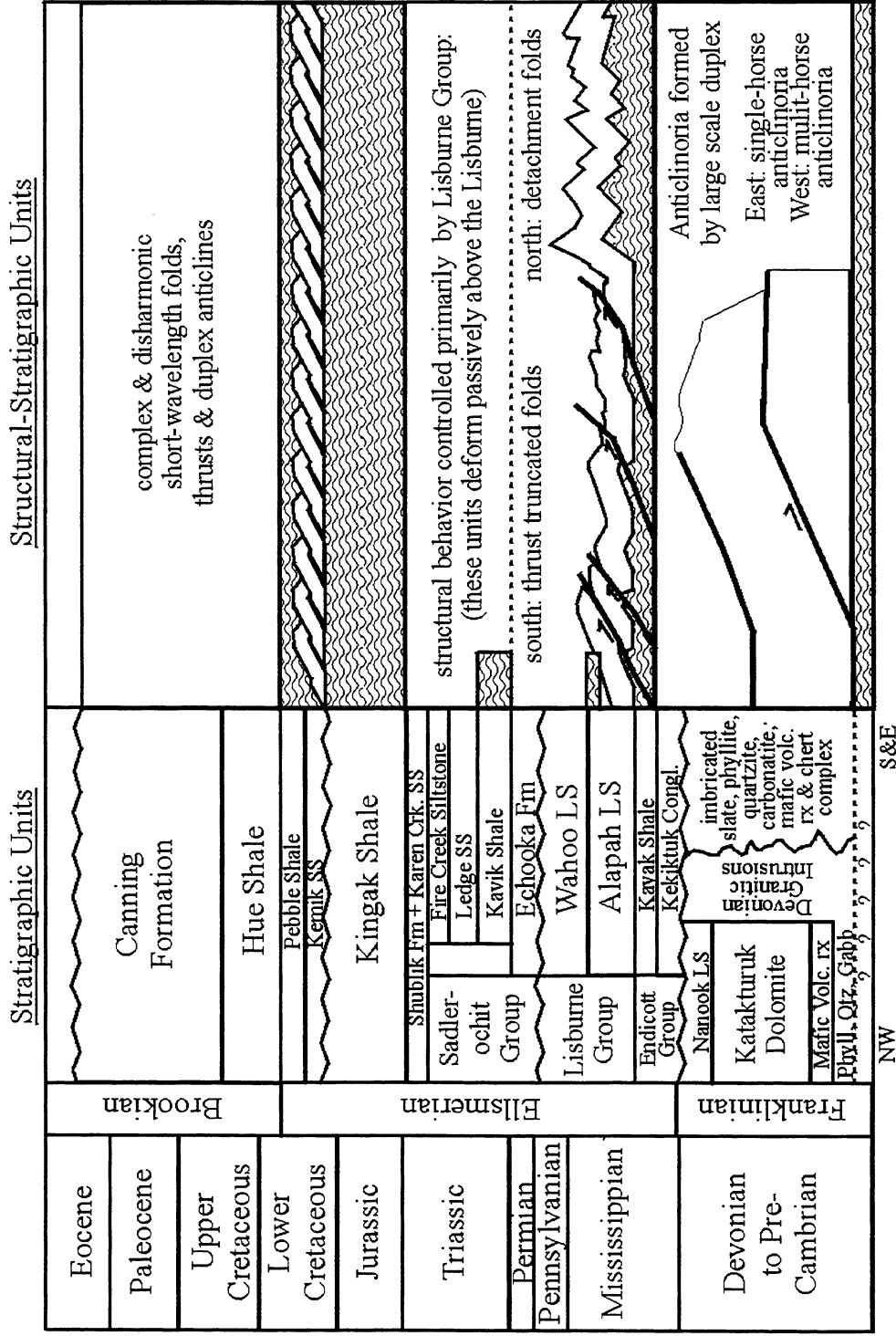


Figure 6: Lithostratigraphy and mechanical stratigraphy of the northeastern Brooks Range. Detachment units are stippled (modified from Wallace and Hanks 1990, and Wallace, 1993)

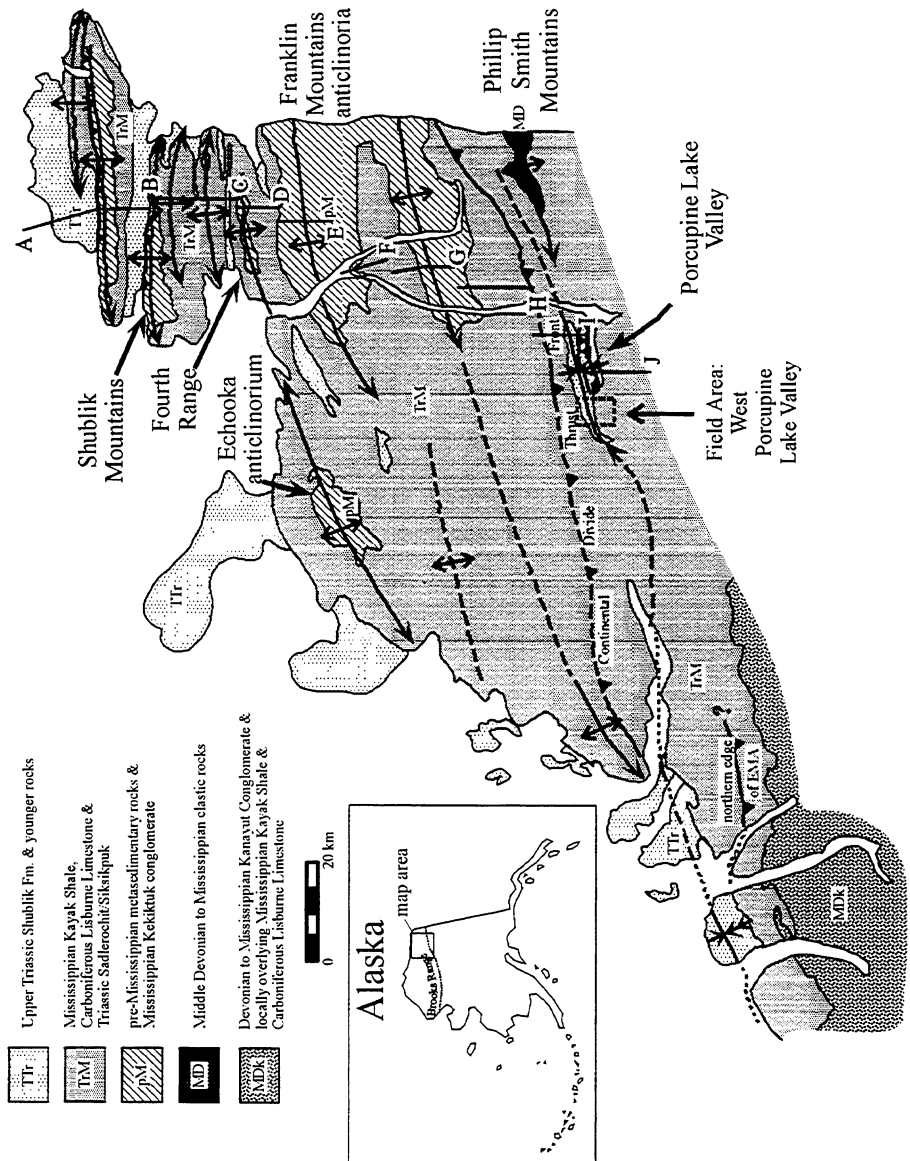


Figure 7: The geologic map of the western portion of the northeastern Brooks Range. Section lines F through J correspond with the cross section in figure 8.

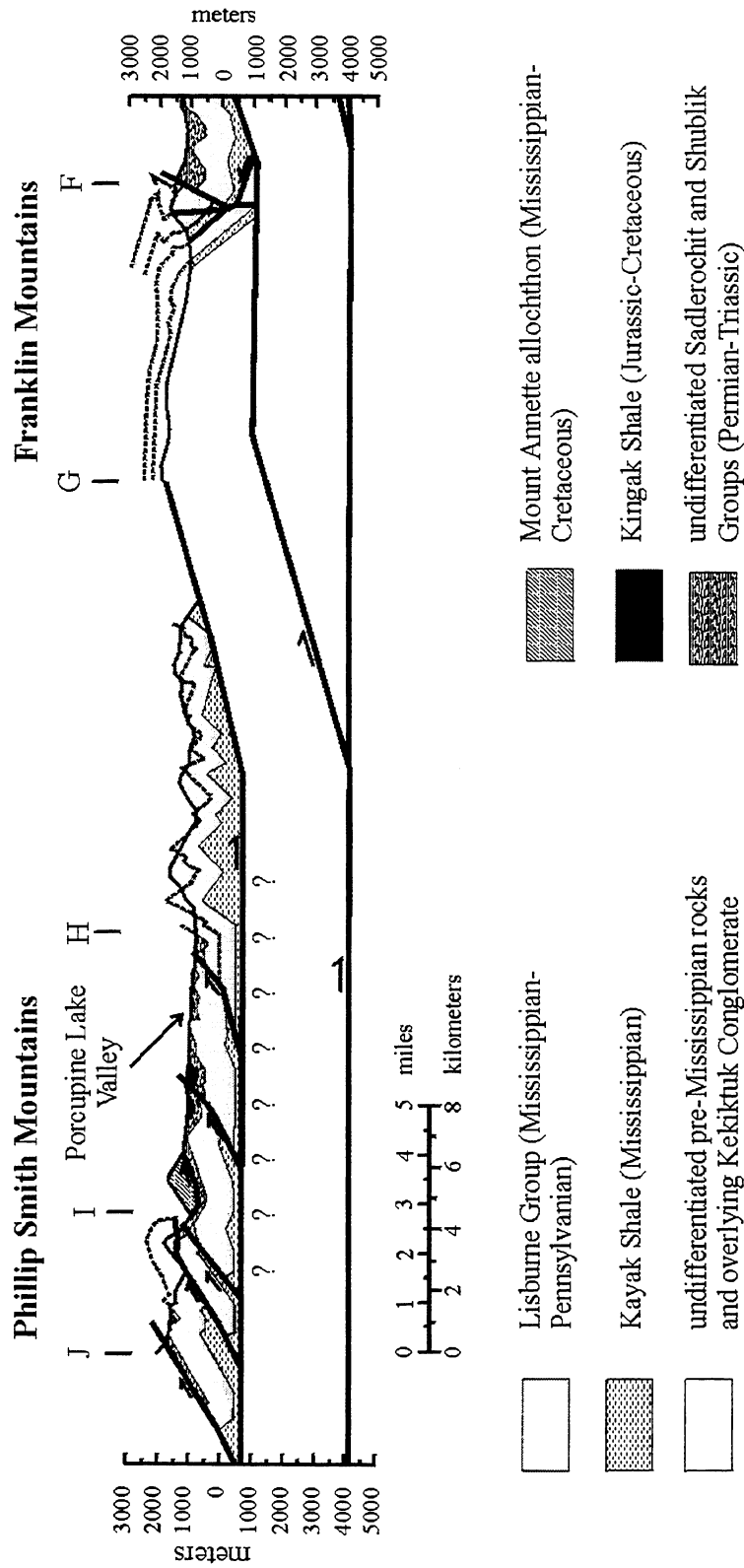


Figure 8: Cross section through the northeastern Brooks Range. See figure 7 for section line locations (letters F-J on cross section correspond to letters on figure 7). Note the difference in structural behavior of the Lisburne group between the Porcupine Lake area and the southernmost Franklin Mountains (north of the "H" section boundary). Modified from: Wallace, 1993.

SYSTEM	GROUP	STRATIGRAPHIC UNIT	LITHOLOGY	DESCRIPTION	DEPOSITIONAL ENVIRONMENT					
					INTERTIDAL	RESTRICTED	OPEN	PLAT-FORM	OPEN MARINE	
PERMIAN	SADLEROCHIT GROUP	Ivishak Formation (part)		Quartzose sandstone and shale						
		Echooka Formation		Siltstone and glauconitic sandstone						
PENNSYLVANIAN	LISBURNE GROUP	Wahoo Limestone	upper member	Oncolitic and peloid packstone and grainstone Ooid and (or) <i>Dorezella</i> packstone and grainstone Ooid grainstone Cryptalgal and (or) dolomitized mudstone	Cyclical, alternating with bryozoan-pelmatozoon limestone					
			lower member	Bryozoan-pelmatozoon grainstone and packstone						
		Alapah Limestone	upper member	Spiculitic dolostone and dolomitic lime mudstone-wackestone, cryptalgal laminites						
			middle member	Bryozoan-pelmatozoon limestone						
			lower member	Cyclical, crossbedded, skeletal grainstone alternating with peloidal skeletal packstone. Algal limestone and spiculitic dolostone and limestone in lower part						
		MISSISSIPPIAN	ENDICOTT GROUP	Itkilyariak Formation		Sandy limestone				
				Kayak Shale		Black shale, containing some sandstone and limestone				
Kekiktuk Conglomerate				Quartzose sandstone and conglomerate						
PRE-MISSISSIPPIAN		Main Capleson Limestone								
		Nanoak Limestone								
		Katakaturuk Dolomite								
		Sedimentary, metamorphic, and igneous rocks, undivided		Sedimentary, metamorphic, and igneous rocks						

Figure 9: Generalized lithostratigraphy of the Endicott, Lisburne, and Sadlerochit groups in the northeastern Brooks Range.
(From: Krumhardt et al., 1996)

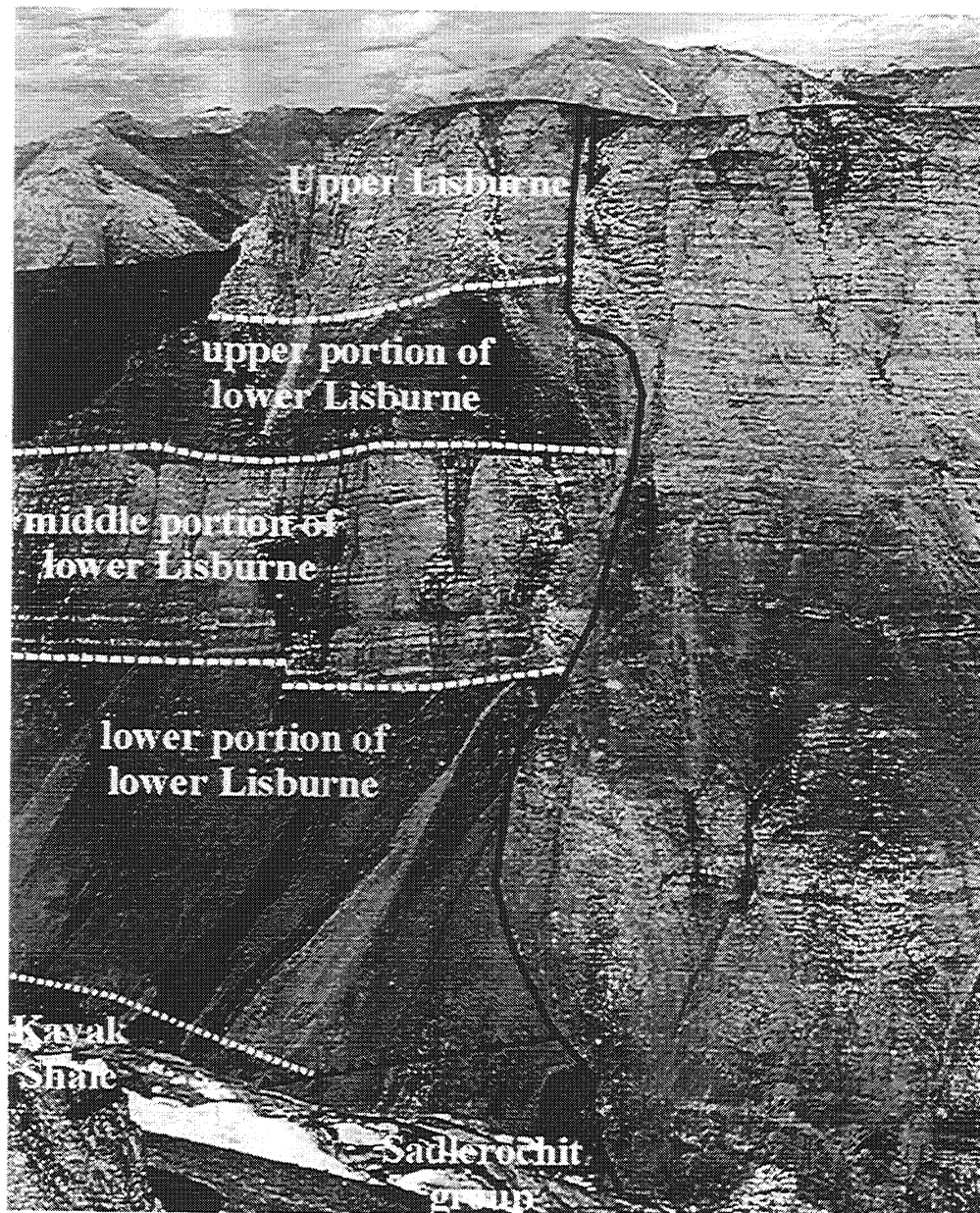


Figure 10: Photograph of the stratigraphy in West Porcupine Lake Valley. View is toward the northeast at the northwestern most Lisburne in the field area. The full thickness of the upper Lisburne is not shown here. Partial sections of the upper Lisburne are shown either side of the normal fault. The upper and lower portions of the lower Lisburne tended to be both recessive in their weathering patterns and mechanically weaker than the upper Lisburne or the middle portion of the lower Lisburne. Note the thrust, which places Lisburne and Kayak Shale above the Sadlerochit group.

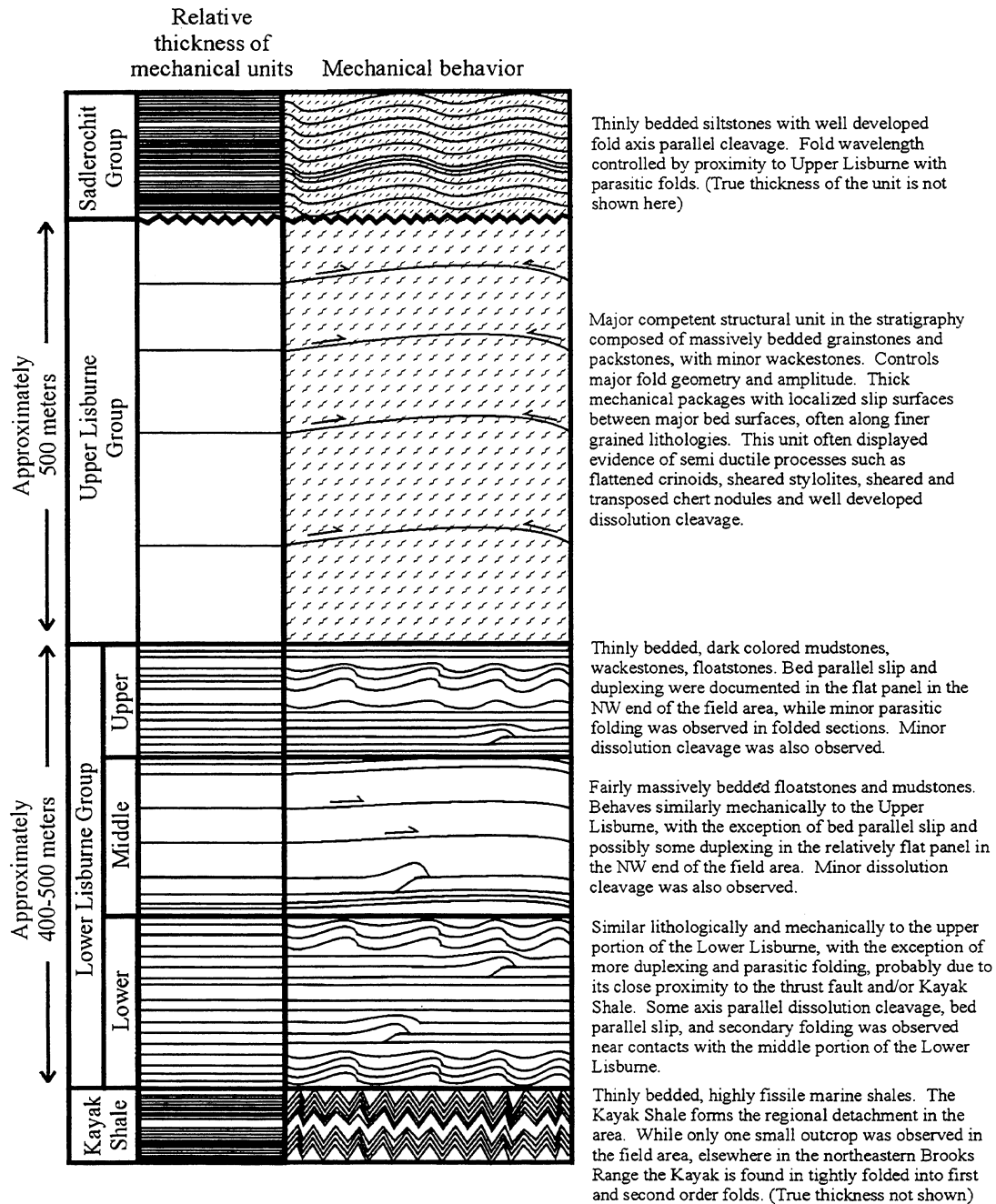


Figure 11: Generalized Mechanical Stratigraphy of the Kayak Shale, Lisburne Group, and Sadlerochit Group in West Porcupine Lake Valley. Thicknesses of units are approximate. The full thickness of Sadlerochit Group and Kayak Shale are not shown.



Legend

Contacts, faults, and fold axes are solid where precisely located, dashed where approximate, dotted where inferred (see below).

Faults
 Thrust fault
 other faults

Folds: general geometry map symbol
 symmetric anticline
 asymmetric anticline
 overturned anticline
 overturned/tilted anticline
 monocline
 symmetric syncline
 asymmetric syncline
 overturned syncline
 -arrows indicate direction of plunge

Contacts and Symbols
 Sadlerochit: S
 Upper Lisburne: uL
 Lower Lisburne: lL
 Kayak Shale: K

Strike and Dip Symbols
 m measured bedding dip 0-90 horizontal vertical
 m measured overturned bedding
 estimated bedding
 estimated overturned bedding (dips away from curve)
 m measured cleavage

Figure 12: Geologic map of West Porcupine Lake Valley. Township and range grid boxes are 1 mile square. Line of section corresponds with the cross section in figure 13.

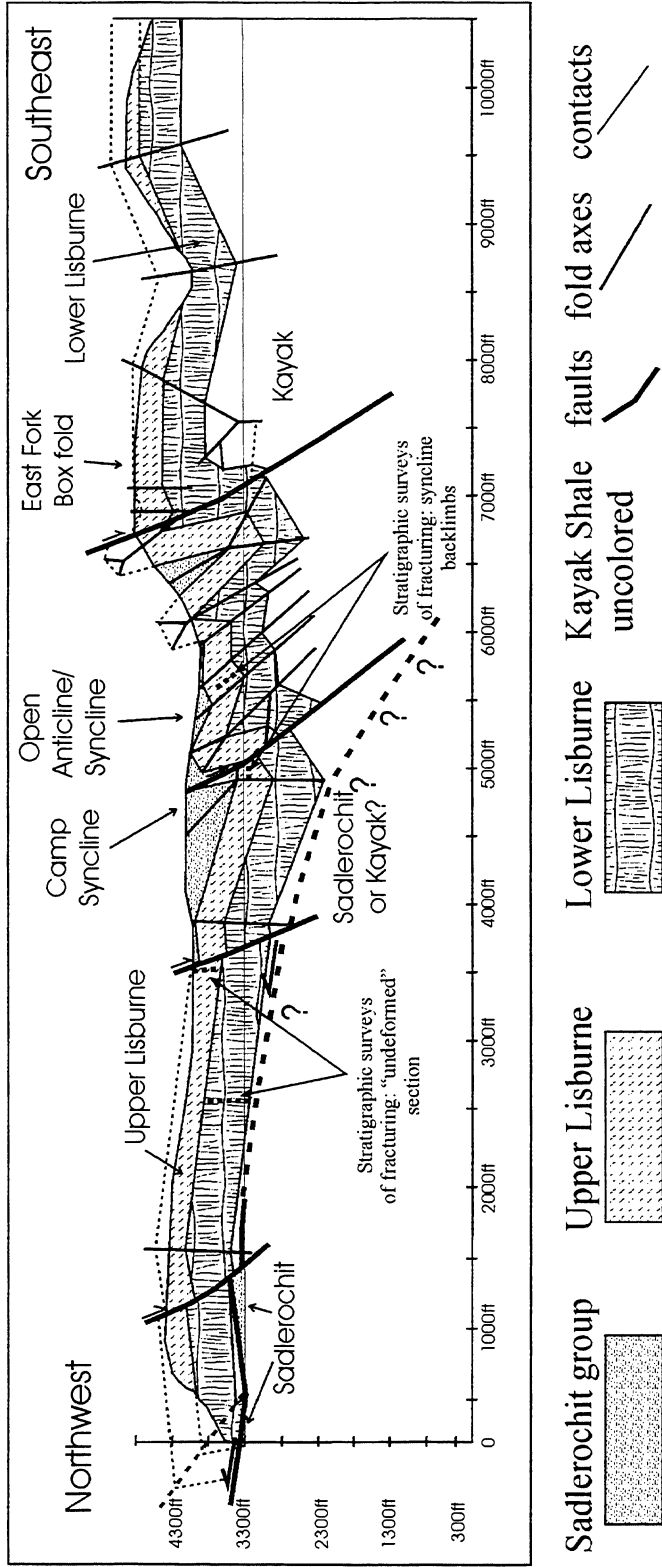


Figure 13: Unbalanced cross section through West Porcupine Lake Valley. Section line shown on figure 12. Photographs of Camp Syncline, Open Anticline, and Open Syncline are shown in following figures

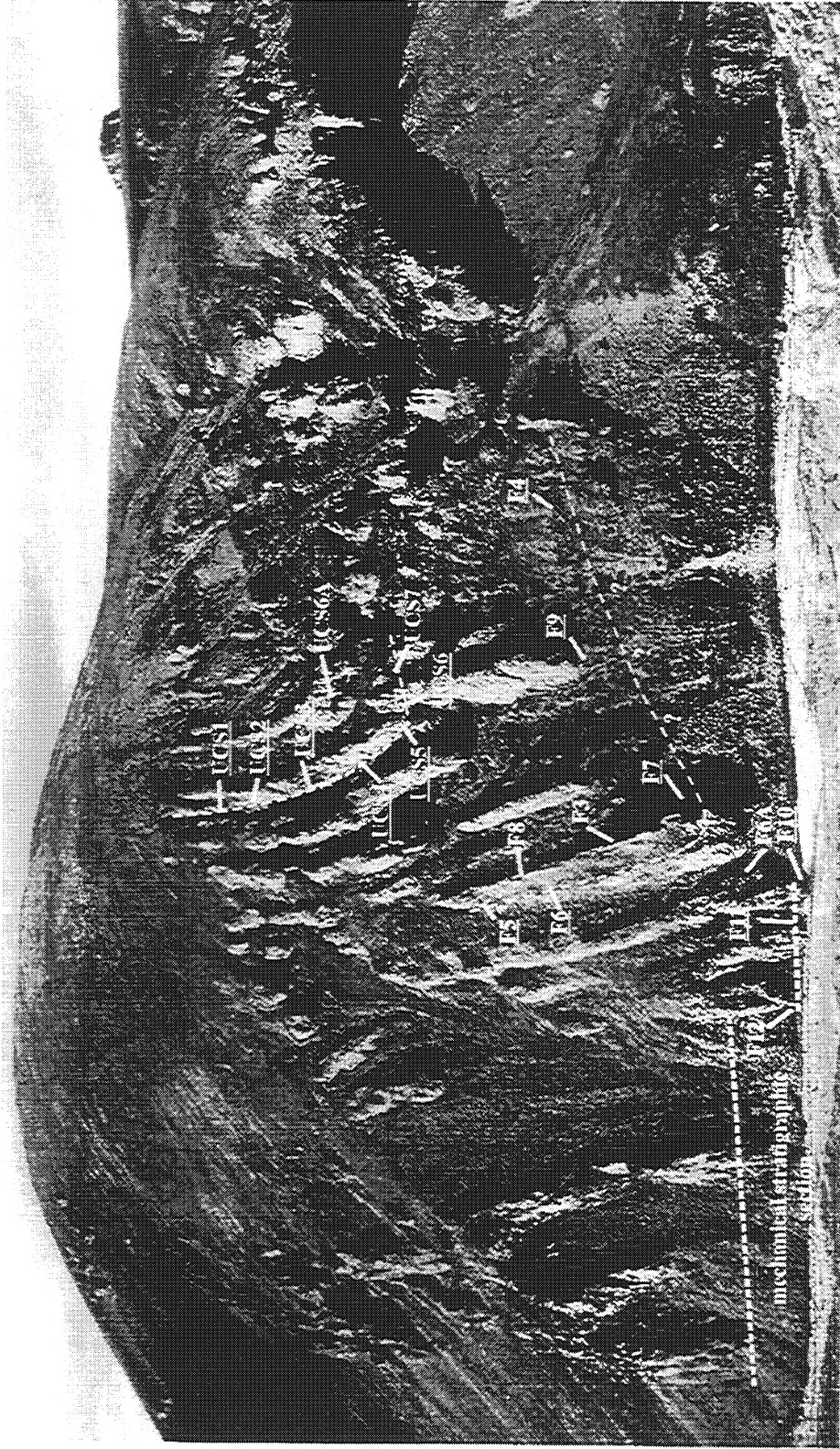


Figure 14: West view of Camp Syncline with sample locations. Underlined sample locations designate detailed fracture sampling method, non-underlined sample locations designate generalized fracture sampling method, and dotted line indicates the location of stratigraphic survey.

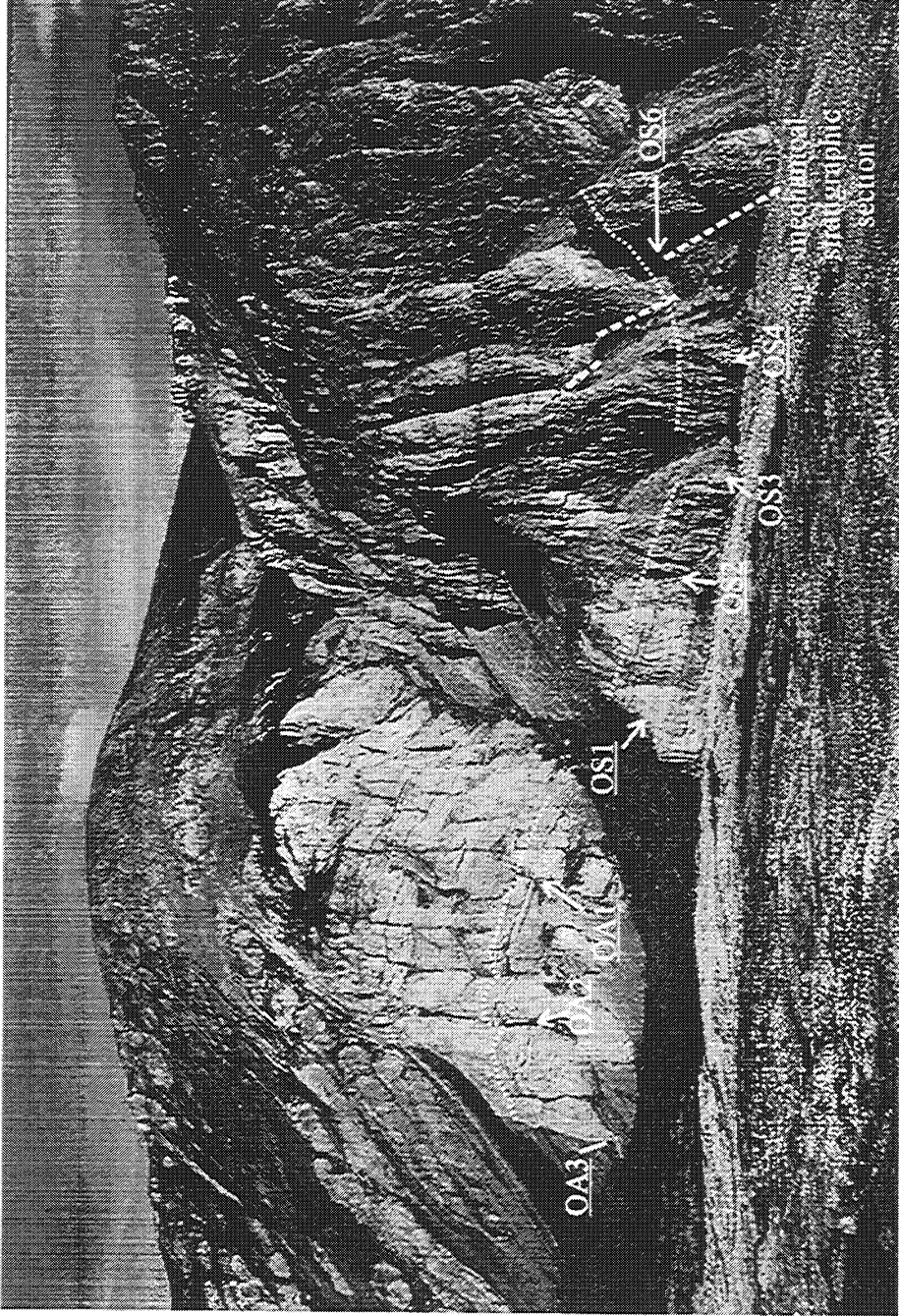


Figure 15: Northeast view (strike sub-perpendicular) of open anticline and syncline with sample locations. Underlined sample locations designate detailed fracture sampling method, non-underlined sample locations designate generalized fracture sampling method, and dotted line indicates the location of stratigraphic survey.

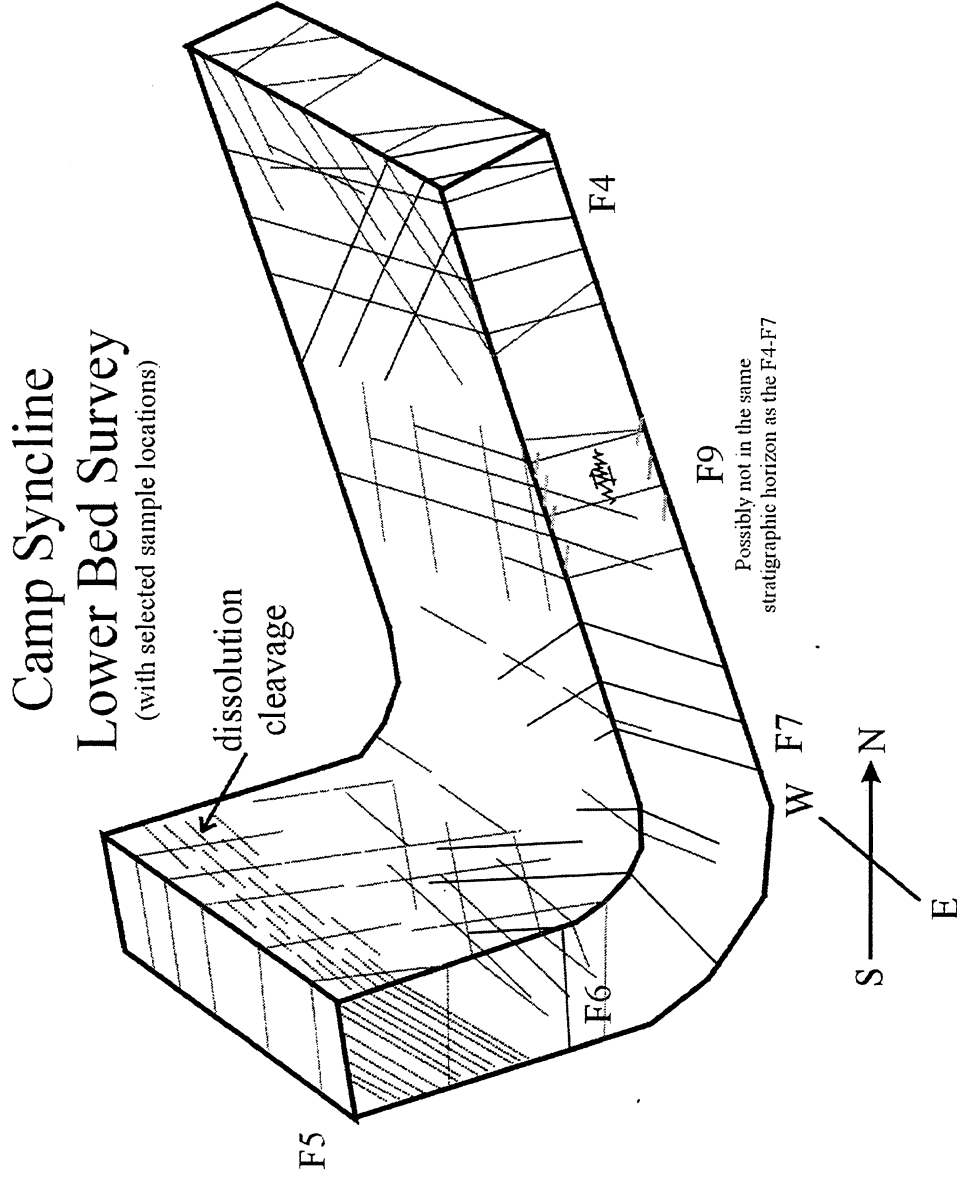


Figure 16: Preliminary interpretive sketch of selected fracture sets recorded in the lower portion of Camp Syncline. This sketch is not representative of the spacing of fractures throughout the fold, but shows the general fracture orientations.

Flow modeling

A.V. Karpov, J. L. Jensen, Texas A&M University and
C. L. Hanks, University of Alaska Fairbanks

Introduction

An essential part of the study of fractured systems includes fracture distribution analysis and development of statistical models describing the behavior of various fracture features (e.g. height and spacing). The assigned distribution types and parameters are being used in fracture set generation and fluid flow modeling in the Lisburne formation.

Literature Overview

Fracture Statistical Properties

It is generally recognized that a variety of different mathematical and statistical models can describe fractures. Many studies of fracture property statistical behavior are available in the literature. A few results and conclusions, as well as different approaches in data analysis, are covered here.

Dershowitz and Einstein (1988) cite various studies on observed distribution types of fracture properties. Distributions for fracture trace length include exponential, lognormal, hyperbolic and Gamma-1 distributions. Models based on different processes suggest three distributions: random placement processes lead to exponential distributions; multiplicative processes as they occur in breakage lead to lognormal distributions; and continuity of the process from smallest to largest sizes produces hyperbolic (fractal) distributions. However, a rigorous association of fracture size distribution with underlying geologic processes does not exist at present.

Fracture spacing often follows an exponential distribution, which is natural if fractures are created by a Poisson or Markov process. In the Poisson process, fractures are located independently according to a uniform distribution; a Markov process implies a dependence of fracture location on the preceding one. There is also evidence of lognormal distributions of fracture spacing (e.g. Rouleau and Gale, 1985). Wu and Pollard (1995) argue that lognormal spacing distributions imply under-developed fractures as opposed to normal distribution, which was suggested to indicate that a fracture set is exceptionally well developed or "saturated."

Guo et al. (1999) inspected thirty-six sets of surface fractures mapped from satellite images and aerial photos. Twenty-five hypothesized probability distribution functions were used to fit each data set. The best-fit distribution was selected using a chi-square goodness-of-fit value. Fracture lengths were best-fit by PearsonVI, PearsonV, lognormal2, or extreme-value distributions; the spacing data were best-fit by PearsonVI or lognormal distributions.

There are also cases where different size distributions can be observed in the same geological processes. Korvin (1989), as quoted in Korvin (1992), analyzed the statistical geometry of the network of faults on the structural map of the Paleozoic Basement of the Gulf of Suez. The trend

sides (N10-60° W) of the fault blocks were exponentially distributed, the “cross trend“ block sides (N20-70° E) were lognormally distributed.

Reported values of fractal dimensions vary; they appear to depend on how uniformly the sampling is performed through the whole range of scales, as well as on sampling methods. Barton (1992) found that the fractal dimension of intervals in a borehole was in the range of 0.6 – 0.8, while the dimension of two-dimensional patterns of fractures on related outcrops was in the range of 1.6-1.8.

Fracture Property Assessment

The variety of possible distribution types that can potentially mimic fracture geometry raises a question of adequate techniques for choosing and validating statistical models. Histograms and descriptive statistics provide a general “feel” of a data set but seldom allow fitting a unique distribution type to the observed values. Data located at the ends of the observed range, i.e. the extreme values, are especially hard to model using histograms. Since several analytical curves can approximate an analyzed histogram there is a need to use more sophisticated techniques.

Jensen et al (1997, p. 84) suggest probability plots to test the hypothesis of a normal distribution of a sample. The procedure can be easily adjusted to test other hypotheses. Rouleau and Gale (1985) used this approach, for example, when they tested exponential, log-normal and Weibull as candidate distributions to fit fracture spacing data. They also performed Kolmogorov - Smirnov goodness-of-fit tests to validate candidate distributions. This allowed quantitative comparison between possible statistical models for the best-fit selection. A similar approach was implemented by Guo et al (1999), using chi-squared goodness-of-fit statistics to choose best candidates for data fitting. Hoskins and Wallis (1997) address a problem of fitting a frequency distribution to samples drawn from different sites using L-moments. More details are given in Appendix A.

Lisburne Formation Fracture Analysis

Data Description

The object of our analysis is two fracture sets in the relatively undeformed section of the Lisburne carbonates (massive grainstones of the lower Wahoo Limestone): an early NNW-oriented set of extension fractures and a later ENE-oriented set of extension and shear fractures. Outcrop photographs provided quantitative information about fracture height and spacing. These data were obtained by screening fracture properties along scan-lines on the photograph. Thus, for the NNW set, we had 100 values of fracture height and 98 values of fracture spacing. There were 26 height and 25 spacing values available for ENE fractures.

Analysis Results

The first step in the data analysis was an inspection of general statistical characteristics of the fracture properties. All property distributions are skewed to the left, which is very typical

behavior. Further analysis was undertaken, particularly testing if the properties come from the exponential or lognormal distribution models.

NNW fractures

NNW fracture height

Probability plot analysis suggests the exponential model may be more appropriate than lognormal (Fig. 1). To further assess the suitability of the two distribution models, Monte Carlo simulations were performed. Ten lognormally and ten exponentially distributed sets were generated with the mean and standard deviation of the actual data set (Fig. 1). The exponential model, though poorly fitting heights below 1.2 meters, mimics the larger values fairly well. The lognormal model tends to predict larger values than actual for heights greater than 10 meters. Since larger fractures may dominate fluid flow, the exponential height model seems to be more appropriate. This assessment, however, overlooks an important feature of the exponential model.

The exponential model has only one parameter. Attempting to choose the value which best suits the larger heights causes a substantial misfit with approximately two-thirds of the data (i. e. heights below 7 meters). The degree of mismatch could significantly influence flow assessments. Therefore, the lognormal model becomes the preferred distribution because it has two parameters and still gives an acceptable fit.

An L-moment plot was also used to assess fracture height distribution (Fig. 2). The NNW height does not tend definitely to any of the standard distributions, lying in the vicinity of exponential, lognormal, Pearson III and generalized Pareto curves on the plot. A special type of simulation, “jack-knifing” was applied to look at possible variations of the sample points on the L-moment plot (Appendix B). Results of the simulations (Fig. 3) show a fairly “tight” cloud for NS fracture height, apparently due to the large sample size and therefore, lower variability (comparing to EW sample). Thus, any of several models could be used for height in this set according to the L-moment procedure. For fracture height we therefore chose the lognormal model.

NNW fracture spacing

NNW fracture spacing on the probability plots is poorly approximated by the exponential model for both small and large values. The lognormal distribution, on the contrary, fits fairly well, including the extreme values (Fig. 4). The L-moment plot (Fig. 2) also shows the lognormal model as the best fit for this property. The sample point is located exactly on the lognormal curve.

Thus, a lognormal distribution was used for the NNW fracture spacing.

ENE fracture set

Similar to the NNW set analysis, the ENE set was assessed for appropriate height and spacing distribution models.

ENE fracture height

A probability plot (Fig. 5) shows that fracture height is well approximated by a lognormal distribution. Although both the exponential and lognormal models both capture the large and medium fracture behavior, the lognormal model better suits fractures smaller than 1.5 meters. The cloud of simulated points on the L-moment plot (Fig. 3) is also located further from the exponential point than from the lognormal curve. While some of the points are located almost on the lognormal curve, most of the cloud is in the vicinity to the generalized Pareto distribution, which has a power-law form in this region of the L-moment plot (Hoskins and Wallis, 1997). Montroll and Schlesinger (1983) argue that sometimes the lognormal distribution can mimic power-law behavior and it is hard to distinguish between them.

The lognormal model appears to be a good final selection for the ENE fracture height.

ENE fracture spacing

As with the fracture height, the fracture spacing is well fit by the lognormal model on the probability plots (Fig. 6). However, on the L-moment plot (Fig. 3), the sample cloud is somewhat apart from the majority of the standard curves, being close only to the Generalized Extreme Value distribution. Perhaps, such deviation is due to the small sample size (25 points). Based on the probability plots for the ENE fracture spacing, the lognormal model was chosen.

Fracture Modeling

After the distribution type selection we need to assign specific parameter values, such as mean and standard deviation, to each fracture property. We can do so by minimizing the error between the model and sample points, iterating parameters of the model. Table 1 shows the results of these iterations.

Table 1. Model distribution types and parameters for fracture properties

Fracture set	NS			EW		
	Distribution	mean	st dev	distribution	mean	st dev
Height	lognormal	7.78	6.09	lognormal	5.11	4.4
Spacing	lognormal	1.57	1.61	lognormal	1.97	1.73

The selected statistical models for the fracture properties are not considered to be final. As the study progresses, we should be flexible in the model assignment, adjusting it if additional data become available and comparing different models in sensitivity studies.

Preliminary results of fracture generation (using Fracman) are shown in Figs 7 and 8. The input for the model is shown in Table 2

Table 2 Input parameters for fracture generation in Fracman.

Model: Poisson Rectangles
 Region: Box 10x10x10 m³

Fracture set	NS			EW		
	distribution	mean	st dev	distribution	mean	st dev
Orientation of trend, degrees	constant	330		constant	75	
Orientation of plunge, degrees	constant	0		constant	0	
Height (length in Fracman), m	lognormal	7.78	6.09	lognormal	5.11	4.40
Length(width in Fracman), m	correlated, Length=(0.5-1.0)xheight					
Intensity, P ₃₂ , m ² /m ³		7.5E-01			6.6E-01	

The limitations and assumptions of this model include:

1. Orientation of fracture trend and plunge is constant.
 2. No quantitative length data are available at this point. Based on geological experience in the area, values 0.5 - 1.0 times the height value were used.
 3. Appropriate fracture spacing is obtained by adjusting the fracture intensity, which has a constant value.
 4. No fracture termination percent is assigned.
- This model and variants will be used for flow modeling.

Future Work

Further work will focus on fluid flow modeling of the simulated fractures (using the Fracman software). This work will comprise:

1. Transmissivity and sensitivity studies to quantify the effects of the fractures on flow. This includes both a sensitivity analysis of the parameter values used in the fracture modeling and an assessment of the relative contributions to flow of the various fracture sets.
2. A modeling different borehole orientations and locations in the fractured domain. This will give guidelines to the optimal borehole trajectory for the modeled fracture distributions.
3. The work will be extended to apply similar assessments in the more highly deformed sections of the Lisburne Group.

Acknowledgements

We thank Golder and Associates for the use of FracMan software in this project.

References

1. Barton, C.C. 1995. Fractal Analysis of Scaling and Spatial Clustering of Fractures, in *Fractals in the Earth Sciences* (C. C. Barton and P.R.LaPointe, eds.) Plenum Press, New York and London
2. Barton, C.C. 1992. in *Fractals in the Earth Sciences* (C. C. Barton and P.R.LaPointe, eds.) (Geologic Society of America Memoir, 1992).
3. Dershowitz, W.S., and Einstein, H. H. 1988. Characterizing Rock Joint Geometry with Joint System Models”, *Rock Mechanics and Rock Engineering*, No. 21, p. 21-51.
4. Guo, G., George, S. A., and Lindsey, R. P., 1999. Statistical Analysis of Surface Lineaments and Fractures for Characterizing Naturally Fractured Reservoirs, in R. Schatzinger and J. Jordan, eds., *Reservoir Characterization – Recent Advances, AAPG Memoirs 71*, p. 221-250

5. Hosking, J. R. M. and Wallis, J. R., *Regional Frequency Analysis*, Cambridge University Press, Cambridge, United Kingdom (1997)
6. Jensen, J. L. et al., *Statistics for petroleum engineers and geoscientists*, Prentice Hall, Upper Saddle River, NJ (1997)
7. Lorenz, J. C. and Hill, R.E. 1995. Subsurface Fracture Spacing: Comparison of Inferences From Slant/Horizontal and Vertical Cores”, *SPE Formation Evaluation*, March 1995, p. 66-72.
8. Montroll, E. W. and Schlesinger, M. F., 1983. Maximum Entropy Formalism, Fractals, and 1/f Noise: A Tale of Tails, *J. Stat. Phys.*, 32: 209-230
9. Rock fractures and fluid flow: contemporary understanding and applications, Committee on Fracture Characterization and Fluid Flow et al., National Academy Press, Washington, DC (1996)
10. Rouleau, A., and Gale, J. E., 1985. Statistical Characterization of the Fracture System in the Stripa Granite, Sweden, *International Journal of Rock Mechanics and Mining Sciences*, Vol. 22, p. 353
11. Wu, H., and Pollard, D.D.: “An Experimental Study of the Relationship Between Joint Spacing and Layer Thickness”, *Journal of Structural Geology*, v. 17, 1995, p. 887-905.

Appendix A. Sample L-moment calculations

Hoskins and Wallis (1997) formulated several important principles of the regional frequency analysis, some of which are relevant to our task:

1. Frequency analysis should be robust. In many cases, it is unreasonable to expect a model to be an exact representation of a physical process. Much more important the modeling procedure to be *robust*, i.e. it “should yield quantile estimates whose accuracy is not seriously degraded when the true physical process deviates from the model’s assumptions in a plausible way.”
2. Use Monte Carlo simulation to establish the properties of a frequency analysis procedure, or to compare two or more procedures.
3. Frequency distributions need not to be “textbook” distributions. For an adequate modeling, it is wise to include candidates having a wide range of moderate- and heavy-tailed behavior or distributions with enough free parameters.
4. L-moments are useful summary statistics. Sample moment statistics, particularly skewness and kurtosis, are often used to judge the closeness of an observed sample to a postulated distribution. However, these statistics have algebraic bounds depending on a sample size and therefore they are not reliable in certain cases. A better approach uses L-moment statistics which are “able to characterize a wider range of distributions and, when estimated from a sample, are more robust to the presence of outliers in the data.” The authors propose a plot of L-skewness versus L-kurtosis for various standard distribution types. This plot is used for diagnostic purposes, i.e. location of sample points on the diagram can show the best-fit distribution. A procedure of L-moment calculation is described below.

Estimation of L-moments is based on a sample of size n , arranged in ascending order. Let $x_{1:n} \leq x_{2:n} \leq \dots \leq x_{n:n}$ be the ordered sample. It is convenient to begin with an estimator of the probability weighted moment β_r . An unbiased estimator of β_r is

$$b_r = n^{-1} \binom{n-1}{r}^{-1} \sum_{j=r+1}^n \binom{j-1}{r} x_{j:n}$$

This may alternatively be written as

$$b_0 = n^{-1} \sum_{j=1}^n x_{j:n} ,$$

$$b_1 = n^{-1} \sum_{j=2}^n \frac{(j-1)}{(n-1)} x_{j:n} ,$$

$$b_2 = n^{-1} \sum_{j=3}^n \frac{(j-1)(j-2)}{(n-1)(n-2)} x_{j:n} ,$$

and in general

$$b_r = n^{-1} \sum_{j=r+1}^n \frac{(j-1)(j-2)\dots(j-r)}{(n-1)(n-2)\dots(n-r)} x_{j:n}$$

The sample L-moments are defined by

$$l_1 = b_0$$

$$l_2 = 2b_1 - b_0$$

$$l_3 = 6b_2 - 6b_1 + b_0$$

$$l_3 = 20b_3 - 30b_2 + 12b_1 - b_0$$

and in general

$$l_{r+1} = \sum_{k=0}^r p_{r,k}^* b_k ; \quad r=0,1,\dots, n-1$$

where

$$p_{r,k}^* = (-1)^{r-k} \binom{r}{k} \binom{r+k}{k} = \frac{(-1)^{r-k} (r+k)!}{(k!)^2 (r-k)!}$$

Appendix B. Jack-knifing Analysis

Assume we have a sample of size n . Any statistical properties, for example L-Skewness (T_3) and L-Kurtosis (T_4) are calculated for whole set. The jack-knifing starts with a removal of the first data point. T_3 and T_4 now are re-calculated for the remaining $n-1$ data points. Then, the first is replaced and the second data point is removed from the full set of n numbers. Another pair of L-moments is calculated, etc. The procedure is repeated until the last (n^{th}) data point is removed and the L-moments are calculated. As a result we have $n-1$ L-moment pairs calculated for subsets with one removed point and L-moments calculated for the full data set. This is illustrated on Fig. 3 where, for each fracture property, we can see point clouds formed by the n values.

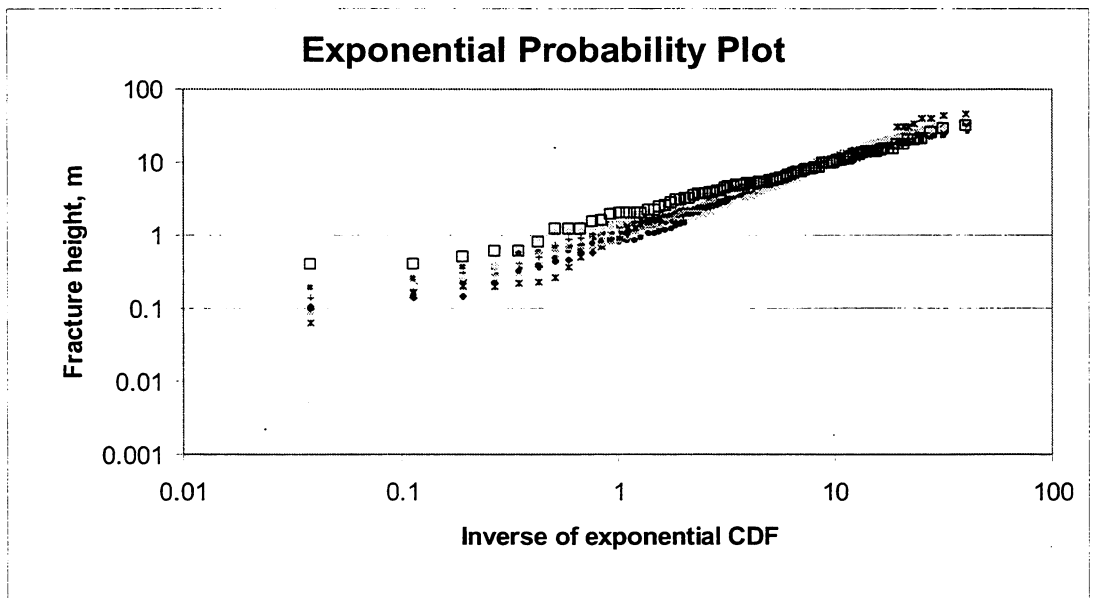
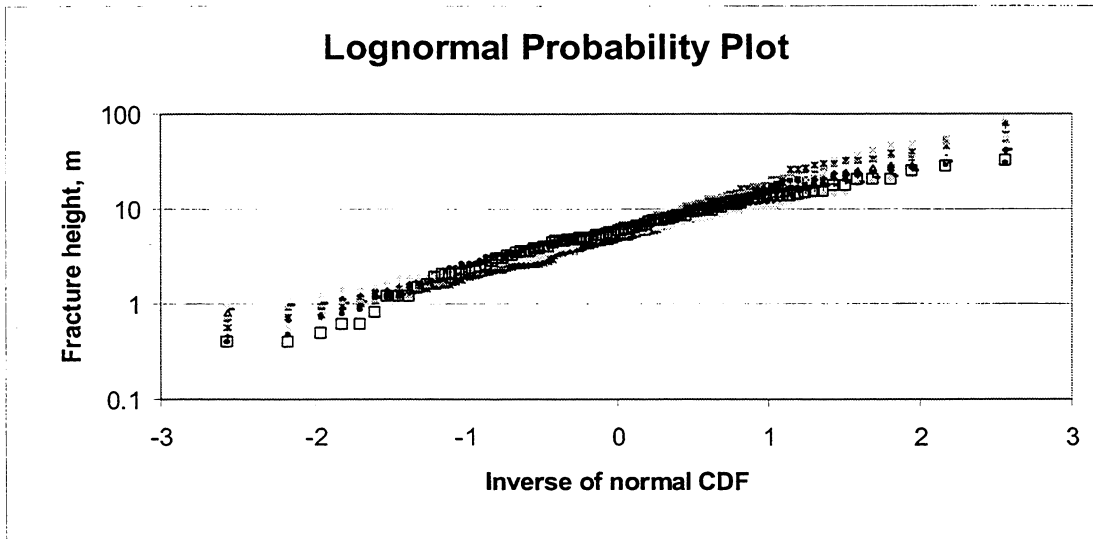


Figure 1 Results of Monte Carlo simulations on probability plots for NS fracture height. Squares represent sample, dots show simulated values.

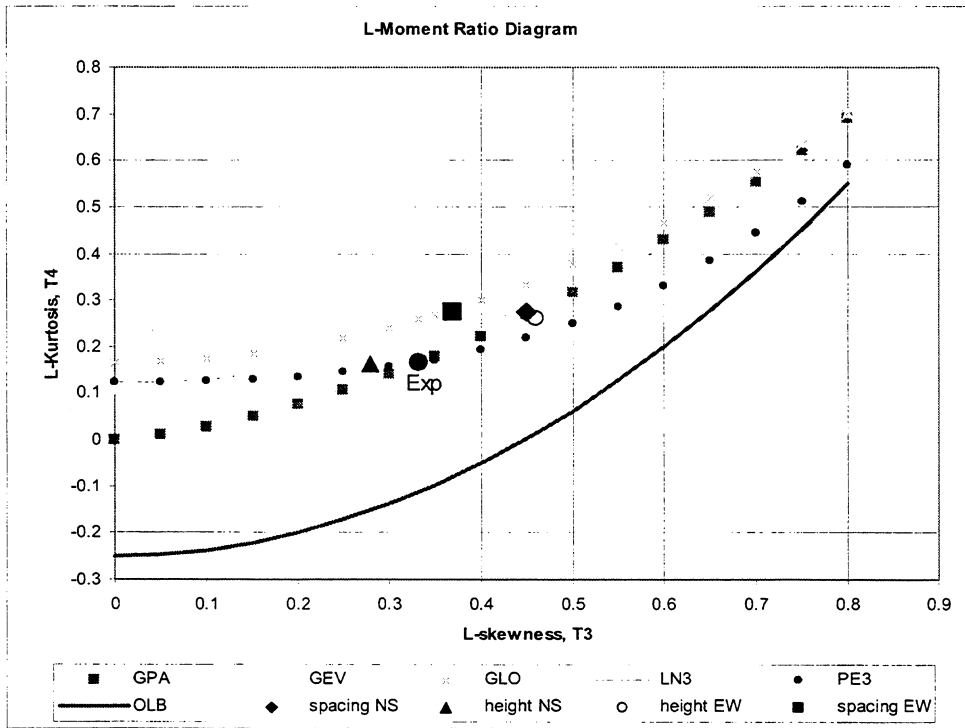


Figure 2 L-moment plot with fracture height and spacing sample points.

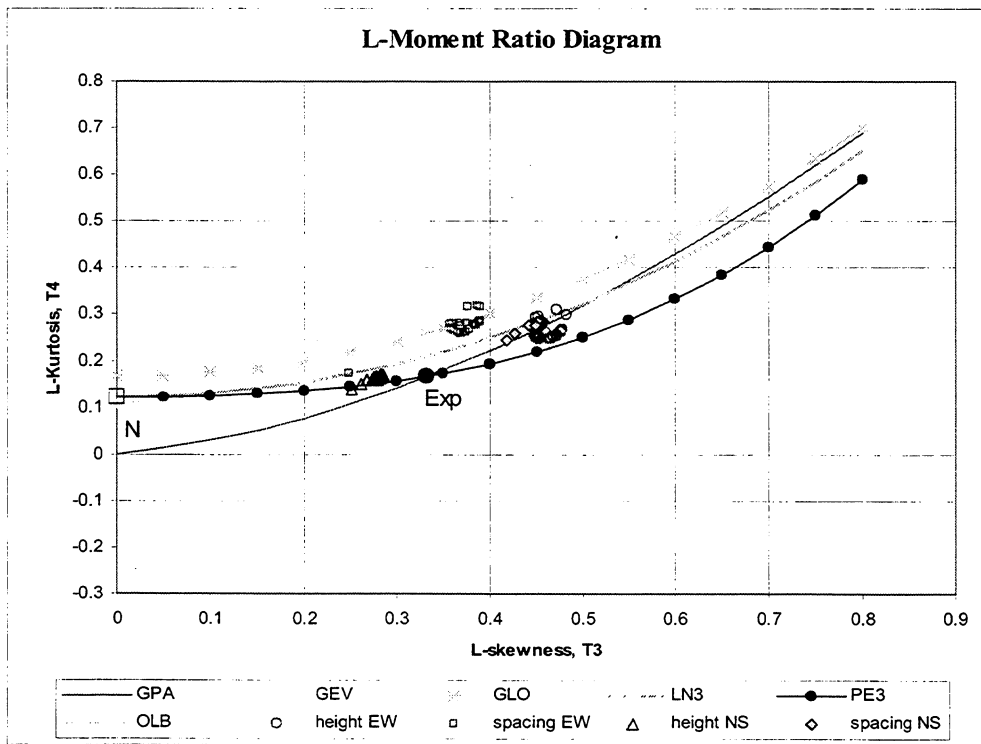


Figure 3 "Jack-knifing" simulation results shown on L-moment plot.

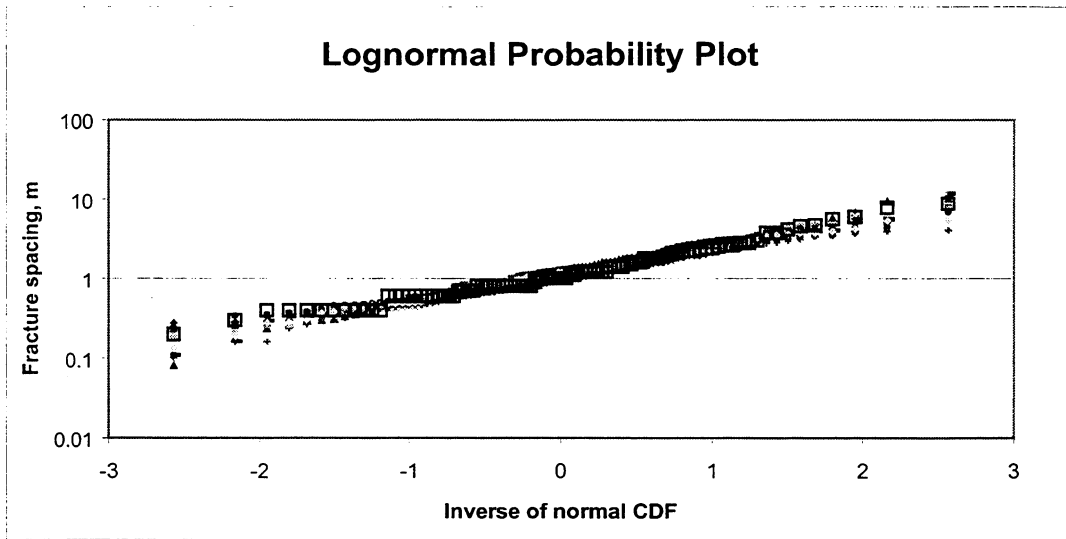


Figure 4 Probability plots for NS fracture spacing. Squares represent sample, dots show simulated values.

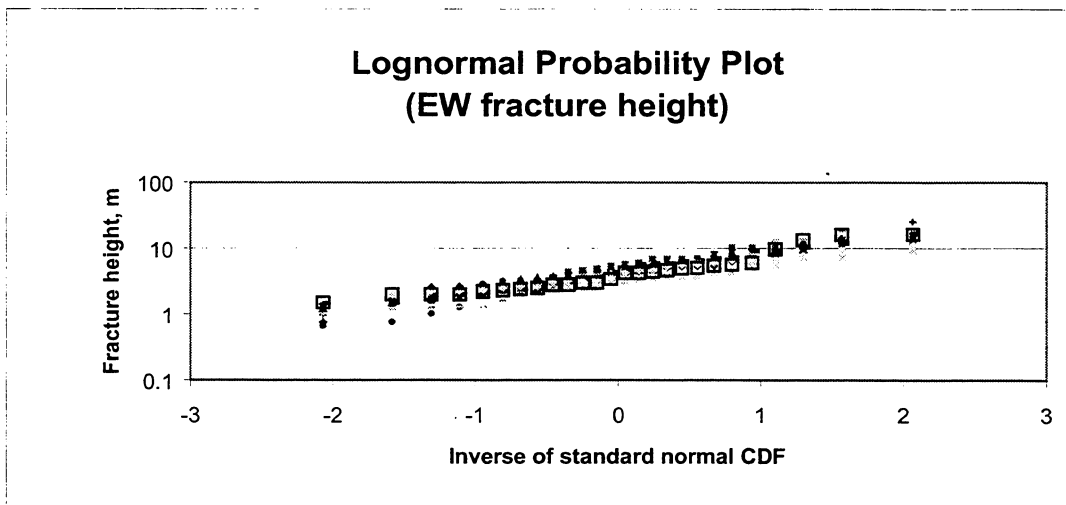


Figure 5 Probability plots for EW fracture height. Squares represent sample, dots show simulated values.

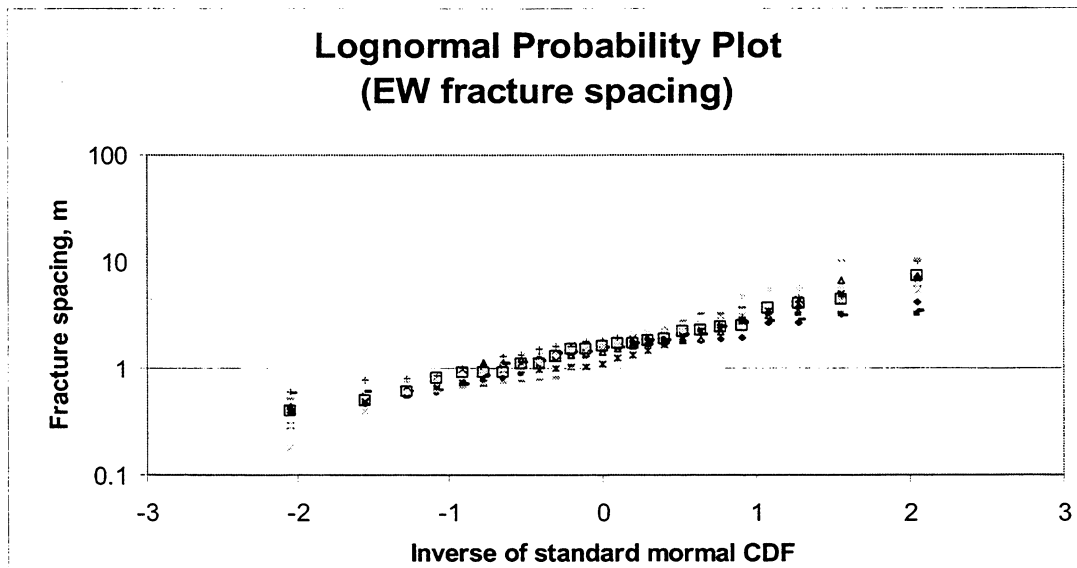


Figure 6 Probability plots for EW fracture spacing. Squares represent sample, dots show simulated values.

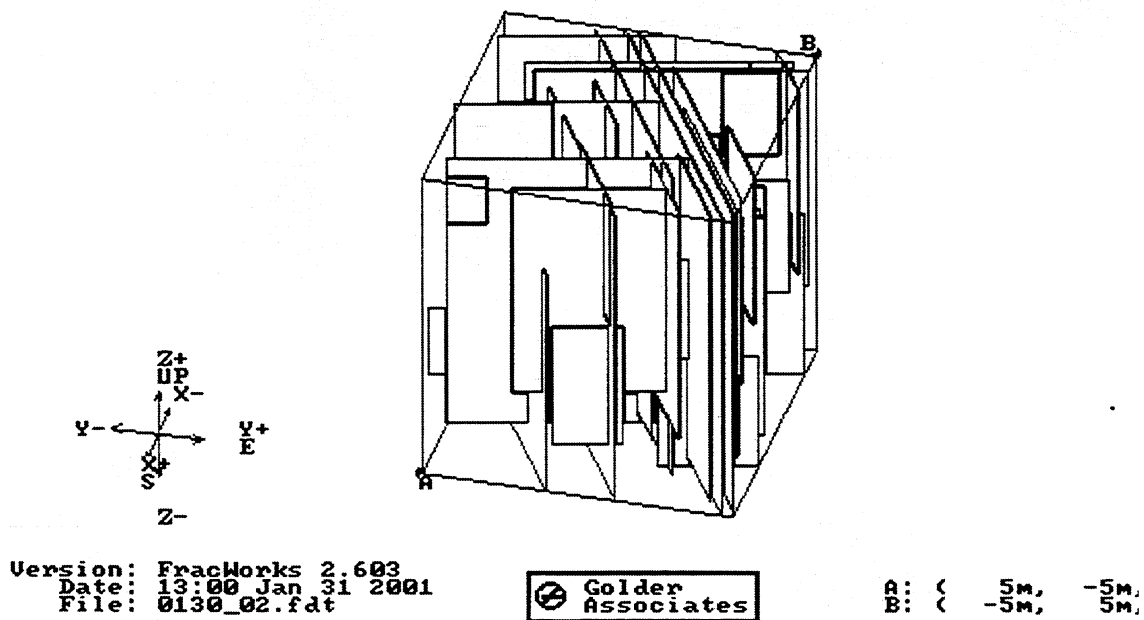


Figure 7 Fracman model of megafractures (10x10x10 m³)

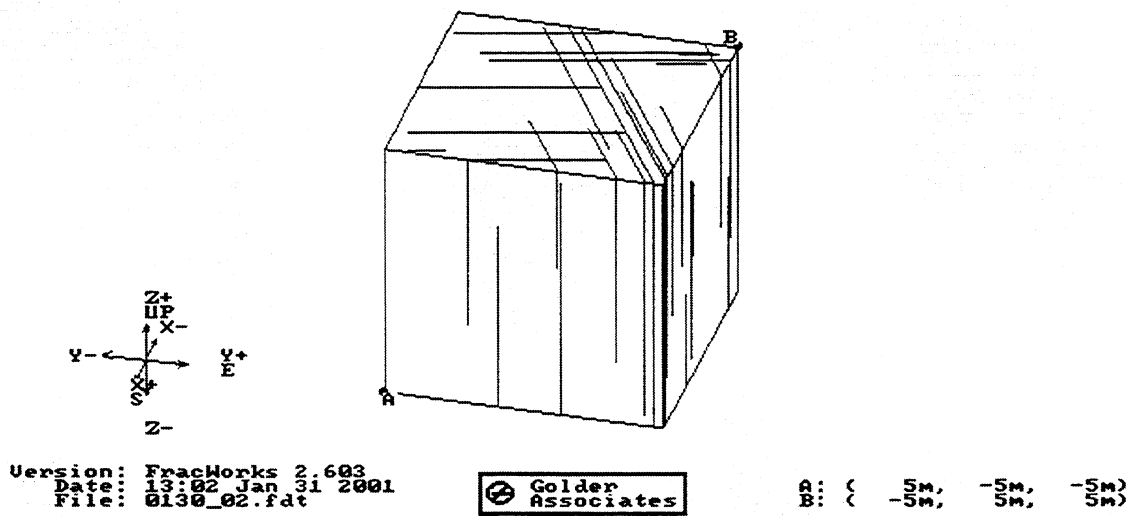


Figure 8 Fracman model showing only fracture traces (10x10x10 m³)

